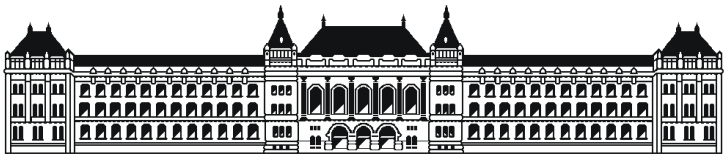

Budapest University of Technology and Economics
Department of Measurement and Information Systems

Digital Sound Synthesis of Two-Dimensional Vibrating Bodies

Master's thesis

Written by
Márton Albert

Supervisors:

Dr. László Sujbert
Budapest University of Technology and Economics, Department of Measurement and Information Systems

Prof. Dr.-Ing. Rudolf Rabenstein
Friedrich-Alexander-University of Erlangen-Nuremberg, Chair of Multimedia Communications and Signal Processing

2010

Budapesti Műszaki és Gazdaságtudományi Egyetem
Méréstechnika és Információs Rendszerek Tanszék

DIPLOMATERV FELADAT (ezt adják. . .)

Márton Albert
szigorló villamosmérnök hallgató részére
(nappali tagozat villamosmérnöki szak)

Digital Sound Synthesis of Two-Dimensional Vibrating Bodies
(a feladat szövege a mellékletben)

A tervfeladatot összeállította és a tervfeladat tanszéki konzulense:

Dr. László Sujbert
docens

A záróvizsga tárgyai:

Első tárgy
Második tárgy
Harmadik tárgy

A tervfeladat kiadásának napja:
A tervfeladat beadásának határideje:

dr. Diplomatervfelelős András	*dr. Tanszékvezető Gábor*
adjunktus, diplomaterv felelős	egyetemi tanár, tanszékvezető

A tervet bevette:
A terv beadásának dátuma:
A terv bírálója:

MELLÉKLET

Digital Sound Synthesis of Two-Dimensional Vibrating Bodies

A feladatkiírást a tanszéki adminisztrációban lehet átvenni, és a leadott munkába eredeti, tanszéki pecséttel ellátott és a tanszékvezető által aláírt lapot kell belefűzni (ezen oldal *helyett*, ez az oldal csak útmutatás. Fénymásolat nem jó, ezért mindenki igényeljen megfelelő számú eredeti iratot az adminisztrációban).

Dr. László Sujbert
docens

HALLGATÓI NYILATKOZAT

Alulírott *Márton Albert*, a Budapesti Műszaki és Gazdaságtudományi Egyetem hallgatója kijelentem, hogy ezt a diplomatervet meg nem engedett segítség nélkül, saját magam készítettem, és a diplomatervben csak a megadott forrásokat használtam fel. Minden olyan részt, amelyet szó szerint, vagy azonos értelemben, de átfogalmazva más forrásból átvettem, egyértelműen, a forrás megadásával megjelöltem.

Tudomásul veszem, hogy az elkészült diplomatervben található eredményeket a Budapesti Műszaki és Gazdaságtudományi Egyetem, a feladatot kiíró egyetemi intézmény saját céljaira felhasználhatja.

Budapest, May 21, 2010

Márton Albert
hallgató

Contents

Kivonat

Jelen munka a kétdimenziós, görbült, változó vastagságú, ortotróp héjak fizkai alapú modellezéséről szól, ami alkalmas lehet a harang hangjának modellezésére. A modellezéshez a függvénytranszformációs technikát alkalmaztuk, amelynek egyik lépését a véges differencia módszer segítségével végeztük el.

A modellezés első lépése egy megfelelő fizikai modell, vagyis differenciálegyenlet létrehozása. A görbült héjakat alapvetően csatolt differenciálegyenlet renszerrel lehet leírni, amelyben nemlinearitás is felmerül. Ennek elkerülése érdekében létrehoztunk egy olyan egyszerűsített egyenletet, amely a lemez transzverzális kitérését leíró egyenlettől egyetlen, differenciálhányados nélküli tagban különbözik. A kapott egyenlet általánosan görbült, változó falvastagságú ortortóp héjakra is használható.

A modellezés második lépése a kapott egyenlet számítógépen való implementálása. Ehhez először ismertetjük a főbb hangmodellezési technikákat, majd a két felhasznált technikát részletesen bemutatjuk. Közben kitérünk az adjungált differenciáloperátor fogalmára, és számítási módjaira, ami fontos szerephez jut a függvénytranszformációs technika alkalmazásakor. Ezenkívűl előállítjuk a véges differencia módszernek egy olyan változatát, amit használni tudunk a felmerülő sajátérték-problémák numerikus megoldására. Végül a javasolt hibrid modellt alkazzuk egy közönséges hengeres és egy harangformájú héjra, valamint bemutatunk néhány eközben felmerülő problémát.

Abstract

This thesis is about the physics-based modeling of two-dimensional orthotropic curved shells with variable thickness, which could be suitable for the synthesizing of the sound of bells. The functional transformation method is employed, but one of its steps is performed by the help of the finite difference method.

The first task of the modeling is to derive an appropriate physical model, that is a differential equation. Curved shells can be described basically by means of a coupled system of differential equations, wherein often arise nonlinearities too. To avoid this, we introduce a simplified shell equation which differs from the plate equation in one term only, containing no derivatives. The resulting equation can be applied to universally curved orthotropic shells with variable thickness too.

The second step of the modeling is the implementation of the differential equation. Towards this, the most important modeling methods are outlined first, then the applied methods are introduced in detail. The concept of adjoint differential operator is outlined too, which plays in important rule in the functional transformation method. In addition a modified version of the finite different method is introduced, which is capable to solve the arising eigenvalue-problems numerically. Finally the proposed hybrid method is applied to ordinary cylindrical shells and a bell-shaped shell. Several arising difficulties are presented too.

Introduction

Physics-based sound synthesis is one of the most active field of sound synthesis and according to the increasing growth of the speed of computers the perspectives are widening continually. Several methods have evolved, which model the vibrations of the resonator part of the musical instruments. Two methods are employed in this thesis, the finite difference and the functional transformation method. The former one is a widely used, relatively simple method, while the second one, which is developed at the Chair of Multimedia Communications and Signal Processing of the University Erlangen-Nuremberg, is a less known but much more practical method.

By the physics-based modeling of musical instruments the starting-point is usually a differential equation, which describes the motion of the resonator part of the instrument. These resonators can be treated usually as one or two-dimensional vibrating bodies, most of them can be described by means of a single differential equation. In the vibration of curved shells, however, plays the in-plane motion an important role too. Accordingly, they can be described basically by coupled system of differential equations, which can be nonlinear too. The implementation of such a differential equation is rather complicated. Hence, one of our aims was to develop a simplified governing equation, which is based on a single differential equation for the sake of simplicity, but takes the additional stiffness arising due to the curvature into account in the possible restricted manner.

The functional transformation method was applied to such types of vibrating bodies previously, which can be treated analytically. In many possible cases, however this can not be carried out, hence our second aim was to develop a method which is suitable to treat these cases numerically. The main task of this method is to solve an eigenvalue-problem of a differential operator. This gives the kernels of a transform arising in the functional transformation method. In this thesis we adopt the finite different method to solve this eigenvalue-problem. In this way a hybrid method is constructed, which is able to treat two-dimensional shells possessing cylindrical symmetry and variable thickness.

The thesis begins with the overview of the most important sound synthesis methods in section 1. Several considerations and the introduction of the concept of adjoint differential operator can be found in section 2. In the following two sections the applied sound synthesis methods are introduced, the functional transformation method in section 3, while the finite difference method in section 4. In section 5 we develop the governing equation of the orthotropic plate and reveal what happens if we take the in-plane motions into account too. In section 6 the simplified equation of the cylindrical shell is deduced first, then the

equation is adopted to arbitrary curved shells. Several variants of the shell equation are implemented in section 7 by the help of the developed synthesis method. In section 8 the achieved results and the possible directions of development are summarized. The physical concepts on which the derivations of the differential equations are based can be found in Appendix F.1.

This thesis is based on the report written at the University of Erlangen-Nuremberg in the spring semester 2009. Two sections are dropped out, while the section dealing with the required physical concepts is removed to the Appendix. The section treating the sound synthesis methods, the introduction of the adjoint operator and the finite different method, and the application of the resulting hybrid method were added posterior.

Chapter 1

About Sound Synthesis

In this chapter the aim of sound synthesis and the main trends of it are presented. Only an overview of the relevant and widely used methods is given, a wider and more detailed overview can be found in [18]. Two methods are employed in this thesis, these will be detailed in chapters 3 and 4.

1.1 The Aim of Sound Synthesis

The practical purpose is seemingly the reproduction of the sounds of different musical instruments and hereby to create a device, which is capable to replace the instrument. This proves useful in certain cases only, however. In the case when the real instrument is expensive or/and hardly movable, it can be beneficial to create a substitute model indeed, things are like this in the cases of the piano and church organ. In most cases, however, the set-up of the musical instrument is not too complex and can be built at a relatively low price, while the sound or physical process can be far too difficult which raises the price of the model. Cases in point are the flutes, by which the vocal tract of the musician have to taken in consideration too by modeling. Not to mention that the musicians are used to the manner of playing of the instrument in question. In fact this is what they make master themselves of during the practice, and for this reason it can not be modified. This makes the model costly in certain cases. In the case of the string instruments for example, probably almost the complete instrument should be built up to let a musician capable to play on it, similar is the situation by the flutes too. In pipe organ and piano models the wide-spread MIDI keyboards seem to be utilizable. Though the reaction of the strings or the trackers are not modeled, it is an accepted resort.
A further difficulty is to create a loudspeaker-system, which is capable to play-back the synthesized sounds, and this is not only a question of quality but of power too. The sound of church bells reach the threshold of pain in the near-field for example. Thus the cost of a loudspeaker-system of appropriate quality and power have to be taken into account too, if one wants to replace a musical instrument with its model.

The substitution of real instruments with those models is thus questionable in the most cases but the physics-based sound synthesis has at least three other kind of motivation.

On the one hand one get acquainted with the physical concepts operating the musical instrument in question during the preparation of the model. Usually we do not use the physical models derived from a group of phenomena to describe the phenomena in question only, but we try to wide the scope of the model by means of generalization (which has to be verified of course). Analogously, we do not get information of the investigated musical instrument only, and herewith we arrived at the other two motivations of physics-based sound synthesis. On one hand, the created model can be used to produce the sound of new, costly or not at all build able instruments. On the other hand, in the case of a suitably accurate model, it can be of assistance to the designing and development of real musical instruments.

This thesis is motivated by these latter three factor, especially the first one. Thus we did not aspire to create a substitute model, but much rather to describe the physical problem and to collect the relevant knowledge.

1.2 Sound Synthesis Methods

According to the employed method the sound synthesis methods can be divided into three families. Namely we can speak about physics-based modeling, signal-based modeling and abstract methods. These latter ones are usually discussed with the sampling synthesis together, which is owing to its simplicity and effectiveness a widely used method, but is rather a kind of sound compression than sound synthesis.

1.2.1 Abstract Methods & Sampling Synthesis

The methods based upon abstract algorithms have evolved in the early years of sound synthesis. All of them intended to generate – by the human auditory system – pleasant and natural considered sounds. Of this kind are the harmonious sounds for example, in which the frequencies of overtones are the multiples of the one of the fundamental.

FM Synthesis In the case of FM synthesis we are producing harmonious-like sounds exploiting the properties of frequency-modulated signals. In the simplest case the output signal of a sine wave generator (carrier) is modulated by an other sine wave (signal), in this way we get a spectrum periodically distributed around the carrier frequency, with a period of the signal frequency. In the case of the so-called feedback FM synthesis one can keep hands on the model parameters easier, thanks to various feedbacks.

Waveshaping Synthesis This method utilizes the overtones arising from the nonlinear distortion. It is easily implementable: we store the nonlinear characteristic curve in a vector or table, then addressing this table with a sine-wave signal the read values form the desired output signal. The structure of harmonics is controllable by means of the characteristic curve.

Karplus-Strong Algorithm Karplus and Strong developed a very simple method to model percussion and plucking string instruments. They were able to model the initial sharp transients and the clearer, more periodic falloff sound by means of a Wavetable, filled up with random-like data and having various low-pass filters in its feedback.

Sampling Synthesis The denomination refers practically speaking to play-back of sounds recorded in advance. It differs from the simple repetition therein, that on behalf of the reduction of data to store, not the entire sustained sound, but only the initial transient and one period of the steady sound are stored. At the play-back these components are interlaced and the latter one iterated, altering its volume according to the falloff (at best imitating the frequency dependence of the falloff by means of filtering). It is conventional also to reduce the amount of required data by means of pitch shifter[1] and other compression methods.

1.2.2 Signal-based Sound Synthesis

In the case of signal-based sound synthesis, we study the sound of the musical instrument in question, try to get the relevant properties of the sound and generate the synthesized sound on the grounds of this knowledge.

In contrast to the abstract methods these methods are capable to model the sound of real musical instruments. Since we take only the properties of the sound into consideration, the complexity of the sound presents the difficulty and it is irrelevant how complicated the mechanism creating the sound is. The signal-based method is very universal in the sense, that it is adaptable to several instruments by altering the values of its parameters only, in contrast to the physics-based methods where this can be said only of instruments having similar structure. Basically, the signal-based models are appropriate to model slowly varying sounds, rather circumstantial transformations need to be done to consider the transients too. Along with the sampling synthesis, its utmost disadvantage is that it needs a new record or set of parameters for each note.

The signal-based approach can be divided into two truly distinct synthesis methods, the other ones differ in the employed apparatus only, or include several supplements.

Additive Synthesis As the denomination refers to, this method composes the synthesized sound by means of summing simpler signals. These signals are usually sine-waves with different frequencies. Their amplitudes (and frequencies) are modulated by the help of slowly-varying control signals.

In the case of the resynthesis of real sounds, the control signals are extracted from the original sound and are approximated by a set of linear functions for the sake of variability and reduction of the amount of data. The difference between the original and resynthesized sounds is the error function, which contains spectral components of small amplitude and the transient respectively. From this error function the transient is retrievable by the help of spectral analysis, while the rest is usually approximated by means of a quasi random

[1] Not the entire gamut is stored, and the missing tones are obtained from the adjacent tones by means of pitch shifting.

function with given amplitude spectrum. Both technics are employed by the transient modeling synthesis, only the latter one by the spectral modeling synthesis.

Subtractive Synthesis We speak about subtractive synthesis or source-filter synthesis if we create the desired sound from a more complex one by the help of time-variant filtering. Since the human voice is generated in the same wise, in the case of voice synthesis the model parameters are determinable from the physical concepts of voice generation. In the case of musical instruments we can only recline upon the sound itself.

The signal of departure is usually some broadband or harmonic-rich sound. If the desired sound is harmonious we can set out from an impulse train of the wanted frequency for example. By means of time-variant filtering the change of formants over the time can be modeled too.

1.2.3 Physics-based Sound Synthesis

The denomination refers to the fact that we start out from the behaviour of the body which is generating the sound. The modeling consists of two steps in this case, the first one is the construction of a physical model: we examine the sound generation mechanism and the properties of sound radiation and simplify them with the fidelity in view. The second step is the implementation of the physical model typically on a computer or an appropriate hardware.

This is the most dynamically developing branch of sound synthesis in our days. The utmost advantage of it is that the arising model behaves musical instrument-like, its parameters are, in contrast to the signal-based models related to the instrument itself and are well interpretable also to the musicians. It is very beneficial in the case of such instruments, which sound is determined by more factors. Of this kind is the violin. The sound of the violin depends on the speed and pressure of the bow, we can sound given a tone on more than one string, the strings can be plucked, the gentle fluctuation of the place of fingers – the vibrato – results in a tone of new character too. In the case of the signal-based synthesis for each of these playing styles an extra set of parameters needs to be set up, which is, taking the combinations of playing styles into account too, almost hopeless. In the case of physics-based sound synthesis, however, the modifications are evident and well determined. These methods have usually the highest computing demand, however.

To find out, what is negligible during the construction of the physical model, we have to examine the sound of the instrument and the properties of the human auditory system too. We do not need to model the torsional motion of the bars of a carillon for example, since it produces sounds with low efficiency. Sometimes certain components of the arisen sound are not audible due to the properties of the auditory system or other effects.

Finite Different Method The starting-point of this method is the differential equation describing the motion of the resonator part of the musical instrument in question. In the case of many instruments this equations is already known. Modeling the violin, the piano or the guitar, to a first approximation the governing equation of the ideal string

has to be utilized with boundary conditions according the type of termination. In the case of a drum, the differential equation of the ideal membrane is the starting-point. In the case of the marimba and xylophone the governing equation of the rod has to be applied. These equations are, in the case of simple initial and boundary conditions, analytical solvable. Since, however in a suitably elaborate model both the equation and the boundary conditions are difficult, we can rely on numerical computation only. Thus, the solution is sought in discrete spatial and temporal points, and the differential equation has to be transformed into a difference equation accordingly. In this way we get a recurrence equation finally, which gives the values of the sought function in every spatial points on the grounds of the values in the preceding time-step. The top disadvantage of this method is, that the the time-step has to be chosen gratuitously small for the sake of the stability.

Digital Waveguide Similarly to the finite difference method, the solution of the governing differential equation is sought, but now we utilize the knowledge, that every functions of the form $y(x,t) = y_+(x - ct)$ and $y(x,t) = y_-(x + ct)$ are solutions of the ideal string equation for example. Here c is the frequency independent velocity of the arbitrary waveforms running in the positive and negative directions, respectively. The digital waveguide model consists of two delay lines which carry the two waves, running in opposite direction. On the ends, carrying out the transformations according to the terminations, the signal is sent in the other delay line. This corresponds to the reflection on the boundaries. On any point of the string, the sought quantity is determined as the sum of the corresponding values in both delay lines. By means of an adequate filtering the losses and dispersion can be modeled too. This is the most-used method. Since we fulfilled a part of the solution of the equation in advance, it has a lower computational demand as the finite difference method does.

Finite Element Method The motion of a distributed vibrating system can be approximated by means of numerous, to each other connected simple ideal mechanical elements (masses, springs and dampers). In this way we have to solve a number of simple equations. We do not need, thus the differential equation, what is favorable in the case of bodies with complicated geometry (e.g. church bell). It can be shown (see [4]) that the difference equation can be derived from the mass-spring model of the string for example.

Functional Transformation Method This method sets out from the governing partial differential equation, similarly to the finite difference method. It employs, however functional transformations, and generates a multidimensional analogue of the transfer functions used in system theory. The differential equations arising in physical-based sound synthesis are initial and boundary value problems. In the functional transformation method the temporal derivatives are removed first by means of the well-known Laplace-transform. Then we construct an other transformation to remove the spatial derivatives from the remaining boundary value problem. In this way, an algebraic equations arises which contains the transforms of the sought and excitation functions and some optional additive terms accord-

ing to the initial conditions. This is rearranged into a multidimensional transfer function form which is then discretized and the inverse transformations are carried out. This method results in an alternative description of the system, which is implementable by the help of a digital filter bank. Feeding this filter bank with the temporal function of the separated excitation function we get the values of the sought function at fixed spatial coordinates in the output.

1.3 The Two Steps of Bysics-based Sound Synthesis

In this section we want to pan out about the two steps of physics-based sound synthesis.

The first step is thus to create a physical-mathematical model about the system in question. In the cases of the finite difference and functional transformation methods this model is the differential equation of the vibrating body. We usually achieve the desired model by means of several simplifying steps. Our choice of what we consider negligible influences decisively, how relevant our model will be. We can easily commit such a fault which results in a model describing either not the system, we want to model with it, or even a physically unreal system.

As a first simplification we usually enter the concept of *neutral surface* or *middle surface*. This is the surface in a bent plate which is neither stretched nor compressed during bending movements. The motion of this surface will be determined only. The second simplification is to take only certain type of motion into account. In the case of percussion instruments we are concerned in such vibrations which are accountable for the radiated sound principally. These are the transversal or bending waves. Sought is thus the differential equation describing the transversal deflection $w(x_1, x_2, t)$ of the middle surface. It can happen, however, that we have to determine the in-plane motion of the middle surface too, to be able to get the transversal deflection correctly. This is the case by the strings of the piano, where certain components of the sound can be modeled in this wise only[2]. In such a case the differential equations describing the different type of motions get coupled with each other, and often cause nonlinearity too.

The differential equations can be determined on the grounds of considerations of geometry, kinematics, elasticity theory and dynamics, the required concepts are reviewed in Appendix F.1. The derivation of the equations can be decomposed into five more or less well separable tasks, which are in every case similar. For the sake of the uniform and transparent presentation these steps will be reviewed here, and we will follow them in chapters 5 and 6. Note, that sometimes this treatment can seem circuitous and the related books usually do not separate these tasks, but by the reason of perspicuity it will be helpful.

The five steps of the deduction of governing differential equations of mechanical vibrating systems are the following:

1. **Kinematics (strain – displacement relation):** Developing the relationship between the deflection function w and the strains ϵ by means of simple geometrical

[2]See in [1].

considerations. As it was detailed the transversal deflection w is a special part of the displacement vector $\mathbf{u}(\mathbf{r})$. Similarly, usually we do not need to determine the complete ϵ strain tensor either, but only the relevant components.

2. **Hooke's law (stress – strain relation):** Determining the stress σ according to the strain ϵ by the help of Hooke's law.

3. **Resultants (moment of force & tension – stress relation):** Introducing new quantities, which makes easier to develop the balance equations for a differential element of the mechanical system. These new quantities are different types of moments and in-plane force densities. They can be determined by integration over thickness.

4. **Balance of moments (shearing force – moment of force relation):** Determining the Q shear forces according to the M torques by the help of balance of moment equations (section F.1.2).

5. **Balance of forces (displacement – shearing force relation):** Developing the relation between the deflection w, its derivatives and the shear force Q and in-plane force densities N by the help of Newton's second law (section F.1.1).

Note, that these steps can be carried out in different order too, the advantage of this sequence is, that we use always the results of the preceding steps and in this way the deduction has a linear structure.

It is often worthwhile to treat more derivatives together and designate with a *differential operator* for the sake of transparency. Differential operator is the Laplace operator of Laplace's and Poisson's equations for example, but we can define other ones too, if it facilitates our work.

The second step of physics-based sound synthesis is the implementation of the given mathematical model. This is a signal processing and programming task, which is determined by means of the chosen method fairly accurately. Some unique solutions can be needed but usually one of the methods overviewed in the preceding section is used.

Chapter 2

Preliminary Considerations

In this section some considerations arising during the derivation of the differential equations is presented and the applied modeling method is presented.

2.1 Physical, Geometrical and Mathematical Considerations

One of our aims was to be able to describe a relatively general family of the two-dimensional vibrating bodies. The differential equations of the isotropic plate and the membrane are relatively simple and well-known. Some generalizations are are proposed in the followings.

One of them is to assume orthotropy instead of isotropy. This means different physical properties in different directions (see F.1.6). As a result the number of elastic properties increase and the spatial differential operator of the governing equation decomposes in more terms. An other possible generalization is to take the variable thickness into account. For the sake of this the thickness and consequently other terms have to be considered the function of the spatial coordinates. The third possibility is to consider the curved plates or shells. In this case further elastic effects have to be considered. The shells have an additional stiffness due to their curvature, this is demonstrated on a differential element of a cylindrical shell on figure 2.1. Applying a transversal force f_e on the shell, in-plane forces N arise and the differential element is contracted (or stretched). Thus the shell has a bigger resistance against the excitation. We will try to take this effect into account in a manner simply enough to let the functional transformation method applicable. The upper three generalization can be considered simultaneously too, we will perform this in section 7.

During application of the functional transformation method the concept of the adjoint of differential operators will be required, the mathematical concept of this adjoint is presented in the following subsection.

2.1.1 Not Self-adjoint Differential Equations

The concept of adjoint of differential operators can be introduced on the grounds of the same property of matrices, as it can be found in [8]. Here a short outline is presented about the association detailed there.

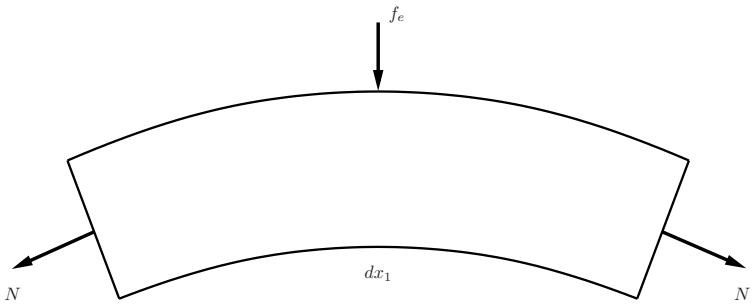

Figure 2.1: *In-plane forces arise due to transversal excitation force in the curved shell.*

2.1.1.1 The Adjoint Operator

Our starting-point is the fact that a differential operator can be concerned as a matrix of infinite size, or in other words as a system of infinite number of equations and variables. This can be seen on the grounds of the possibility of approximation of differential operators by the help of the finite difference method. This will be presented in section 4.

The adjoint of a matrix is usually defined as the conjugate of the transpose. This operation can be carried out in the case of finite sizes only, and is not helpful in point of view of the differential equations. It is possible, however to define the adjoint matrix in a way which is applicable in the case of infinite sizes too. Wee need for this definition the fundamental transposition rule of matrix calculus only:

$$\widetilde{AB} = \tilde{B}\tilde{A}. \tag{2.1}$$

Since the inner product of of two vectors $\langle v_1, v_2 \rangle = \tilde{v}_1 v_2$ is a scalar[1], which adjoint is the conjugate, we can write

$$[\tilde{v}_1 v_2]^* \equiv \tilde{v}_2 v_1, \tag{2.2}$$

where the asterisk represents conjugation. If we write v_2 as Av_3, we get that

$$[\tilde{v}_1 A v_3]^* \equiv \tilde{v}_3 \tilde{A} v_1. \tag{2.3}$$

This fundamental identity is called *bilinear identity*. The adjoint of the infinite sized matrices representing the differential operators have to satisfy this equation as well. Moreover the identity can be used as the definition. According to the association between differential operators and matrices (see section 4) the bilinear identity (2.3) can be adapted to

[1] The v_i vectors are column vectors.

differential operators, thus with a more practical notation

$$\langle u, A\{v\}\rangle^* \equiv \left\langle v, \tilde{A}\{u\}\right\rangle \tag{2.4}$$

where $A\{.\}$ is the operator in question, $\tilde{A}\{.\}$ is the adjoint of it, while u and v are arbitrary continuous sufficiently differentiable functions. This counterpart of the bilinear identity is called *Green's identity*. The inner product in the identity is defined by

$$\langle g, f\rangle = \int g^*(x) f(x) \mathrm{d}x, \tag{2.5}$$

where x represents a point in the multi-dimensional space, $\mathrm{d}x$ is the volume element and the integration should be carried out on the domain of definition. In the case of real functions the conjugation can be skipped, accordingly Green's identity is

$$\int A\{v(x)\}u(x)\mathrm{d}x = \int v(x)\tilde{A}\{u(x)\}\mathrm{d}x. \tag{2.6}$$

By the help of this identity we can determine if a pair of operators are in adjoint relation, moreover we can determine the adjoint of a given operator.

2.1.1.2 Determination of the Adjoint Operator

The differential operators, in them selfs give not an unambiguous description about the system, the missing information is in the boundary conditions. As we will see in section 4, a differential operator in itself corresponds to an incomplete system of equations. Thus boundary conditions have to be considered too by the application of Green's identity. In this way the identity gives not the adjoint operator only, but the adjoint boundary conditions too. The adjoint operator can be determined analytically in two steps, as it is presented in [8].

Extended Green's Identity In the first step we concern functions u and v in the Green's identity (2.6) sufficiently differentiable only, they do not have to fulfill the boundary conditions. In this case the right side is not zero, and a term called *boundary term* arises. This depends on the values of functions u and v and its derivatives on the boundaries, that is

$$\int \left(u(x)A\{v(x)\} - v(x)\tilde{A}\{u(x)\}\right)\mathrm{d}x \equiv \text{boundaryterm}. \tag{2.7}$$

This identity is called *extended Green's identity*. Let us assume that we succeed to write the integrand in the following from:

$$u(x)A\{v(x)\} - v(x)\tilde{A}\{u(x)\} \equiv \sum_\alpha \frac{\partial}{\partial x_\alpha} F_\alpha(u, v), \tag{2.8}$$

where the terms $F_\alpha(u, v)$ are bilinear functions of u and v and x_α are the independent variables. Now, considering $F_\alpha(u, v)$ as components of a vector, we can write according to

Gauss's integral theorem that

$$\int \Big(u(x)A\{v(x)\} - v(x)\tilde{A}\{u(x)\} \Big)\, \mathrm{d}x \equiv \int \sum_{\alpha} \frac{\partial}{\partial x_\alpha} F_\alpha(u,v)\mathrm{d}x = \int \sum_{\alpha} F_\alpha(u,v)\nu_\alpha \mathrm{d}S, \tag{2.9}$$

where ν_α are the components of the outward pointing unit normal field of the boundary S. Thus we got the desired form where the right side is the boundary term, which will determine the adjoint boundary conditions.

Let us examine if the extended Green's identity (2.7) can be written in the form of (2.8). The effect of a linear differential operator $A\{.\}$ on a function $v(x)$ can be written as the linear combination of $v(x)$ and its derivatives. A typical term is thus

$$q(x)\frac{\partial w(x)}{\partial x_i}, \tag{2.10}$$

where $q(x)$ is a given function of variables x_i and $w(x)$ is an arbitrary partial derivative of $v(x)$. We can reduce the order of derivative, by applying the product rule of differentiation on the product of $u(x)q(x)w(x)$:

$$u(x)q(x)\frac{\partial w(x)}{\partial x_i} = \frac{\partial}{\partial x_i}\left[u(x)q(x)w(x)\right] - \frac{\partial}{\partial x_i}\left[u(x)q(x)\right] w(x). \tag{2.11}$$

This step can be applied on the second term on right side (by emphasizing a new derivative from the derivatives included in $w(x)$) again and again, in this way we can liberate $v(x)$ from all derivatives. This argument can be used to all terms of the operator and we can rewrite the product $uA\{v\}$ in such a way, where $v(x)$ is unhinged from each last term, while the remaining terms are of the form $\frac{\partial}{\partial x_\alpha}F_\alpha(u,v)$, that is

$$u(x)A\{v(x)\} = v(x)\tilde{A}\{u(x)\} + \sum_{\alpha} \frac{\partial}{\partial x_\alpha} F_\alpha(u,v). \tag{2.12}$$

We have thus arrived at the desired formula and we got a method for the derivation of the adjoint operator and the boundary term.

Adjoint Boundary Conditions The second step is the determination of the adjoint boundary conditions. These are determined by means of the demand that the right side of the Green's identity must be zero. Thus the boundary conditions are those conditions which we have to put on $u(x)$ beyond the conditions on $v(x)$ to let the boundary term disappear.

This is thus the analytical method of determination of the adjoint operator, based on the definition. As we will see we can proceed much easier by the help of the finite difference method. Namely if the matrix of the differential operator is given, it is enough take its adjoint. We will use this latter method in our model.

2.2 The Applied Modeling Method

We will use the functional transformation method and the finite difference method together, constructing a relatively universal method. We will see in next section that during the application of the functional transformation method one has to solve a function-valued eigenvalue-problem. This means the solution of a boundary value problem, which is solvable analytically in special cases only. According to [5] the separation of variables can be used in the case of the rectangular plate only if the plate has at least two opposite edges simply supported. Thus the problem of the rectangular plate with all the edges free can not be solved analytically either. For this reason we will solve the eigenvalue problems by the help of the finite difference method.

In this way we keep the advantage of the functional transformation method, that is it results in an effectively implementable parallel filter bank structure. But at the same time we extend its applicability to problems which are analytically not or hardly solvable.

Chapter 3

Functional Transformation Method

In this section we introduce the Functional Transformation Method by following up the introduction presented in [7], [14] and [13], respectively. In section 3.1 we shortly summarize the steps required, then in section 3.2 the details on the specific example of the string is introduced. In section 3.3 the method is adopted to non self-adjoint operators, finally in section 3.4 we analyse the results, and give some notices.

We assume the partial differential equation of the process given, and our aim is to transform the equation into an other equivalent description, which is capable for digital modeling. In this case this will be a parallel filter bank, where the coefficients are calculated from the physical properties of the process.

3.1 The Steps of the Functional Transformation Method

The denomination alludes to the way how we get the coefficients of the filter bank from the governing equation: functional transformations need to be done on the initial and boundary value problem.

The steps and the equivalent descriptions of the system, which we get among the transformations can be surveyed in the following enumeration and in figure 3.1.

1. Applying the **Laplace transformation** to the initial-boundary-value problem. In this way we get a boundary-value problem, where the temporal derivatives are represented by means of the initial conditions and multiplication of the powers of complex frequency s.

2. We apply the so-called **Sturm–Liouville transformation** to the boundary-value problem, which behaves the same way in point of the space variable as the Laplace transformation does in point of the temporal variable. Our most important task is to find the transformation kernel of the Sturm-Liouville transformation, which is different for every initial-boundary-value problem. This can be determined analytically in certain cases, but we have to resort to numerical methods mostly.

3. With the preceding two steps we turned the problem into an algebraic equation, without any derivatives. This can be easily **rearrang**ed into a continuous-time mul-

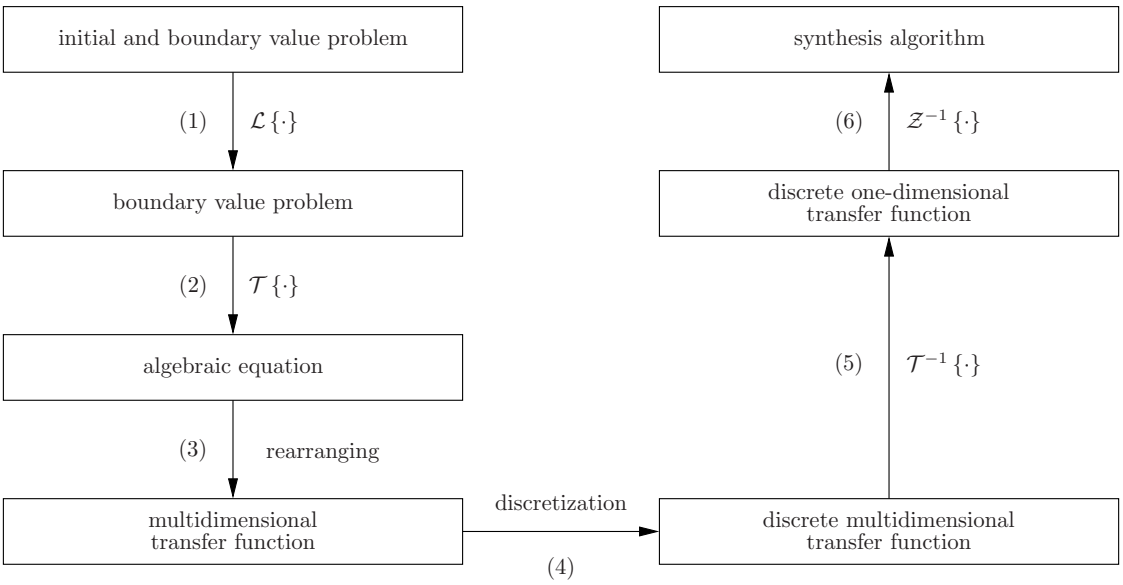

Figure 3.1: *The essential steps of the functional transformation method.*

tidimensional transfer function, which gives the relation of the sought function to the excitation function.

4. We rewrite the continuous-time transfer function into a discrete-time transfer function by the help of the **impulse-invariant transformation**. This way we arrive at a discrete multidimensional transfer function. This new description of the system will be well suited for implementing on an appropriate digital hardware.

5. We have to fulfill in the discrete-time domain the inverse of the first two transformations, firstly let us use the **inverse Sturm-Liouville transformation**. This way we get a description containing the discrete complex-frequency and the spatial variable. This description can be interpreted as a number of one-dimensional transfer functions connected parallel.

6. The last step is to apply the **inverse z-transform** to the problem, which yields the filter bank realization in the discrete time domain. Since the coefficients of every single filters can be determined on the grounds of their transfer functions, this last step do not have to be done from the point of view of implementation.

3.2 An Example: The String

In this section the steps of the functional transformation method will be applied to the vibrating ideal string, on both end fixed. This problem is universal enough to be able to

represent the method, but not too complex, to let us see the matter beyond the computation.

The investigated problem is thus, the transverse vibration of the string, both end fixed, and subjected to certain axial tension. This tension together with the bending moments arising in the bent string produce the restoring forces. Let us designate the mass density of the string material by ρ, and the cross section by A, in this case the linear mass density is ρA. The string constitutes according to the restoring forces and the mass density a vibrating system. We can describe this vibrating system by the help of a partial differential equation.

Our starting point is thus the governing equation of the transverse vibration, and the corresponding boundary and initial conditions. These are in this case

$$\frac{EI}{\rho A}\frac{\partial^4}{\partial x^4}y(x,t) - \frac{T_s}{\rho A}\frac{\partial^2}{\partial x^2}y(x,t) + \frac{\partial^2}{\partial t^2}y(x,t) + \frac{d_1'}{\rho A}\frac{\partial}{\partial t}y(x,t) + \frac{d_3'}{\rho A}\frac{\partial^3}{\partial t \partial x^2}y(x,t) = \frac{1}{\rho A}f'(x,t), \tag{3.1}$$

where

$$y(x,t)\big|_{t=0} = 0, \tag{3.2a}$$

$$\frac{\partial}{\partial t}y(x,t)\bigg|_{t=0} = 0, \tag{3.2b}$$

and

$$\begin{aligned} y(x,t)\big|_{x=0} &= 0, & y(x,t)\big|_{x=l} &= 0, \\ \tfrac{\partial^2}{\partial x^2}y(x,t)\Big|_{x=0} &= 0, & \tfrac{\partial^2}{\partial x^2}y(x,t)\Big|_{x=l} &= 0. \end{aligned} \tag{3.3}$$

Here $y(x,t)$ stands for the transversal deflection of the string, where x and t are the spatial and temporal coordinates, respectively. The arising material constants and coefficients along with their designations and units are summarized in table 3.1.. The derivation of the equation can be found in [5] for example.

Renaming the coefficients and the excitation in equation (3.1) in the same way as it can be found in [7], we can turn it into a simpler form:

$$S^4\frac{\partial^4}{\partial x^4}y(x,t) - c^2\frac{\partial^2}{\partial x^2}y(x,t) + \frac{\partial^2}{\partial t^2}y(x,t) + d_1\frac{\partial}{\partial t}y(x,t) + d_3\frac{\partial^3}{\partial t \partial x^2}y(x,t) = f(x,t), \tag{3.4}$$

where

$$S^4 = \tfrac{EI}{\rho A} \qquad c^2 = \tfrac{T_s}{\rho A} \qquad d_1 = \tfrac{d_1'}{\rho A} \qquad d_3 = \tfrac{d_3'}{\rho A} \qquad f(x,t) = \tfrac{1}{\rho A}f'(x,t). \tag{3.5}$$

Thus, the initial-boundary problem is given, we are before the first step of section 3.1, in the first box on figure 3.1 so far.

Table 3.1: *Physical constants and parameters of the differential equation.*

Symbols	Designations	Units
E	Young's modulus	$\frac{N}{m^2}$
I	Second moment of area	m^4
ρ	Density	$\frac{kg}{m^3}$
A	Cross-section area	m^2
T_s	Tension	N
d_1'	Frequency independent damping	$\frac{kg}{s\,m}$
d_3'	Frequency dependent damping	$\frac{kg\,m}{s}$

3.2.1 Laplace Transform

The first step is to apply the Laplace transformation to the governing equation (3.4). The Laplace transformation of a function of one variable is

$$\mathcal{L}\{y(t)\} = Y(s) = \int_0^\infty y(t)K_{\mathcal{L}}(t,s)\mathrm{d}t = \int_0^\infty y(t)e^{-st}\mathrm{d}t, \tag{3.6}$$

where $K_{\mathcal{L}}(t,s) = e^{-st}$ is the transformation kernel of the Laplace transformation. According to the differentiation theorem of the Laplace transformation, we can write for the derivatives of $y(t)$ the followings

$$\mathcal{L}\left\{\frac{\partial}{\partial t}y(t)\right\} = sY(s) - y(t)|_{t=0}\,, \tag{3.7a}$$

$$\mathcal{L}\left\{\frac{\partial^2}{\partial t^2}y(t)\right\} = s^2Y(s) - s\,y(t)|_{t=0} - \frac{\partial}{\partial t}y(t)\bigg|_{t=0}. \tag{3.7b}$$

In the case of our problem, however, accordingly to the initial conditions (3.2) the first term matters only. The first step of section 3.1 ends thus with

$$S^4\frac{\partial^4}{\partial x^4}Y(x,s) - c^2\frac{\partial^2}{\partial x^2}Y(x,s) + s^2Y(x,s) + d_1sY(x,s) + d_3s\frac{\partial^2}{\partial x^2}Y(x,s) = F(x,s), \tag{3.8}$$

where $Y(x,s) = \mathcal{L}\{y(x,t)\}$, and $F(x,s) = \mathcal{L}\{f(x,t)\}$. The boundary conditions are according to the linearity of the Laplace transform the followings

$$\begin{aligned} Y(x,s)\big|_{x=0} &= 0 & \qquad Y(x,s)\big|_{x=l} &= 0 \\ \tfrac{\partial^2}{\partial x^2}Y(x,s)\Big|_{x=0} &= 0 & \qquad \tfrac{\partial^2}{\partial x^2}Y(x,s)\Big|_{x=l} &= 0. \end{aligned} \tag{3.9}$$

Thus, we were able to eliminate the temporal derivatives and we arrived at the boundary value problem. We will remove the spatial derivatives in the next step.

3.2.2 Sturm–Liouville Transform

The Sturm-Liouville transformation can be universally written in the same form as the Laplace transformation, the transform of $Y(x,s)$ with respect to x is thus

$$\overline{Y}(n,s) = \mathcal{T}\left\{Y(x,s)\right\} = \int_0^l Y(x,s)K(n,x)\mathrm{d}x, \tag{3.10}$$

where n is the spatial frequency variable, while $K(n,x)$ is the transformation kernel of the SLT. Our aim is to determine the transformation kernel in such a way, that if we apply the SL transformation to equation (3.8), it turns the spatial derivatives into a multiplication by a function of the spatial frequency variable $\beta(n)$. We can write this requirement in a simple form by means of grouping the spatial derivatives into an operator

$$L_w\left\{Y(x,s)\right\} = S^4\frac{\partial^4}{\partial x^4}Y(x,s) + (d_3 s - c^2)\frac{\partial^2}{\partial x^2}Y(x,s). \tag{3.11}$$

Our aim is thus

$$\mathcal{T}\left\{L_w\left\{Y(x,s)\right\}\right\} = \beta(n)\overline{Y}(n,s). \tag{3.12}$$

If this is realized, equation (3.8) turns into the desired form

$$\beta(n)\overline{Y}(n,s) + s^2\overline{Y}(n,s) + d_1 s\overline{Y}(n,s) = \overline{F}(n,s), \tag{3.13}$$

where $\overline{F}(n,s) = \mathcal{T}\{F(x,s)\}$. For the sake of the upper requirement, we have to create the transformation kernel $K(n,x)$ adequately. Namely, two conditions have to be fulfilled, on the one hand

$$\mathcal{T}\left\{L_w\left\{Y\right\}\right\} = \int_0^l L_w\left\{Y\right\}K\mathrm{d}x = \int_0^l Y\tilde{L}_w\left\{K\right\}\mathrm{d}x, \tag{3.14}$$

on the other hand

$$\tilde{L}_w\left\{K\right\} = \beta(n)K. \tag{3.15}$$

In this case we get for the Sturm–Liouville transform of $L_w\left\{Y\right\}$ that

$$\mathcal{T}\left\{L_w\left\{Y\right\}\right\} = \int_0^l Y\tilde{L}_w\left\{K\right\}\mathrm{d}x = \int_0^l Y\beta(n)K\mathrm{d}x = \beta(n)\int_0^l YK\mathrm{d}x = \beta(n)\mathcal{T}\left\{Y\right\}. \tag{3.16}$$

The first condition is fulfilled automatically if the operator $\tilde{L}_w$ is the adjoint of L_w[1]. The second condition is an eigenvalue problem concerning the operator $\tilde{L}_w$.
Thus we have to determine the adjoint of L_w at first, than the eigenfunctions of this adjoint operator have to be found. These are the transformation kernels. The eigenvalues $\beta(n)$ corresponding to the eigenvectors are the factors, by which the transformed function $\overline{Y}(n,s)$ has to be multiplied to give $\mathcal{T}\left\{L_w\left\{Y\right\}\right\}$.

In the case of the string the adjoint operator can be determined analytically, integration by parts has to be employed practically as we have seen in section 2.1.1.2. The deduction

[1] This is the reason for the designation.

can be found in in [7], herein we give the solution only. The adjoint operator is

$$\tilde{L}_w \{K(n,x)\} = S^4 \frac{\partial^4}{\partial x^4} K(n,x) + (d_3 s - c^2) \frac{\partial^2}{\partial x^2} K(n,x), \tag{3.17}$$

while the adjoint boundary conditions are

$$\begin{aligned} K(n,x)\big|_{x=0} &= 0, & K(n,x)\big|_{x=l} &= 0, \\ \tfrac{\partial^2}{\partial x^2} K(n,x)\Big|_{x=0} &= 0, & \tfrac{\partial^2}{\partial x^2} K(n,x)\Big|_{x=l} &= 0. \end{aligned} \tag{3.18}$$

These agree with the operator L_w and the boundary conditions belonging to it, that means that the operator with the given boundary conditions is self-adjoint[2].

Now we can determine the transformation kernels $K(n,x)$, which are the solution of the eigenvalue problem (3.15) with boundary conditions (3.18). Since this is an ordinary eigenvalue problem, but the exact process depends on the operator and the boundary conditions, we transmit the result only[3]. The eigenfunctions are thus

$$K(n,x) = \sin\left(n\pi \frac{x}{l}\right), \tag{3.19}$$

while the eigenvalues are functions of the physical parameters as follows

$$\beta(n,s) = S^4 \left(\frac{n\pi}{l}\right)^4 - \left(s d_3 - c^2\right) \left(\frac{n\pi}{l}\right)^2. \tag{3.20}$$

We have thus the exact form of the Sturm-Liouville transformation, which is defined, in the case of the string, by (3.10), (3.19) and (3.20), respectively.

Note, that we could choose β, or $n\pi/l$ too as spatial frequency variable, as these and n are mutually expressible with each other. Choosing either of the alternatives, it is clear, that the spatial frequency variable has not a continuous codomain. Taken n, the codomain is the set of positive integers. The transformation kernel $K(n,x)$ and the transform $\overline{Y}(n,s)$ are thus in fact two sets of functions, that is $(K(1,x), K(2,x), \ldots)$ and $\left(\overline{Y}(1,x), \overline{Y}(2,x), \ldots\right)$ respectively. Accordingly, the inverse Sturm–Liouville transformation will be a function series expansion.

After the Laplace transformation the Sturm-Liouville transformation has been applied too, we are thus in the third box of figure 3.1, after the second step. Equation (3.13) is the desired algebraic equation.

[2]Note that if one would lay down homogeneous conditions on Y' and Y'', the adjoint boundary conditions would concern K and $K^(3)$ and the operator L_w would not be self-adjoint.

[3]The solutions for the string with supported ends, the bar with free ends and the membrane with various types of boundary conditions can be studied for example in [7].

3.2.3 Rearranging the algebraic equation

The algebraic equation (3.13) can be easily rearranged into the form of a multidimensional transfer function concerning $\overline{F}(n,s)$:

$$\bar{G}(n,s) = \frac{1}{\bar{P}(n,s)} = \frac{\bar{Y}(n,s)}{\bar{F}(n,s)} = \frac{1}{s^2 + d_1 s + \beta(n,s)}, \tag{3.21}$$

which agrees the third step, and we arrived at the fourth box on figure 3.1.

It is apparent, that function (3.21) describes a second order, continuous-time system for each value of n. Let's express the denominator by means of the poles

$$\bar{P}(n,s) = s^2 + d_1 s + \beta(n,s) = (s - s_n)(s - s_n^*). \tag{3.22}$$

Seeking the poles in the form of

$$s_n = \sigma(n) + j\omega(n), \tag{3.23}$$

and taking into account equation (3.20) too, we get the imaginary and real parts of the poles as

$$\begin{aligned} \sigma(n) &= \frac{1}{2}\left(d_3\left(\frac{n\pi}{l}\right)^2 - d_1\right) \\ \omega(n) &= \sqrt{S^4\left(\frac{n\pi}{l}\right)^4 + c^2\left(\frac{n\pi}{l}\right)^2 - \sigma(n)^2}. \end{aligned} \tag{3.24a}$$

The poles are thus functions of the physical properties and determine the transfer function (3.21) at the same time.

3.2.4 Impulse-invariant Transform

According to section 3.1 we have to turn the continuous-time system, described by (3.21) into a discrete-time system. Since this equation describes a second order continuous-time system for each value of n, our object is, to turn these systems into a discrete one, with n as a parameter. Two well known methods for this purpose are the bilinear and the impulse-invariant transformations. The former is capable to transform the transfer functions without any aliasing effects, but now, we are able to control the bandwidth by means of the number of the used second order filters, i.e. the modes. Thus, using the more complicated bilinear transformation has no benefits in this case.

Accordingly, the impulse-invariant transformation will be used. Let decompose, thus, the transfer function into partial fractions, which gives

$$\bar{G}(n,s) = \frac{1}{s^2 + d_1 s + \beta(n)} = \frac{1}{(s - s_n)(s - s_n^*)} = \frac{\frac{1}{s_n - s_n^*}}{s - s_n} + \frac{\frac{1}{s_n^* - s_n}}{s - s_n^*}, \tag{3.25}$$

the discrete-time transfer function is on the grounds of rules of the impulse-invariant trans-

formation

$$\bar{G}^d(n,z) = \frac{\frac{1}{s_n - s_n^*}}{1 - e^{s_n T} z^{-1}} + \frac{\frac{1}{s_n^* - s_n}}{1 - e^{s_n^* T} z^{-1}}, \tag{3.26}$$

where T is the discrete time-step and z the discrete complex frequency, d in the exponent refers to discrete functions. Our result takes shape after some calculation, in accordance with the deconvolution (3.23), as

$$\bar{G}^d(n,z) = \frac{1}{\omega(n)} \frac{e^{\sigma(n)T} \sin(\omega(n)T) z}{z^2 - 2e^{\sigma(n)T} \cos(\omega(n)T) z + e^{2\sigma(n)T}}. \tag{3.27}$$

We realized the fourth step, the fifth transformation will be the inverse Sturm-Liouville transformation.

Note, that we treated the spatial frequency variable n as a parameter in this section, discretization was made only on the temporal variable. The discrete-time multidimensional transfer function is thus the function of the continuous-spatial and the discrete-time frequency variable, respectively.

3.2.5 Inverse Sturm-Liouville Transform

According to (3.27) we can write $\overline{Y}^d(n,z)$ as followings

$$\overline{Y}^d(n,z) = \overline{G}^d(n,z)\overline{F}^d(n,z). \tag{3.28}$$

As it was mentioned in section 3.2.2, the inverse Sturm-Liouville transformation gives the original function, in the case of self-adjoint spatial differential operators, in terms of an orthogonal series expansion, thus

$$Y^d(x,z) = \mathcal{T}^{-1}\left\{\overline{Y}^d(n,z)\right\} = \sum_n \frac{1}{N(n)} \overline{Y}^d(n,z) K(n,x), \tag{3.29}$$

where

$$N(n) = \int_0^l (K(n,x))^2 \, \mathrm{d}x. \tag{3.30}$$

Note, that in the case of non self-adjoint operators the inverse SL transformation differs from the above expression, we will pan out about this in section 3.3. We can write thus on the grounds of the equations (3.28) and (3.29)

$$Y^d(x,z) = \mathcal{T}^{-1}\left\{\overline{Y}^d(n,z)\right\} = \sum_n \frac{1}{N(n)} \overline{G}^d(n,z)\overline{F}^d(n,z) K(n,x). \tag{3.31}$$

After substituting the discrete multidimensional transfer function (3.27) we get

$$Y^d(x,z) = \sum_n \frac{1}{N(n)} \frac{e^{\sigma(n)T}}{\omega(n)} \sin(\omega(n)T) \frac{z}{z^2 - 2e^{\sigma(n)T} \cos(\omega(n)T) z + e^{2\sigma(n)T}} \overline{F}^d(n,z) K(n,x). \tag{3.32}$$

It is practical to restrict the set of the possible $f(x,t)$ excitation functions to the form

$$f(x,t) = f_x(x)f_t(t). \tag{3.33}$$

Thus we suppose, that the spatial distribution of the excitation does not alter with time and the excitation can be separated into a product of a space and a time dependent function. This seems to be fair in the case of the struck or plucked string. With this assumption we have

$$\begin{aligned} F(x,s) &= f_x(x)F_t(s), \\ \overline{F}(n,s) &= \bar{f}_x(n)F_t(s), \\ \overline{F}^d(n,z) &= \bar{f}_x(n)F_t^d(z). \end{aligned} \tag{3.34}$$

Introducing some notations for the sake of simplicity

$$a(n,x) = \frac{1}{N(n)} \frac{e^{\sigma(n)T}\sin(\omega(n)T)}{\omega(n)} \bar{f}_x(n)K(n,x), \tag{3.35a}$$

$$H^d(z) = \frac{z}{z^2 - 2e^{\sigma(n)T}\cos(\omega(n)T)z + e^{2\sigma(n)T}}, \tag{3.35b}$$

whereby the z-transform of the sought function can be written as

$$Y^d(x,z) = \sum_n a(n,x)H^d(z)F_t^d(z). \tag{3.36}$$

It is clearly visible the possibility of realization by means of a parallel filter bank from this form. The transfer function of the filters are $H^d(z)$, the outputs are weighted with $a(n,x)$, and the input signal of each filter is the $f_t[k]$ excitation function.

Let us label the output of the certain filters as followings

$$\hat{Y}^d(n,z) = H^d(z)F_t^d(z) = \frac{z}{z^2 - 2e^{\sigma(n)T}\cos(\omega(n)T)z + e^{2\sigma(n)T}} F_t^d(z). \tag{3.37}$$

from here, by the help of rearranging

$$\hat{Y}^d(n,z)z^2 = 2e^{\sigma(n)T}\cos(\omega(n)T)\hat{Y}^d(n,z)z - e^{2\sigma(n)T}\hat{Y}^d(n,z) + F_t^d(z)z, \tag{3.38}$$

thus, with the notation

$$c_1 = 2e^{\sigma(n)T}\cos(\omega(n)T), \tag{3.39a}$$

$$c_2 = -e^{2\sigma(n)T} \tag{3.39b}$$

we get

$$\hat{Y}^d(n,z) = c_1\hat{Y}^d(n,z)z^{-1} + c_2\hat{Y}^d(n,z)z^{-2} + F_t^d(z)z^{-1}. \tag{3.40}$$

By the help of this expression we are able to sketch the structure of the filter bank, see figure 3.2. We do not need to perform the inverse z-transformation, we will do it for the

sake of completeness, however.

3.2.6 Inverse Z-transform

According to equations (3.36), (3.37), and the linearity of the z-transformation, we can write

$$y^d(x,k) = \sum_n a(n,x)\hat{y}^d(n,k), \tag{3.41}$$

where $\hat{y}^d(n,k)$ is the inverse z-transform of $\hat{Y}^d(n,z)$, and on the grounds of equation (3.40)

$$\hat{y}^d(n,k) = \mathcal{Z}^{-1}\left\{\hat{Y}^d(n,z)\right\} = c_1\hat{y}^d(n,k-1) + c_2\hat{y}^d(n,k-2) + f_t^d(k-1), \tag{3.42}$$

in accordance with the time shifting property of the Z-transformation

$$\mathcal{Z}\left\{x(k-\kappa)\right\} = z^{-\kappa}X(z). \tag{3.43}$$

Our result is thus the following

$$y^d(x,k) = \sum_{n=1} a(n,x)\left[c_1\hat{y}^d(n,k-1) + c_2\hat{y}^d(n,k-2) + f_t^d(k-1)\right]. \tag{3.44}$$

We obtained the discrete-time description of the model. This is a parallel filter bank (see figure 3.2), which is easily and effectively implementable in real-time applications. Each filter corresponds to a mode of the vibration, and the parameters are given according (3.39), (3.24), (3.20), and (3.5) directly by means of the physical parameters.

As we mentioned previously in section 3.2.4, the bandwidth of the model is controllable by of the number of modes (n_{max}). Let us, thus choose n_{max} as follows

$$\begin{aligned} \omega(n_{max}) &\leq 2\pi f_s/2 \\ \omega(n_{max}+1) &> 2\pi f_s/2 \end{aligned} \tag{3.45a}$$

where $f_s = 1/T$ is the sampling frequency. Depending on the computational capacity we can choose n_{max} smaller of course. Thus, our result is more precisely

$$y^d(x,k) = \sum_{n}^{n_{max}} a(n,x)\left[c_1\hat{y}^d(n,k-1) + c_2\hat{y}^d(n,k-2) + f_t^d(k-1)\right]. \tag{3.46}$$

The number of parallel filters is thus n_{max} and they span a predefined frequency range.

3.3 Extension to Non Self-adjoint Problems

This section provides an extension of the previously introduced method to non self-adjoint problems. Only those steps which differ from the self-adjoint case are introduced. A more detailed description can be found in [12].

We have seen in section 3.2.2, that we had to solve the Sturm–Liouville eigenvalue

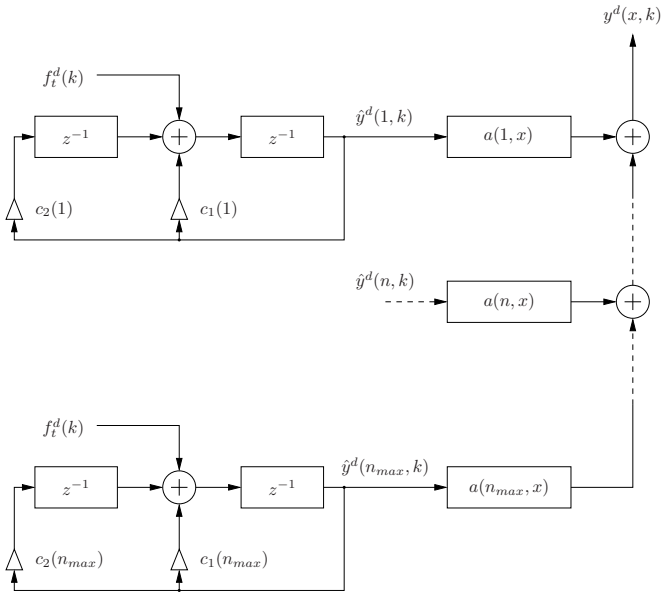

Figure 3.2: *The synthesis algorithm as a parallel filter bank.*

problem (3.15) of the adjoint operator given by (3.14) to be able to remove the spatial differential operator. In the case of the string the operator L_w was self-adjoint, so the inverse Sturm–Liouville transformation was given by means of a series expansion with the $K(n,x)$ functions. In the case of non self-adjoint operators, however the eigenvectors of $\tilde{L}_w$ do not form an orthogonal system, and thus can not be used as the basis of the expansion.

In this cases the eigenfunctions of the original operator L_w, thus the solutions of equation

$$L_w\left\{J(n,x)\right\} = \beta(n)J(n,x) \tag{3.47}$$

has to be determined too. This, and equation (3.15) are the adjoint boundary value problems of each other. It can be shown, that their eigenvalues are the same, and the eigenvectors form a biorthogonal system, thus

$$\langle J(n,x), K(m,x)\rangle = \int J(n,x)K(m,x)\mathrm{d}x = 0 \quad \text{ha} \quad (n \neq m). \tag{3.48}$$

We demonstrate that function $Y^d(x,z)$ has to be expressed by means of a series expansion of $J(n,x)$, thus we seek the function in the form

$$Y^d(x,z) = \sum_n a_n J(n,x). \tag{3.49}$$

Multiplying this equation by $K(m,x)$ and integrating over the entire domain we get, according to the biorthogonal property of functions J and K, one and only not zero term on the right side. Namely the term in which $n = m$, that is

$$\int Y^d(x,z)K(m,x)\mathrm{d}x = a_m \int J(m,x)K(m,x)\mathrm{d}x. \tag{3.50}$$

The coefficients a_m are thus, after introducing the designation $N_m = \langle J(m,x), K(m,x)\rangle$, expressible by means of the transform $\overline{Y}^d(m,z)$:

$$a_m = \frac{\int Y^d(x,z)K(m,x)\mathrm{d}x}{N_m} = \frac{\overline{Y}^d(m,z)}{N_m}. \tag{3.51}$$

The sought function $Y^d(x,z)$ is thus given by the sum

$$Y^d(x,z) = \sum_n \frac{\overline{Y}^d(n,z)}{N_n} J(n,x). \tag{3.52}$$

This is the inverse Sturm–Liouville transformation in the non self-adjoint case.

Accordingly, we have to solve two eigenvalue problems. We use the eigenfunctions of the adjoint problem in the SL transformation, but the eigenfunctions of the original operator form the basis of the series expansion in the inverse SL transformation.

3.4 Summary

We managed to convert the governing differential equation of the string into a parallel filter bank structure. The process is similar for the rod, the membrane, the plate or the cylindrical shell. The steps are the same, the difference lies in the values of $\sigma(n)$ and $\omega(n)$ and the shape of the transformation kernels K and J. Thus it is sufficient to determine these quantities and to modify the parameters of the filter bank accordingly. Either a new instrument is investigated or the underlying governing equation is refined, the parallel filter bank remains.

The eigenvalue problem (3.47) of the transformation kernel J is actually the equation solved after separation of variables in the well-known process of solving differential equations. Thus functions $J(n,x)$ describe the form of the modes. The inverse Sturm–Liouville transformation expresses the sought function by means of these mode shape functions. Thus our model can be considered as the superposition of the time-varying mode shape functions.

Since no spatial discretization has been done, we can choose an arbitrary point of the domain of definition, in which we want to calculate the sought function. We can assume an excitation with arbitrary spatial distribution too. Only the weighting factor $a(n,x)$ has to be calculated accordingly.

According to the parallel filter structure this model suggests the additive synthesis with the significant difference that the coefficients of the filters are not obtained from the study of the voice but from physical parameters. The functional transformation method combines thus the benefits of the physical and additive modeling. Namely the voice is controlled by the physical properties but the computational demand is commensurable to the one of additive models and can be run efficiently on DSP-s according to the filter structure. This has of course a price, the amount of the preliminary computation. In the case of the finite difference method the difference equation is solved directly, the computational

demand is high, but we are able to solve easily nonlinear equations too. In the case of the digital waveguide we use d'Alambert's solution which reduces the computational demand drastically, but it is hard to apply the method on dispersive systems for example. In the case of the functional transformation method we arrive at the most simple parallel filter structure at the expense of the most preliminary computation.

Chapter 4

Finite Difference Method

We introduce the finite difference method in this section, that is the way how one can turn the differential equations into a recurrence equation, which we mentioned in section 1.2.3. This is one of the simplest methods to solve a differential equation numerically. It could be used to implement the investigated differential equations directly, but as we mentioned this is a relatively computation costly method, thus it is not worthy to use it in real-time applications for the present. We will use it to compute the transformation kernels of the functional transformation method. This do not need to be calculated in real-time as long as we do not want to alter the parameters of the instrument during the usage.

4.1 Derivation of the Recurrence Equation

We set out from the definition of the derivative and since it does not presents difficulty, we start with the two-dimensional case.

4.1.1 The Difference Quotients

The partial derivative of a function of two variables with respect to one of the variables is defined as the ordinary derivative with respect to the variable in question[1]. That is the partial derivative of $v(x_1, x_2)$ with respect to x_1 is

$$\frac{\partial v(x_1, x_2)}{\partial x_1} = \lim_{\Delta x_1 \to 0} \frac{v(x_1 + \Delta x_1, x_2) - v(x_1, x_2)}{\Delta x_1}. \tag{4.1}$$

In the case of the finite difference method we determine the sought function (the transversal deflection for example) in certain predefined points of the domain of definition (the plate or shell) only. In the simplest case these points are defined by means of an equidistant partition in both directions, in this way the points form an equidistant grid (see figure 4.2), and the difference quotients are expressible by means of simple formulas. We will see in section 7.2 that sometimes the geometry prevents this kind of division, in such cases the

[1] See [2] for example.

formulas get elaborate. Let thus the partition in both directions be

$$x_{1min} \leq x_1 \leq x_{1max} \quad \Rightarrow \quad x_{1min} = x_{11}, x_{12}, \ldots, x_{1n} = x_{1max}, \tag{4.2a}$$

$$x_{2min} \leq x_2 \leq x_{2max} \quad \Rightarrow \quad x_{2min} = x_{21}, x_{22}, \ldots, x_{2m} = x_{2max}. \tag{4.2b}$$

With this partition, the number of points is nm, while the step-size in directions x_1 and x_2 are $\Delta x_1 = (x_{1max} - x_{1min})/(n-1)$ and $\Delta x_2 = (x_{2max} - x_{2min})/(m-1)$ respectively. Let us introduce a simplifying designation as well, let the values of $v(x_1, x_2)$ in the above defined points be

$$v(x_{1i}, x_{2j}) \equiv v_{i,j}. \tag{4.3}$$

Since the function is given in predefined points only, we are not able to determine the limit in the formula (4.1) of the derivative, and we have to use approximation. One possibility is the so-called *forward difference*

$$\left.\frac{\partial v(x_1, x_2)}{\partial x_1}\right|_{(x_{1i}, x_{2j})} \cong \frac{v_{i+1,j} - v_{i,j}}{\Delta x_1} \equiv \frac{\Delta_1 v}{\Delta x_1}, \tag{4.4}$$

where, adopted the customary designation, Δ_i stands for the finite difference in the numerator. The subscript indicates the variable, according to which the difference have to be taken. The so-called *backward* and *central* differences are in use too, which are the followings

$$\begin{aligned} \frac{\nabla_1 v}{\Delta x_1} &\equiv \frac{v_{i,j} - v_{i-1,j}}{\Delta x_1}, \\ \frac{\delta_1 v}{2\Delta x_1} &\equiv \frac{v_{i+1,j} - v_{i-1,j}}{2\Delta x_1}. \end{aligned} \tag{4.5}$$

4.1.2 The Error of Difference Quotients

We can estimate the errors of the various difference quotients by the help of the Taylors series. Let us see the central difference for example. Applying the Taylor expansion on function $v(x_1, x_2)$, we can write

$$\begin{aligned} v_{i+1,j} = v_{i,j} &+ \left(\left.\frac{\partial v}{\partial x_1}\right|_{(x_{1i}, x_{2j})} \Delta x_1 \right) + \left(\frac{1}{2!} \left.\frac{\partial^2 v}{\partial x_1^2}\right|_{(x_{1i}, x_{2j})} {\Delta x_1}^2 \right) + \\ &+ \left(\frac{1}{3!} \left.\frac{\partial^3 v}{\partial x_1^3}\right|_{(x_{1i} + \Theta_a \Delta x_1, x_{2j})} {\Delta x_1}^3 \right), \\ v_{i-1,j} = v_{i,j} &- \left(\left.\frac{\partial v}{\partial x_1}\right|_{(x_{1i}, x_{2j})} \Delta x_1 \right) + \left(\frac{1}{2!} \left.\frac{\partial^2 v}{\partial x_1^2}\right|_{(x_{1i}, x_{2j})} {\Delta x_1}^2 \right) - \\ &- \left(\frac{1}{3!} \left.\frac{\partial^3 v}{\partial x_1^3}\right|_{(x_{1i} - \Theta_b \Delta x_1, x_{2j})} {\Delta x_1}^3 \right), \end{aligned} \tag{4.6}$$

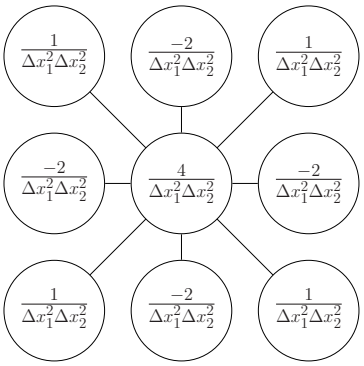

Figure 4.1: *The stencil of the differential operator* $L\{.\} = \frac{\partial^4}{\partial x_1^2 \partial x_2^2}$

where $(0 < \Theta_a, \Theta_b < 1)$, and we get for the difference quotient that

$$\frac{\delta_1 v}{2\Delta x_1} = \left.\frac{\partial v}{\partial x_1}\right|_{(x_{1i}, x_{2j})} + \frac{1}{3!} \left.\frac{\partial^3 v}{\partial x_1^3}\right|_{(x_{1i}+\Theta_a \Delta x_1, x_{2j})} \frac{{\Delta x_1}^2}{2} + \frac{1}{3!} \left.\frac{\partial^3 v}{\partial x_1^3}\right|_{(x_{1i}-\Theta_b \Delta x_1, x_{2j})} \frac{{\Delta x_1}^2}{2} = \left.\frac{\partial v}{\partial x_1}\right|_{(x_{1i}, x_{2j})} + O(\Delta x_1^2). \tag{4.7}$$

Thus if v is three times differentiable with respect to x_1, than the discretization error is proportional to the square of spacing Δx_1. It can be shown in the same way, that the error of the forward and backward differences is proportional to the step-size.

4.1.3 Higher-order Difference Quotients

Since the higher order derivatives are defined as the derivatives of the lower ones, the higher order difference quotients can be derived from the first order quotient. We can get the second order central difference quotient with respect to x_2 in the following manner[2]

$$\frac{\partial^2 v}{\partial x_2^2} \cong \Delta_2(\nabla_2 v_{i,j}) = \nabla_2(\Delta_2 v_{i,j}) = \frac{v_{i,j+1} - 2v_{i,j} + v_{i,j-1}}{\Delta x_2^2}. \tag{4.8}$$

It can be shown that this approximation has an error of order of $\Delta^2 x_2$.

We can establish the higher order and mixed difference quotients with the same technique. The finite difference quotients approximating the third and fourth order and the

[2]See in [19] for example.

twice second order mixed derivatives are the followings:

$$\begin{aligned}
\frac{\partial^3 v}{\partial x_1^3} &\cong \frac{v_{i+2,j} - 2v_{i+1,j} + 2v_{i-1,j} - v_{i-2,j}}{2\Delta x_1^3}, \\
\frac{\partial^4 v}{\partial x_1^4} &\cong \frac{v_{i+2,j} - 4v_{i+1,j} + 6v_{i,j} - 4v_{i-1,j} + v_{i-2,j}}{\Delta x_1^4}, \\
\frac{\partial^4 v}{\partial x_1^2 \partial x_2^2} &\cong \frac{v_{i+1,j+1} - 2v_{i,j+1} + v_{i-1,j+1} - 2v_{i+1,j} + 4v_{i,j} - 2v_{i-1,j}}{\Delta x_1^2 \Delta x_2^2} \\
&\quad + \frac{v_{i+1,j-1} - 2v_{i,j-1} + v_{i-1,j-1}}{\Delta x_1^2 \Delta x_2^2}.
\end{aligned} \tag{4.9}$$

The finite differences determine which adjacent function values with what weight have to be taken in the approximation of the given derivative at the given point. These data can be illustrated by the help of the so-called *stencil*. In the case of the upper mixed finite difference the stencil is illustrated in figure 4.1.

4.1.4 The Differential Operator as a Matrix

Consider a differential equation in operator form

$$D\{v\} = f. \tag{4.10}$$

Since the function is sought in points given by (4.2) only, it is worthwhile to apply the designation (4.3) to function f too. For the sake of the matrix form we have to modify our designation further, however. Let us construct two one-dimensional arrays from the values of $v_{i,j}$ and $f_{i,j}$ as follows: let form the function values at points $x_1 = x_{11}, x_{12}, \ldots, x_{1n}, x_2 = x_{21}$ the first n element of the arrays. Let the function values at $x_1 = x_{11}, x_{12}, \ldots, x_{1n}, x_2 = x_{22}$ form the next n element, and so on. In this case the one-dimensional arrays are

$$\mathbf{v} = [v_{1,1}, v_{2,1}, v_{3,1}, \ldots, v_{n,1}\ ,\ v_{1,2}, \ldots, v_{n,2}\ ,\ v_{1,3},\ \ldots\ ,\ v_{1,m}, v_{2,m}, \ldots, v_{n,m}]^T\ , \tag{4.11a}$$

$$\mathbf{f} = [f_{1,1}, f_{2,1}, f_{3,1}, \ldots, f_{n,1}\ ,\ f_{1,2}, \ldots, f_{n,2}\ ,\ f_{1,3},\ \ldots\ ,\ f_{1,m}, f_{2,m}, \ldots, f_{n,m}]^T\ , \tag{4.11b}$$

where $\mathbf{v}^T$ stands for the transpose of $\mathbf{v}$. This designation corresponds to a numbering of the points (see figure 4.2).

Let us suppose as an example, that the differential equation (4.10) stands for

$$\frac{\partial^2 v}{\partial x_1^2} + \frac{\partial^2 v}{\partial x_2^2} = f. \tag{4.12}$$

The finite difference approximation of this equation in point (x_{1i}, x_{2j}) is

$$\frac{v_{i+1,j} - 2v_{i,j} + v_{i-1,j}}{\Delta x_1^2} + \frac{v_{i,j+1} - 2v_{i,j} + v_{i,j-1}}{\Delta x_2^2} = f_{i,j}, \tag{4.13}$$

or switching over to our new notation (4.11) and entering the designation $S_1 = 1/\Delta x_1^2$ and $S_2 = 1/\Delta x_2^2$, we can say that the $i + (j-1)n$-th element of $\mathbf{f}$ depends on the following

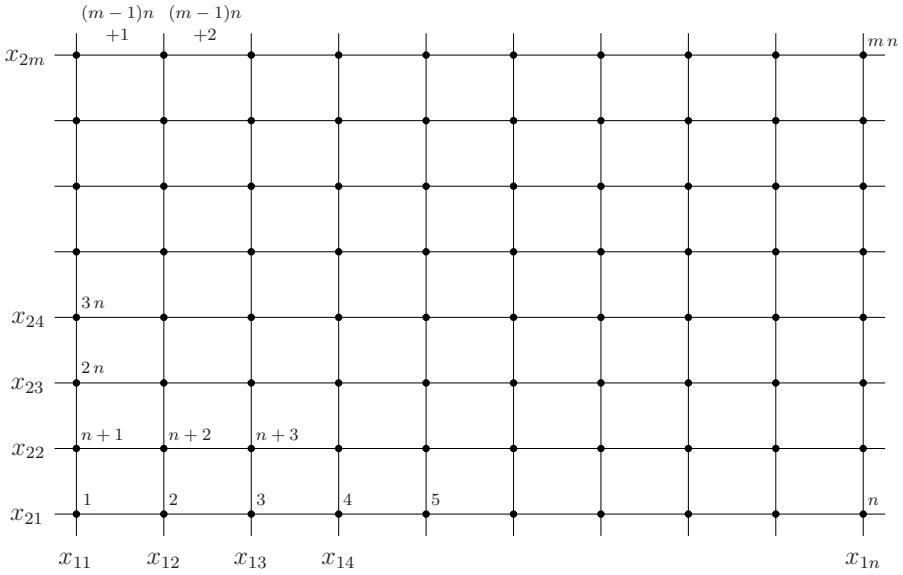

Figure 4.2: *The serial numbers of the points of domain of definition.*

elements of $\mathbf{v}$

$$\begin{aligned} &S_1 v_{i+1+(j-1)n} - 2S_1 v_{i+(j-1)n} + S_1 v_{i-1+(j-1)n} + \\ &+S_2 v_{i+jn} - 2S_2 v_{i+(j-1)n} + S_2 v_{i+(j-2)n} = f_{i+(j-1)n}. \end{aligned} \tag{4.14}$$

This linear combination is, of course, expressible by means of a matrix too

$$\mathbf{D}\mathbf{v} = \mathbf{f}, \tag{4.15}$$

where the quadratic block matrix $\mathbf{D}$ of size $(nm \times nm)$ has the following form in this case

$$\mathbf{D} = \begin{pmatrix} \mathbf{B} & S_2\mathbf{I} & 0 & 0 & \cdots & 0 & 0 & 0 \\ S_2\mathbf{I} & \mathbf{B} & S_2\mathbf{I} & 0 & & 0 & 0 & 0 \\ 0 & S_2\mathbf{I} & \mathbf{B} & S_2\mathbf{I} & & 0 & 0 & 0 \\ 0 & 0 & S_2\mathbf{I} & \mathbf{B} & & 0 & 0 & 0 \\ \vdots & & & & \ddots & & & \\ 0 & 0 & 0 & 0 & & \mathbf{B} & S_2\mathbf{I} & 0 \\ 0 & 0 & 0 & 0 & & S_2\mathbf{I} & \mathbf{B} & S_2\mathbf{I} \\ 0 & 0 & 0 & 0 & & 0 & S_2\mathbf{I} & \mathbf{B} \end{pmatrix}. \tag{4.16}$$

Herein matrix $\mathbf{I}$ is the unit matrix of size $(n \times n)$, while $\mathbf{B}$ is a quadratic matrix of the

same size, which is

$$\mathbf{B} = \begin{pmatrix} -2(S_1+S_2) & S_1 & 0 & \cdots & 0 & 0 \\ S_1 & -2(S_1+S_2) & S_1 & & 0 & 0 \\ 0 & S_1 & -2(S_1+S_2) & & 0 & 0 \\ \vdots & & & \ddots & & \\ 0 & 0 & 0 & & -2(S_1+S_2) & S_1 \\ 0 & 0 & 0 & & S_1 & -2(S_1+S_2) \end{pmatrix}. \tag{4.17}$$

Thus we managed to convert the differential equation (4.12) into the matrix representation (4.15) by the help of the finite different method. It is apparent that we get the differential equation back when $\Delta x_1 \to 0$ and $\Delta x_2 \to 0$, but the size of matrix $\mathbf{D}$ and vectors $\mathbf{v}$ and $\mathbf{f}$ become infinite. We referred to this matrix – differential operator connection in section 2.1.1.2, as we defined the adjoint differential operator.

One can construct the matrix $\mathbf{D}$ corresponding to any differential operator in the same way. We will use this version of the finite difference method to solve the Sturm–Liouville eigenvalue-problems arising in the functional transformation method.

As we mentioned in section 2.1.1.2, the differential operator gives not a complete description about a system, we need boundary conditions too.

4.1.5 Boundary Conditions

The upper derived matrix $\mathbf{D}$ gives a correct description about the differential operator in those points only, where all those points exist which are necessary for the approximation of the operator in the point in question. In the case of the upper example, matrix $\mathbf{D}$ sees four adjacent points on the edges and three adjacent points in the corners only, thus $\mathbf{D}$ is not enough to determine the functional value in this points.

The conditions on the sought function and its derivatives prescribed by the boundary conditions can be described by the help of finite difference approximations also. Let the boundary conditions corresponding to the operator, defined by equation (4.12), be the followings for example

$$\left.\frac{\partial^2 v}{\partial x_1^2}\right|_{(x_{1min},x_2)} = 0, \tag{4.18a}$$

$$\left.\frac{\partial v}{\partial x_1}\right|_{(x_{1max},x_2)} = 0, \tag{4.18b}$$

$$\left.\frac{\partial^2 v}{\partial x_2^2}\right|_{(x_1,x_{2min})} = 0, \tag{4.18c}$$

$$\left.\frac{\partial v}{\partial x_2}\right|_{(x_1,x_{2max})} = 0. \tag{4.18d}$$

We have at least two different possibility to take the boundary conditions into consideration.

Virtual Points One possible solution is to consider *virtual points* outside the domain of the operator. With the help of these the finite difference operator can be expressed in the same form on the edges too. In this case these points are defined by the coordinates

$$(x_{10}, x_{2i}), \tag{4.19a}$$
$$(x_{1(n+1)}, x_{2i}), \tag{4.19b}$$
$$(x_{1i}, x_{20}), \tag{4.19c}$$
$$(x_{1i}, x_{2(m+1)}) \tag{4.19d}$$

beyond the edges

$$(x_1, x_2) = (x_{1min}, x_2), \tag{4.20a}$$
$$(x_1, x_2) = (x_{1max}, x_2), \tag{4.20b}$$
$$(x_1, x_2) = (x_1, x_{2min}), \tag{4.20c}$$
$$(x_1, x_2) = (x_1, x_{2max}) \tag{4.20d}$$

In these points the values of $v_{i,j}$ are expressed by means of the finite different approximations of the boundary conditions. In our example the following algebraic equations can be derived from the boundary conditions (4.18):

$$\frac{v_{0,j} - 2v_{1,j} + v_{2,j}}{\Delta x_1^2} = 0, \tag{4.21a}$$
$$\frac{v_{n+1,j} - v_{n-1,j}}{2\Delta x_1} = 0, \tag{4.21b}$$
$$\frac{v_{i,0} - 2v_{i,1} + v_{i,2}}{\Delta x_2^2} = 0, \tag{4.21c}$$
$$\frac{v_{i,m+1} - v_{i,m-1}}{2\Delta x_2} = 0, \tag{4.21d}$$

where $(i = 1, 2, \ldots, n)$ and $(j = 1, 2, \ldots, m)$. Thus $v_{0,j}, v_{n+1,j}, v_{i,0}$ and $v_{i,m+1}$ are all expressible from values inside the domain of the operator. We can say according the first equation for example that $v_{0,j} = 2v_{1,j} - v_{2,j}$. Thus as we are evaluating the stencil corresponding to $\mathbf{D}$ in points $v_{1,j}$, and we need the S_1-fold of points $v_{0,j}$, we can take them into account as $S_1(2v_{1,j} - v_{2,j})$. Accordingly, the stencil suffers some distortion near by the edges. We can take into account other types of boundary conditions in the same way.

One-sided Differential Quotients In the case of the other method we are distorting the finite differences of the boundary conditions in such a way that they rely on values inside the domain of the operator only. In the upper example we have to use backward differences to approximate the boundary condition on edge $(x_1, x_2) = (x_{1max}, x_2)$ for example. Note that by the help of the Taylor series we are able to construct any non-symmetric finite difference quotient for the approximation of any derivative.

It can come up the question if the upper two methods leads to different result, that is

they result in different distortion of the stencil. Let us thus investigate the edge $(x_1, x_2) = (x_{1max}, x_2)$ of our example. According to the first method we get that along this edge $v_{n+1,j} = v_{n-1,j}$, thus $v_{n-1,j}$ has to be taken $2S_1$ times instead of S_1 times.
In the second case we get on the grounds of the backward difference that $v_{n,j} = v_{n-1,j}$. The difference operator has not to be considered on points (x_{1n}, x_{2j}), where the solution is determined by the upper equation. The difference operator is thus in point $(x_{1(n-1)}, x_{2j})$ $S_1(v_{n-2,j} - v_{n-1,j}) + S_2(v_{n-1,j+1} - 2v_{n-1,j} + v_{n-1,j-1}) = f_{n-1,j}$. It is apparent thus that the two methods result in different stencil.

4.2 The Eigenvalue Problem

We want to use the matrix representation of differential operators to solve the eigenvalue problem (3.15) arising in the functional transformation method. The eigenvalue problem of a differential operator can be expressed as

$$D\{v\} = \lambda_n v. \tag{4.22}$$

On the right side of equation (4.10) can thus be found not a given function f, but the multiple of v itself. Here do we profit by the matrix representation as we do not have to change anything in our upper train of thought. We have to simply write

$$\mathbf{Dv} = \lambda_n \mathbf{v} \tag{4.23}$$

where $\mathbf{D}$ can be determined as formerly. The difference is only, that we are seeking not the specific solution of the linear algebraic system of equations (4.15) in view of $\mathbf{f}$, but those vectors $\mathbf{v}$ and corresponding scalars λ_n which satisfy equation (4.23). This means the solution of an ordinary matrix eigenvalue-problem, for which long standing numerical methods exist[3], MatLab offers the functions `eig` and `eigs` for eigenvalue calculations (see [16]).

4.3 Non Self-adjoint Problem

We have introduced an analytical method for the derivation of the adjoint of a differential operator in section 2.1.1.2, but we mentioned that the finite different method can be used for this aim too. In our case this will be the more effective way, because with the matrix $\mathbf{D}$ corresponding the original operator in hands we can easily get the matrix corresponding to the adjoint operator as the adjoint of matrix $\mathbf{D}$ (see in [8]). On the grounds of this adjoint matrix we can determine the corresponding differential operator and boundary conditions, that is the adjoint operator. We do not need this last step, however, as the eigenvalue-problem of the adjoint operator will be solved by the help of the adjoint matrix itself.

Note that according to our experiences the matrix of the adjoint operator $\tilde{L}$ coincides

[3] See in [17] for example.

with the adjoint of matrix of the original operator L in certain simple cases, but by the more complex operators some difference occurs. We can not explain this symptom, but we assume, that we can use the adjoint matrix to determine the adjoint eigenfunctions in the case of small step-sizes.

Chapter 5

Plate Equations

In this section the derivation of the differential equations of plates is introduced. In section 5.1 the governing equation of transverse motion is derived following the steps suggested in Appendix 1.3. During the derivation variables are introduced, by the help of which the in-plane motion of the plate can be taken into account too. These are utilized in section 5.2, where the governing equations of in-plane motion of the plate are developed. These and the governing equation of the transverse motion form a coupled system of three differential equations.

5.1 Equation of the Transverse Motion

The well known plate equation of an isotropic plate with constant thickness is

$$D\,\nabla^4 w + \rho h \frac{\partial^2 w}{\partial t^2} = q, \tag{5.1}$$

where $w(x_1, x_2, t)$ is the transverse deflection, D the bending rigidity, ρ the mass density, h the thickness of the plate and q the distributed excitation (force per unit area) applied to the plate, respectively. This equation describes the transverse motion of the plate, and gives no guidance regarding the influence of the in-plane stresses.

In this section a more elaborate governing equation will be derived. We will assume the material of the plate being orthotropic[1] with coordinate axes being the axes of symmetry. The in-plane tension will be taken into account too, which will give rise to take curvatures into account in section 6.

The simplifications will be carried out on the grounds of [9], however, the steps will be arranged according to section 1.3. The notation introduced in Appendix F.1 will be used, which differs slightly from the one used in [9].

Let us consider the neutral surface of the plate, which lies in the case of an orthotropic plate of constant thickness midway through the thickness. We suppose that the lines initially perpendicular to the neutral surface remain straight and perpendicular during the motion. Accordingly, the transversal motion of the plate is completely described by the

[1] See Appendix F.1.6.

transversal motion of the neutral surface. Let us denote the transversal deflection by $w(x_1, x_2)$, where the plane x_1-x_2 is the plane of the plate. Our aim is to derive a governing differential equation for $w(x_1, x_2)$ which can be solved according the excitation and initial and boundary conditions, respectively.

The excitation is the force per unit area acting on the plate and will be denoted by $q(x_1, x_2, t)$.

Let us follow the steps proposed in section 1.3.

5.1.1 Kinematics (strain – displacement relation)

Sought is the relation between the deflection $w(x_1, x_2)$ and the strains arising within the plate. We are not interested in all the possible strains, the normal strains and the shearing strain measured in the plane of the plate will be sufficient. These are according equations (F.1.34) and (F.1.37) expressible by the help of the components of the displacement vector $\mathbf{u}(\mathbf{r})$

$$\epsilon_1 = \frac{\partial u_1}{\partial x_1}, \tag{5.2a}$$

$$\epsilon_2 = \frac{\partial u_2}{\partial x_2}, \tag{5.2b}$$

$$\gamma_{12} = \frac{\partial u_1}{\partial x_2} + \frac{\partial u_2}{\partial x_1}. \tag{5.2c}$$

The components u_1 and u_2 depends not only on the coordinates x_1 and x_2, but also on the curvature of the plate. Thus, the strain varies along the cross-section. Let us consider figure 5.1. For the sake of simplicity depicted is only one coordinate of the plane of plate, the strain can be determined in a same way for both directions, however, thus the abscissa denotes both the coordinates. The displacements u_i on the neutral surface are denoted by $\hat{u}_i$, thus according the figure point p undergoes a displacement of $\hat{u}_i$ and shifts into the point P. The point o above p by a distance of z moves into O and it is clear that it undergoes a smaller displacement. The difference of displacements is $z\,\frac{\partial w}{\partial x_i}$, thus the displacement in the plane above the neutral surface by a distance of z is given by the system of equations

$$u_1 = \hat{u}_1 - z\,\frac{\partial w}{\partial x_1}, \tag{5.3a}$$

$$u_2 = \hat{u}_2 - z\,\frac{\partial w}{\partial x_2}. \tag{5.3b}$$

Substituting these equations into equations (5.2) gives

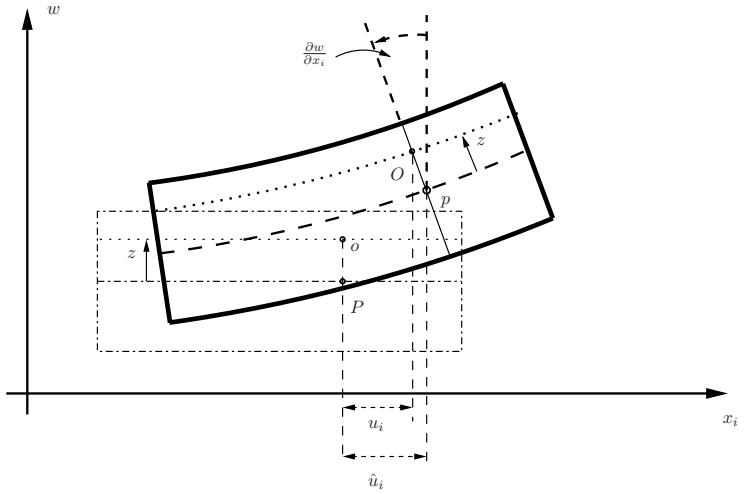

Figure 5.1: *Deformed element of the plate. The points o and p shift into O and P. Due to the bending of the plate element point o undergoes a smaller displacement as p.*

$$\epsilon_1 = \frac{\partial \hat{u}_1}{\partial x_1} - z\,\frac{\partial^2 w}{\partial x_1^2}, \tag{5.4a}$$

$$\epsilon_2 = \frac{\partial \hat{u}_2}{\partial x_2} - z\,\frac{\partial^2 w}{\partial x_2^2}, \tag{5.4b}$$

$$\gamma_{12} = \frac{\partial \hat{u}_1}{\partial x_2} + \frac{\partial \hat{u}_2}{\partial x_1} - 2\,z\,\frac{\partial^2 w}{\partial x \partial y}. \tag{5.4c}$$

We have thus the strains within the plate, expressed by means of the transversal and in-plane displacements of the middle surface.

5.1.2 Hooke's law (stress – strain relation)

The material of the plate is considered orthotropic thus the Hooke's law can be described by means of equations (F.1.51) and (F.1.52). We are interested in strains ϵ_1, ϵ_2 and γ_{12} and the corresponding stresses, thus the rows according ϵ_3, γ_{23} and γ_{31} and the columns according to σ_3, τ_{23} and τ_{31} can be deleted from the compliance matrix. This way we get

$$\begin{pmatrix} \epsilon_1 \\ \epsilon_2 \\ \gamma_{12} \end{pmatrix} = \begin{pmatrix} \frac{1}{E_1} & -\frac{\nu_{12}}{E_1} & 0 \\ -\frac{\nu_{21}}{E_2} & \frac{1}{E_2} & 0 \\ 0 & 0 & \frac{1}{G_{12}} \end{pmatrix} \begin{pmatrix} \sigma_1 \\ \sigma_2 \\ \tau_{12} \end{pmatrix}. \tag{5.5}$$

We have to determine the stiffness matrix from the compliance matrix, since we want to express the stresses by means of the strains. This can be carried out by inverting the compliance matrix, which yields

$$\begin{pmatrix} \sigma_1 \\ \sigma_2 \\ \tau_{12} \end{pmatrix} = \begin{pmatrix} \frac{E_1}{1-\nu_{12}\,\nu_{21}} & \frac{\nu_{12}E_2}{1-\nu_{12}\,\nu_{21}} & 0 \\ \frac{\nu_{21}E_1}{1-\nu_{12}\,\nu_{21}} & \frac{E_2}{1-\nu_{12}\,\nu_{21}} & 0 \\ 0 & 0 & G_{12} \end{pmatrix} \begin{pmatrix} \epsilon_1 \\ \epsilon_2 \\ \gamma_{12} \end{pmatrix}. \tag{5.6}$$

This is Hooke's law concerning the relevant stresses and strains of the plate. Now, we are able to substitute the expressions of strains (5.4) into the Hooke's law and we get

$$\begin{aligned} \sigma_1 &= \frac{E_1}{1-\nu_{12}\,\nu_{21}} \left(\frac{\partial \hat{u}_1}{\partial x_1} - z\,\frac{\partial^2 w}{\partial x_1^2} \right) + \frac{\nu_{12}E_2}{1-\nu_{12}\,\nu_{21}} \left(\frac{\partial \hat{u}_2}{\partial x_2} - z\,\frac{\partial^2 w}{\partial x_2^2} \right), \\ \sigma_2 &= \frac{\nu_{21}E_1}{1-\nu_{12}\,\nu_{21}} \left(\frac{\partial \hat{u}_1}{\partial x_1} - z\,\frac{\partial^2 w}{\partial x_1^2} \right) + \frac{E_2}{1-\nu_{12}\,\nu_{21}} \left(\frac{\partial \hat{u}_2}{\partial x_2} - z\,\frac{\partial^2 w}{\partial x_2^2} \right), \\ \tau_{12} &= G_{12} \left(\frac{\partial \hat{u}_1}{\partial x_2} + \frac{\partial \hat{u}_2}{\partial x_1} - 2\,z\,\frac{\partial^2 w}{\partial x \partial y} \right). \end{aligned} \tag{5.7a}$$

We managed, thus to express the normal and shear stresses by means of the transversal and in-plane deflections of the middle surface.

Note, that by the help of the symmetry constraint (F.1.52a)

$$\nu_{21}E_1 = \nu_{12}E_2 \tag{5.8}$$

the number of independent elastic parameters is reducible to four, but for the sake of simplicity we will use the five material constants, keeping in mind that they are linked with each other by means of the symmetry constraint.

5.1.3 Resultants (moment of force & tension – stress relation)

We can obtain the in-plane normal and shearing force intensities N_1, N_2 and N_{12}, the bending moment intensities M_1 and M_2 and the twisting moment intensity M_{12} depicted on figures 5.2 and 5.3 by integration over the thickness as follows

$$\begin{aligned} N_1 &= \int_{-h/2}^{h/2} \sigma_1 \,\mathrm{d}z, \\ N_2 &= \int_{-h/2}^{h/2} \sigma_2 \,\mathrm{d}z, \\ N_{12} &= \int_{-h/2}^{h/2} \tau_{12} \,\mathrm{d}z, \\ M_1 &= \int_{-h/2}^{h/2} \sigma_1 z \,\mathrm{d}z, \\ M_2 &= \int_{-h/2}^{h/2} \sigma_2 z \,\mathrm{d}z, \\ M_{12} &= \int_{-h/2}^{h/2} \tau_{12} z \,\mathrm{d}z. \end{aligned} \tag{5.9}$$

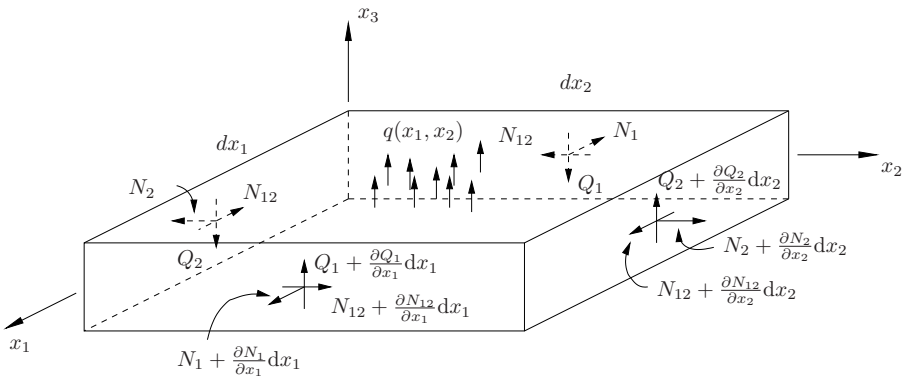

Figure 5.2: *Forces on the plate element*

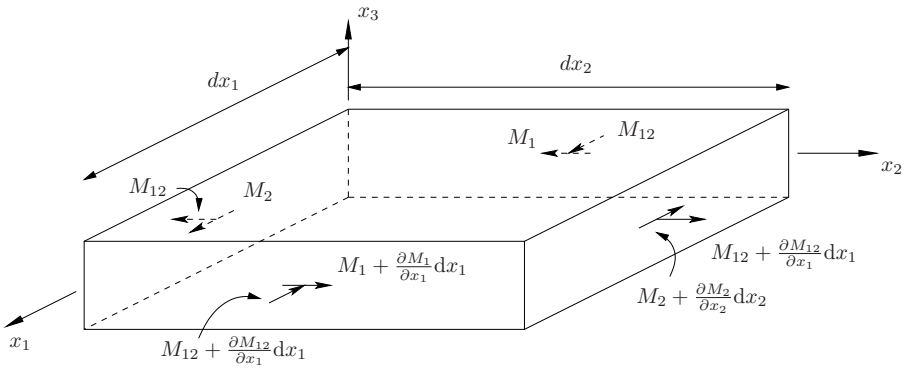

Figure 5.3: *Moments on the plate element*

Let us determine the bending moment M_1 for example, which arises due to the variation of σ_1 through the thickness. The integration gives

$$\begin{aligned} M_1 &= \int_{-h/2}^{h/2} \sigma_1 \, z \, \mathrm{d}z \\ &= \int_{-h/2}^{h/2} \frac{1}{1-\nu_{12}\,\nu_{21}} \left(E_1 \frac{\partial \hat{u}_1}{\partial x_1} z + \nu_{12} E_2 \frac{\partial \hat{u}_2}{\partial x_2} z - E_1 \frac{\partial^2 w}{\partial x_1^2} z^2 - \nu_{12} E_2 \frac{\partial^2 w}{\partial x_2^2} z^2 \right) \mathrm{d}z = \\ &= -D_1 \left(\frac{\partial^2 w}{\partial x_1^2} + \nu_{21} \frac{\partial^2 w}{\partial x_2^2} \right), \end{aligned} \tag{5.10}$$

where equation (5.8) has been employed, and a new variable, the bending rigidity

$$D_1 = \frac{E_1 h^3}{12\,(1-\nu_{12}\,\nu_{21})} \tag{5.11}$$

has been introduced. The terms containing odd powers of z are dropped out due to the integration between symmetrical limits. We obtain the other moment integrals in a similar manner

$$M_2 = -D_2 \left(\frac{\partial^2 w}{\partial x_2^2} + \nu_{12} \frac{\partial^2 w}{\partial x_1^2} \right), \tag{5.12a}$$

$$M_{12} = -2D_k \frac{\partial^2 w}{\partial x_1 \partial x_2}, \tag{5.12b}$$

where

$$\begin{aligned} D_2 &= \frac{E_2 h^3}{12\,(1-\nu_{12}\nu_{21})}, \\ D_k &= G_{12}\,\frac{h^3}{12}. \end{aligned} \tag{5.13}$$

The integrals concerning the in-plane normal and shear force densities are not developed here. We would need the displacements $\hat{u}_i$ to determine these quantities, hence we would get a coupled system of differential equations. This will be developed in section 5.2. In the next steps we will take the in-plane forces into account, however, so we can derive the system of equations easily in section 5.2.

5.1.4 Balance of moments (shearing force – moment of force relation)

The fourth task is to derive the balance of moments equation for the differential plate element (see figures 5.2, 5.3 and 5.4). Since the moments are summed in accordance with the superposition principle, it is sufficient to determine the balance equations only about the axes of coordinate.

Note, that $\mathrm{d}x_1$ and $\mathrm{d}x_2$ are both infinitesimal lengths, thus the surfaces of the plate element given by equations $x_3 = h/2$ and $x_3 = -h/2$ have infinitesimal area too. Therefore there does not arise any moment on these surfaces and there is not any moment about the axis x_3 on the other surfaces. Since there is not any moment about the axis x_3 on the plate

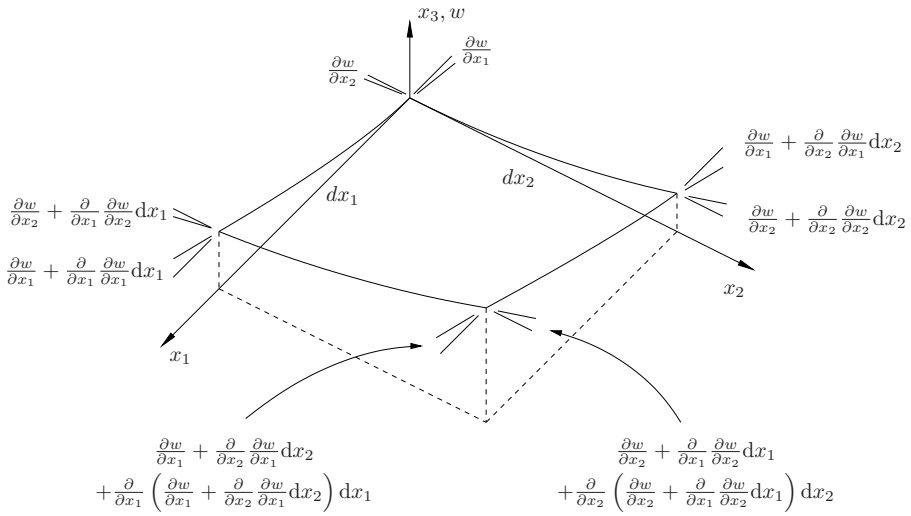

Figure 5.4: *Deformed middle surface of a plate element and the slopes on the edges.*

element, the balance of moments simplifies about this axis to $N_{12} = N_{21}$, which is satisfied automatically in accordance with equation (F.1.25).

Let us derive the balance of moments about axis x_1. Moment arises from shearing force intensity Q_2, from moment intensities M_{12}, M_2 and in the case of the deformed plate (see figure 5.4) from shearing force intensity N_{12}. This last term multiplied by the small angle $\frac{\partial w}{\partial x_1}$. The equation is thus

$$\begin{aligned} 0 \cong \frac{\mathrm{d}L}{\mathrm{d}t} &= Q_2\,\mathrm{d}x_1\frac{\mathrm{d}x_2}{2} + \left(Q_2 + \frac{\partial Q_2}{\partial x_2}\mathrm{d}x_2\right)\mathrm{d}x_1\frac{\mathrm{d}x_2}{2} + \\ &+ N_{12}\,\frac{\partial w}{\partial x_1}\mathrm{d}x_1\frac{\mathrm{d}x_2}{2} + \left(N_{12} + \frac{\partial N_{12}}{\partial x_2}\mathrm{d}x_2\right)\left(\frac{\partial w}{\partial x_1} + \frac{\partial^2 w}{\partial x_2 \partial x_1}\mathrm{d}x_2\right)\mathrm{d}x_1\frac{\mathrm{d}x_2}{2} + \\ &+ M_{12}\,\mathrm{d}x_2 - \left(M_{12} + \frac{\partial M_{12}}{\partial x_1}\mathrm{d}x_1\right)\mathrm{d}x_2 + \\ &+ M_2\,\mathrm{d}x_1 - \left(M_2 + \frac{\partial M_2}{\partial x_2}\mathrm{d}x_2\right)\mathrm{d}x_1. \end{aligned} \tag{5.14}$$

It is apparent, that the moment of inertia was neglected. After simplifications and dividing by $\mathrm{d}x_1\mathrm{d}x_2$ we get

$$\begin{aligned} 0 \cong Q_2 + \frac{\partial Q_2}{\partial x_2}\frac{\mathrm{d}x_2}{2} + N_{12}\frac{\partial w}{\partial x_1} + N_{12}\frac{\partial^2 w}{\partial x_2 \partial x_1}\frac{\mathrm{d}x_2}{2} + \\ + \frac{\partial N_{12}}{\partial x_2}\frac{\partial w}{\partial x_1}\frac{\mathrm{d}x_2}{2} + \frac{\partial N_{12}}{\partial x_2}\frac{\partial^2 w}{\partial x_2 \partial x_1}\frac{\mathrm{d}x_2^2}{2} - \frac{\partial M_{12}}{\partial x_1} - \frac{\partial M_2}{\partial x_2}. \end{aligned} \tag{5.15}$$

If we assume the terms containing $\mathrm{d}x_2$ or partial derivatives of w small enough to be negligible, we arrive at

$$Q_2 - \frac{\partial M_{12}}{\partial x_1} - \frac{\partial M_2}{\partial x_2} \cong 0. \tag{5.16}$$

In the same way we get from the balance of moments about axis x_2

$$Q_1 - \frac{\partial M_1}{\partial x_1} - \frac{\partial M_{12}}{\partial x_2} \cong 0. \tag{5.17}$$

Now, we are able to substitute M_{12} and M_2 from equations (5.12b) and (5.12a) into (5.16). By the help of the symmetry equation (5.8) we arrive at the expression for the shearing force intensity

$$Q_2 = -\frac{\partial}{\partial x_2}\left(D_{12}\frac{\partial^2 w}{\partial x_1^2} + D_2\frac{\partial^2 w}{\partial x_2^2}\right), \tag{5.18}$$

where the notation

$$D_{12} = \nu_{21}D_1 + 2D_k = \nu_{12}D_2 + 2D_k \tag{5.19}$$

is introduced. In the same way we get for Q_1 that

$$Q_1 = -\frac{\partial}{\partial x_1}\left(D_1\frac{\partial^2 w}{\partial x_1^2} + D_{12}\frac{\partial^2 w}{\partial x_2^2}\right). \tag{5.20}$$

We succeed thus to express the shearing force intensities by means of the transverse deflection of the middle surface. The next step is to put down the balance of forces equation.

5.1.5 Balance of forces (displacement – shearing force relation)

Supposing small slopes, that is the tangent and the sine of the angles are taken equivalent and the cosine are taken unity, and considering figures 5.2 and 5.4 we are able to write down Newton's second law in direction x_3 as follows

$$\begin{aligned}
\rho\, h\, \mathrm{d}x_1\, \mathrm{d}x_2\, \frac{\partial^2 w}{\partial t^2} = {} & \frac{\partial Q_1}{\partial x_1}\,\mathrm{d}x_1\,\mathrm{d}x_2 + \frac{\partial Q_2}{\partial x_2}\,\mathrm{d}x_1\,\mathrm{d}x_2 - \\
& - N_1 \mathrm{d}x_2 \frac{\partial w}{\partial x_1} + \left(N_1 + \frac{\partial N_1}{\partial x_1}\mathrm{d}x_1\right)\mathrm{d}x_2\left(\frac{\partial w}{\partial x_1} + \frac{\partial^2 w}{\partial x_1^2}\mathrm{d}x_1\right) - \\
& - N_2 \mathrm{d}x_1 \frac{\partial w}{\partial x_2} + \left(N_2 + \frac{\partial N_2}{\partial x_2}\mathrm{d}x_2\right)\mathrm{d}x_1\left(\frac{\partial w}{\partial x_2} + \frac{\partial^2 w}{\partial x_2^2}\mathrm{d}x_2\right) - \\
& - N_{12} \mathrm{d}x_1 \frac{\partial w}{\partial x_1} + \left(N_{12} + \frac{\partial N_{12}}{\partial x_2}\mathrm{d}x_2\right)\mathrm{d}x_1\left(\frac{\partial w}{\partial x_1} + \frac{\partial^2 w}{\partial x_1 \partial x_2}\mathrm{d}x_2\right) - \\
& - N_{12} \mathrm{d}x_2 \frac{\partial w}{\partial x_2} + \left(N_{12} + \frac{\partial N_{12}}{\partial x_1}\mathrm{d}x_1\right)\mathrm{d}x_2\left(\frac{\partial w}{\partial x_2} + \frac{\partial^2 w}{\partial x_1 \partial x_2}\mathrm{d}x_1\right) + \\
& + q\,\mathrm{d}x_1\,\mathrm{d}x_2,
\end{aligned} \tag{5.21}$$

where ρ is the mass density per unit volume, h is the thickness of the plate and $\frac{\partial^2 w}{\partial t^2}$ is the acceleration of the middle surface in direction x_3. Discarding the third-order differential

terms, and dividing by the area $\mathrm{d}x_1\,\mathrm{d}x_2$, we get

$$\rho\,h\,\frac{\partial^2 w}{\partial t^2} = \frac{\partial Q_1}{\partial x_1} + \frac{\partial Q_2}{\partial x_2} + \frac{\partial}{\partial x_1}\left(N_1\frac{\partial w}{\partial x_1}\right) + \frac{\partial}{\partial x_2}\left(N_2\frac{\partial w}{\partial x_2}\right) + \\ + \frac{\partial}{\partial x_1}\left(N_{12}\frac{\partial w}{\partial x_2}\right) + \frac{\partial}{\partial x_2}\left(N_{12}\frac{\partial w}{\partial x_1}\right) + q. \tag{5.22}$$

This equation can be further simplified by the help of the stress equilibrium equations. The stress equilibrium is generally determined by equation (F.1.23), however if we assume the motion in directions x_1 and x_2 negligible, the static equilibrium equation (F.1.24) can be used. Thus, according the symmetry equation (F.1.25) we get

$$\begin{aligned} \frac{\partial \sigma_{11}}{\partial x_1} + \frac{\partial \sigma_{12}}{\partial x_2} + \frac{\partial \sigma_{31}}{\partial x_3} = 0, \\ \frac{\partial \sigma_{12}}{\partial x_1} + \frac{\partial \sigma_{22}}{\partial x_2} + \frac{\partial \sigma_{32}}{\partial x_3} = 0. \end{aligned} \tag{5.23}$$

In order to apply these equations to the differential element, we have to integrate the stresses σ_{ij} over the surfaces given by x_i = constant. Since the areas of the surfaces determined by equations $x_3 = h/2$ and $x_3 = -h/2$ are infinitesimal, the stresses σ_{31} and σ_{32} vanish. Assuming that integration over the surface x_i = constant and differentiation with respect to x_i are commutable, the equations become according to equations (5.9)

$$\begin{aligned} \frac{\partial N_1}{\partial x_1} + \frac{\partial N_{12}}{\partial x_2} = 0, \\ \frac{\partial N_{12}}{\partial x_1} + \frac{\partial N_2}{\partial x_2} = 0. \end{aligned} \tag{5.24}$$

Thus, equation (5.22) turns into

$$\frac{\partial Q_1}{\partial x_1} + \frac{\partial Q_2}{\partial x_2} + N_1\,\frac{\partial^2 w}{\partial x_1^2} + N_2\,\frac{\partial^2 w}{\partial x_2^2} + 2\,N_{12}\,\frac{\partial^2 w}{\partial x_1 \partial x_2} + q = \rho\,h\,\frac{\partial^2 w}{\partial t^2}. \tag{5.25}$$

Now, we are able to substitute the shearing force intensities Q_1 and Q_2 from equations (5.20) and (5.18). With this last step we arrive at the governing equation of the transversal or bending motion of the orthotropic plate

$$D_1\frac{\partial^4 w}{\partial x_1^4} + 2D_{12}\frac{\partial^4 w}{\partial x_1^2 \partial x_2^2} + D_2\frac{\partial^4 w}{\partial x_2^4} + \rho\,h\,\frac{\partial^2 w}{\partial t^2} = N_1\,\frac{\partial^2 w}{\partial x_1^2} + N_2\,\frac{\partial^2 w}{\partial x_2^2} + 2\,N_{12}\,\frac{\partial^2 w}{\partial x_1 \partial x_2} + q, \tag{5.26}$$

where D_1, D_2, D_{12} and ρ are material parameters and N_1, N_2 and N_{12} are the normal and shearing force densities. The last terms are generally functions of coordinates x_1 and x_2 and time t, and can be computed according equations (5.9). For the sake of this we need to determine the in-plane motion of the plate too, and would get a coupled system of three differential equations. This will be carried out in the next section. However, if the longitudinal motion is neglected, that is we assume $\hat{u}_1 = \hat{u}_2 = 0$, the force densities become equal to zero. With this assumption we arrive at the well-known plate equation, which is

in the orthotropic case

$$D_1 \frac{\partial^4 w}{\partial x_1^4} + 2D_{12} \frac{\partial^4 w}{\partial x_1^2 \partial x_2^2} + D_2 \frac{\partial^4 w}{\partial x_2^4} + \rho\, h\, \frac{\partial^2 w}{\partial t^2} = q. \tag{5.27}$$

This equation turns in the case of isotropy, where $E_1 = E_2 = E$, $\nu_{12} = \nu_{21} = \nu$, and $G = E/2(1+\nu)$ into

$$D \left(\frac{\partial^4 w}{\partial x_1^4} + 2 \frac{\partial^4 w}{\partial x_1^2 \partial x_2^2} + \frac{\partial^4 w}{\partial x_2^4} \right) + \rho\, h\, \frac{\partial^2 w}{\partial t^2} = q, \tag{5.28}$$

or using the more convenient ∇ operator

$$D\, \nabla^4 w + \rho\, h\, \frac{\partial^2 w}{\partial t^2} = q. \tag{5.29}$$

Note, that outgoing from equation (5.26) it is possible to create the governing equation of the membrane too. By assuming the plate being thin enough to be D_1, D_2 and D_{12} negligible, equation (5.26) turns into

$$\rho\, h\, \frac{\partial^2 w}{\partial t^2} = N_1 \frac{\partial^2 w}{\partial x_1^2} + N_2 \frac{\partial^2 w}{\partial x_2^2} + 2\, N_{12} \frac{\partial^2 w}{\partial x_1 \partial x_2} + q. \tag{5.30}$$

Here, the restoring force arises from N_1, N_2 and N_{12}. In the case of the membrane much of the force intensities originate in the tension applied on the edges, the term according the motion gives only a small variation. Thus, the in-plane force intensities can be assumed constant to a first approximation.

We obtained thus the governing equation of the transverse motion of an orthotropic plate. The spatial difference operator is linear, thus we can develop a matrix corresponding to the finite difference operator by the help of the finite difference method overviewed in section 4.

The governing equation can be adapted to plates with variable thickness too. In this case the thickness h and consequently the bending stiffness D_i depends on the coordinates x_i, thus shear forces Q_i have to be determined directly from equations (5.16) and (5.17) and the product rule of differentiation have to be applied.

5.2 Equations of the in-plane Motion

In this section the equation of transverse motion is completed with the equations of in-plane motions. We will see that these equations form a system of coupled differential equations, and contain such products of derivatives, which cause nonlinearities.

We have to develop Newton's second law for the motions in directions x_1 and x_2, that is for $\hat{u}_1$ and $\hat{u}_2$. The situation is a bit more complicated compared with figure 5.4, as shear strains arise in the plane of the plate. The sides of the differential element are not perpendicular to each other any more and not parallel to the coordinate axes either. Every side of the element rotates around every coordinate axis. This makes relatively complicated

to determine the components of the force and moment densities in a given direction for the first sight. The problem can be solved in the following way.

If we determine the rotation matrices about the axes of coordinate with the approximation $\cos(.) = 1$ according to the small angles and multiply them we get the matrix of the general three-dimensional rotation. The six different matrices corresponding the six different order of rotation differs from each other only in terms of order $\sin(.)^2$ or $\sin(.)^3$, thus they can be treated equal. The rotation matrix is

$$\mathbf{R} = \begin{pmatrix} 1 & -\sin(\gamma) & \sin(\beta) \\ \sin(\gamma) & 1 & -\sin(\alpha) \\ -\sin(\beta) & \sin(\alpha) & 1 \end{pmatrix}, \tag{5.31}$$

where α, β and γ are the angles of rotation in the planes perpendicular to x_1, x_2 and x_3, respectively. Since the force and moment densities are parallel to the coordinate axis in the rest position, their components after the rotation can be determined as multiples of the columns of the rotation matrix, namely

$$\mathbf{g}_1 = (g_1, 0, 0)^T \quad \Rightarrow \quad \mathbf{g}_1' = (g_1, g_1 \sin(\gamma), -g_1 \sin(\beta))^T, \tag{5.32a}$$

$$\mathbf{g}_2 = (0, g_2, 0)^T \quad \Rightarrow \quad \mathbf{g}_2' = (-g_2 \sin(\gamma), g_2, g_2 \sin(\alpha))^T, \tag{5.32b}$$

$$\mathbf{g}_3 = (0, 0, g_3)^T \quad \Rightarrow \quad \mathbf{g}_3' = (g_3 \sin(\beta), -g_3 \sin(\alpha), g_3)^T. \tag{5.32c}$$

With these we can determine the components of the force and momentum densities in each direction, and derive Newton's second law concerning the in-plane deflections $\hat{u}_1$ and $\hat{u}_2$. We get in direction x_1

$$\begin{aligned} \rho\, h\, \mathrm{d}x_1\, \mathrm{d}x_2\, \frac{\partial^2 \hat{u}_1}{\partial t^2} = & -N_1\, \mathrm{d}x_2 + \left(N_1 + \frac{\partial N_1}{\partial x_1}\, \mathrm{d}x_1\right) \mathrm{d}x_2 \\ & - N_{12}\, \mathrm{d}x_1 + \left(N_{12} + \frac{\partial N_{12}}{\partial x_2}\, \mathrm{d}x_2\right) \mathrm{d}x_1 \\ & + Q_2 \frac{\partial w}{\partial x_1}\, \mathrm{d}x_1 - \left(Q_2 + \frac{\partial Q_2}{\partial x_2}\, \mathrm{d}x_2\right) \left(\frac{\partial w}{\partial x_1} + \frac{\partial^2 w}{\partial x_2 \partial x_1}\, \mathrm{d}x_2\right) \mathrm{d}x_1 \\ & + Q_1 \frac{\partial w}{\partial x_1}\, \mathrm{d}x_2 - \left(Q_1 + \frac{\partial Q_1}{\partial x_1}\, \mathrm{d}x_1\right) \left(\frac{\partial w}{\partial x_1} + \frac{\partial^2 w}{\partial x_1^2}\, \mathrm{d}x_1\right) \mathrm{d}x_2 \\ & - N_{12} \frac{\partial \hat{u}_1}{\partial x_2}\, \mathrm{d}x_2 + \left(N_{12} + \frac{\partial N_{12}}{\partial x_1}\, \mathrm{d}x_1\right) \left(\frac{\partial \hat{u}_1}{\partial x_2} + \frac{\partial^2 \hat{u}_1}{\partial x_1 \partial x_2}\, \mathrm{d}x_1\right) \mathrm{d}x_2 \\ & + N_2 \frac{\partial \hat{u}_2}{\partial x_1}\, \mathrm{d}x_1 - \left(N_2 + \frac{\partial N_2}{\partial x_2}\, \mathrm{d}x_2\right) \left(\frac{\partial \hat{u}_2}{\partial x_1} + \frac{\partial^2 \hat{u}_2}{\partial x_1 \partial x_2}\, \mathrm{d}x_2\right) \mathrm{d}x_1. \end{aligned} \tag{5.33}$$

Dividing by the differential area $\mathrm{d}x_1 \mathrm{d}x_2$ and neglecting the terms containing differential

lengths we get

$$\rho\, h\, \frac{\partial^2 \hat{u}_1}{\partial t^2} = \frac{\partial N_1}{\partial x_1} + \frac{\partial N_{12}}{\partial x_2} - \frac{\partial}{\partial x_1}\left(Q_1 \frac{\partial w}{\partial x_1}\right) - \frac{\partial}{\partial x_2}\left(Q_2 \frac{\partial w}{\partial x_1}\right) + \frac{\partial}{\partial x_1}\left(N_{12} \frac{\partial \hat{u}_1}{\partial x_2}\right) - \frac{\partial}{\partial x_2}\left(N_2 \frac{\partial \hat{u}_2}{\partial x_1}\right). \tag{5.34}$$

Due to symmetry we can write for deflection $\hat{u}_2$ by means of the change of subscripts that

$$\rho\, h\, \frac{\partial^2 \hat{u}_2}{\partial t^2} = \frac{\partial N_2}{\partial x_2} + \frac{\partial N_{12}}{\partial x_1} - \frac{\partial}{\partial x_2}\left(Q_2 \frac{\partial w}{\partial x_2}\right) - \frac{\partial}{\partial x_1}\left(Q_1 \frac{\partial w}{\partial x_2}\right) + \frac{\partial}{\partial x_2}\left(N_{12} \frac{\partial \hat{u}_2}{\partial x_1}\right) - \frac{\partial}{\partial x_1}\left(N_1 \frac{\partial \hat{u}_1}{\partial x_2}\right). \tag{5.35}$$

The equation concerning deflection w remains the one derived in the preceding section. We copy it here to let the three coupled differential equations see together:

$$\rho\, h\, \frac{\partial^2 w}{\partial t^2} - q = \frac{\partial Q_1}{\partial x_1} + \frac{\partial Q_2}{\partial x_2} + \frac{\partial}{\partial x_1}\left(N_1 \frac{\partial w}{\partial x_1}\right) + \frac{\partial}{\partial x_2}\left(N_2 \frac{\partial w}{\partial x_2}\right) + + \frac{\partial}{\partial x_1}\left(N_{12} \frac{\partial w}{\partial x_2}\right) + \frac{\partial}{\partial x_2}\left(N_{12} \frac{\partial w}{\partial x_1}\right). \tag{5.36}$$

We left the excitation q in the equation to indicate that even if the excitation transversal is, in-plane motion arises due to the coupling. This in-plane motion affects the transversal motion and has thus an effect on the radiated sound.

The in-plane force densities N_1, N_2 and N_{12} can be determined on the grounds of equations (5.9) and (5.7):

$$N_1 = \frac{E_1 h}{1 - \nu_{12}\nu_{21}} \left(\frac{\partial \hat{u}_1}{\partial x_1} + \nu_{21} \frac{\partial \hat{u}_2}{\partial x_2}\right), \tag{5.37a}$$

$$N_2 = \frac{E_2 h}{1 - \nu_{12}\nu_{21}} \left(\frac{\partial \hat{u}_2}{\partial x_2} + \nu_{12} \frac{\partial \hat{u}_1}{\partial x_1}\right), \tag{5.37b}$$

$$N_{12} = G_{12} h \left(\frac{\partial \hat{u}_1}{\partial x_2} + \frac{\partial \hat{u}_2}{\partial x_1}\right). \tag{5.37c}$$

It is apparent that the last four terms of the equations are responsible for the coupling, but these cause the nonlinearity too. The equations can made linear by dropping these terms out, but the coupling between the transversal and in-plane motions would vanish too in this case and the benefit of the model would disappear.

This model offers a possible direction of improvement, but requires the ability of treating nonlinearities too.

Chapter 6

Shell Equations

6.1 The Cylindrical Shell

A number of approaches exist for the derivation of the equation governing the radial motion of the cylindrical shell. The simplest one is the so-called membrane shell, where shearing forces, twisting and bending moments are neglected. The derivation of the corresponding equation and further references to other shell models can be found in [5].

In this section a simplified shell equation is presented, which takes the stiffness arising due the curvature into account, but do not use the in-plane motion and the model remains linear. The idea originates in a possible simplification of the ring equation derived in [5], by which the coupling effect can be avoided. The result is a modified plate equation. We will see, that the difference is only a term containing the deflection w, but no derivatives. This is very helpful from a modeling point of view, since the transformation kernels of the functional transformation method do not need to be modified.

We have to introduce a new coordinate system, which is in this case the cylindrical coordinate system. Thus, the new coordinates r, φ and x_2 are introduced, where r and φ are the polar coordinates in the plane perpendicular to the axis of the cylindrical shell, while x_2 is measured along the axis of the cylindrical shell. It is worthwhile to introduce the arc length x_1 on the surface of the cylindrical shell too (see figures 6.1 and 6.2).

The radial motion of the cylindrical shell can be described by the function $w(\varphi, x_2, t)$, or alternatively by $w(x_1, x_2, t)$. The excitation is the force per unit area $q(\varphi, x_2, t) = q(x_1, x_2, t)$ acting in radial direction.

Let us hence derive our simplified governing equation of the radial motion of cylindrical shell by following up the steps suggested in section 1.3.

6.1.1 Kinematics (strain – displacement relation)

The first step is to relate the strains to the deflection. Similarly to the plate, we have to express the in-plane normal strains ϵ_1, ϵ_2 and the in-plane shearing strain γ_{12} only. These quantities are expressible from the displacement vector $\mathbf{u}(\mathbf{r})$ by means of the following

equations:

$$\begin{aligned}\epsilon_1 &= \frac{\partial u_1}{\partial x_1},\\ \epsilon_2 &= \frac{\partial u_2}{\partial x_2},\\ \gamma_{12} &= \frac{\partial u_1}{\partial x_2} + \frac{\partial u_2}{\partial x_1}.\end{aligned} \tag{6.1}$$

For the sake of simplicity we are neglecting the longitudinal motion in direction x_2, that is we assume $\hat{u}_2 \cong 0$. Due to the bendings strain arises however above and below the middle surface, which can be expressed in the same way as in the case of the plate, thus the longitudinal strain in direction x_2 is

$$u_2 = -z\frac{\partial w}{\partial x_2}. \tag{6.2}$$

In direction x_1, owing to the radial motion strain arises in the middle plane too, the value of which is, on the grounds of figure 6.2,

$$\mathrm{d}\hat{u}_1 = \mathrm{d}x_1' - \mathrm{d}x_1 \cong (w+R)\,\mathrm{d}\varphi - R\mathrm{d}\varphi = w\mathrm{d}\varphi = \frac{w}{R}\mathrm{d}x_1, \tag{6.3}$$

where the contribution of the differential increase $\partial w/\partial x_1$ of w to the value of $\mathrm{d}x_1'$ has been neglected. Thus the deflection w of a differential element causes an elongation $\hat{u}_1$ in direction x_1. Thus higher force is required for the same deflection, since the force has to cover the in-plane strains too. This gives the stability of shell structures (see figure 2.1). The in-plane elongation $\mathrm{d}u_1$ in the plane at a distance z above the middle plane is higher as the one measured in the middle plane by $z(\mathrm{d}\varphi' - \mathrm{d}\varphi)$, where the angle $\mathrm{d}\varphi'$ is (see figure 6.2)

$$\mathrm{d}\varphi' = \mathrm{d}\varphi - \frac{\partial w}{\partial x_1} - \frac{\partial^2 w}{\partial x_1^2}\mathrm{d}x_1 + \frac{\partial w}{\partial x_1} = \mathrm{d}\varphi - \frac{\partial^2 w}{\partial x_1^2}\mathrm{d}x_1. \tag{6.4}$$

Thus the in-plane elongation u_1 is

$$u_1 = \frac{w}{R}x_1 - z\frac{\partial w}{\partial x_1}. \tag{6.5}$$

Substituting this and (6.2) into equations 6.1 gives the strains

$$\begin{aligned}\epsilon_1 &= \frac{w}{R} - z\frac{\partial^2 w}{\partial x_1^2},\\ \epsilon_2 &= -z\frac{\partial^2 w}{\partial x_2^2},\\ \gamma_{12} &= \frac{\partial}{\partial x_2}\left(\frac{w\,x_1}{R}\right) - 2\,z\,\frac{\partial^2 w}{\partial x_1 \partial x_2}.\end{aligned} \tag{6.6}$$

Note, that equation (6.3) is correct in the case when every point of the shell moves radially only. In a real shell, however, longitudinal motion arises which compensate the elongations of the differential elements, thus lower elongations are required. Our model

assigns a higher stiffness to the shell as necessary, this is the price if we want to avoid the coupled system of equations.

6.1.2 Hooke's law (stress – strain relation)

The second step is to relate the strains to the stresses by the help of Hooke's law. In the case of orthotropic material this can be carried out by substituting the determined strains in equation 5.6, that is

$$\begin{aligned}
\sigma_1 &= \frac{E_1}{1-\nu_{12}\nu_{21}}\left(\frac{w}{R} - z\frac{\partial^2 w}{\partial x_1^2} - \nu_{21} z\frac{\partial^2 w}{\partial x_2^2}\right),\\
\sigma_2 &= \frac{E_2}{1-\nu_{12}\nu_{21}}\left(\nu_{12}\frac{w}{R} - \nu_{12} z\frac{\partial^2 w}{\partial x_1^2} - z\frac{\partial^2 w}{\partial x_2^2}\right),\\
\tau_{12} &= G_{12}\left(\frac{\partial}{\partial x_2}\left(\frac{w x_1}{R}\right) - 2\,z\frac{\partial^2 w}{\partial x_1 \partial x_2}\right).
\end{aligned} \tag{6.7}$$

6.1.3 Resultants (moment of force & tension – stress relation)

With these results we are able to determine the moment and force intensities acting on the differential shell element as depicted on figure 6.1. According the definitions 5.9 we can get for the intensities similarly to the treatment in section 5.1.3

$$M_1 = -D_1\left(\frac{\partial^2 w}{\partial x_1^2} + \nu_{21}\frac{\partial^2 w}{\partial x_2^2}\right), \tag{6.8a}$$

$$M_2 = -D_2\left(\nu_{12}\frac{\partial^2 w}{\partial x_1^2} + \frac{\partial^2 w}{\partial x_2^2}\right), \tag{6.8b}$$

$$M_{12} = -2\,D_k\frac{\partial^2 w}{\partial x_1 \partial x_2}, \tag{6.8c}$$

$$N_1 = \frac{E_1}{1-\nu_{12}\nu_{21}}\frac{w\,h}{R}, \tag{6.8d}$$

$$N_2 = \frac{E_2}{1-\nu_{12}\nu_{21}}\,\nu_{12}\,\frac{w\,h}{R}, \tag{6.8e}$$

$$N_{12} = G_{12}\,h\,\frac{x_1}{R}\frac{\partial w}{\partial x_2}, \tag{6.8f}$$

where again

$$D_1 = \frac{E_1 h^3}{12\,(1-\nu_{12}\nu_{21})}, \tag{6.9a}$$

$$D_2 = \frac{E_2 h^3}{12\,(1-\nu_{12}\nu_{21})}, \tag{6.9b}$$

$$D_k = \frac{G_{12}\,h^3}{12}. \tag{6.9c}$$

6.1.4 Balance of moments (shearing force – moment of force relation)

The balance of moments equation about axis x_1 is, expressed by the moment and force densities (see figure 6.1)

$$\begin{aligned} 0 \cong \frac{\mathrm{d}L}{\mathrm{d}t} = {} & Q_2 \mathrm{d}x_1 \frac{\mathrm{d}x_2}{2} + \left(Q_2 + \frac{\partial Q_2}{\partial \mathrm{d}x_2} \mathrm{d}x_2 \right) \mathrm{d}x_1 \frac{\mathrm{d}x_2}{2} + \\ & + N_{12} \frac{\partial w}{\partial x_1} \mathrm{d}x_1 \frac{\mathrm{d}x_2}{2} + \left(N_{12} + \frac{\partial N_{12}}{\partial \mathrm{d}x_2} \mathrm{d}x_2 \right) \left(\frac{\partial w}{\partial x_1} + \frac{\partial^2 w}{\partial x_2 \partial x_1} \mathrm{d}x_2 \right) \mathrm{d}x_1 \frac{\mathrm{d}x_2}{2} + \\ & + M_{12} \mathrm{d}x_2 - \left(M_{12} + \frac{\partial M_{12}}{\partial x_1} \mathrm{d}x_1 \right) \mathrm{d}x_2 + \\ & + M_2 \mathrm{d}x_1 - \left(M_2 + \frac{\partial M_2}{\partial x_2} \mathrm{d}x_2 \right) \mathrm{d}x_1, \end{aligned} \tag{6.10}$$

which is completely the same as equation 5.14 obtained in the case of the plate. Thus, with the same simplifications we arrive at

$$Q_2 - \frac{\partial M_{12}}{\partial x_1} - \frac{\partial M_2}{\partial x_2} \cong 0, \tag{6.11}$$

and

$$Q_1 - \frac{\partial M_1}{\partial x_1} - \frac{\partial M_{12}}{\partial x_2} \cong 0. \tag{6.12}$$

Now, we are able to determine the shearing force intensities, which are according to equations 6.8

$$Q_1 = -\frac{\partial}{\partial x_1} \left(D_1 \frac{\partial^2 w}{\partial x_1^2} + D_{12} \frac{\partial^2 w}{\partial x_2^2} \right), \tag{6.13a}$$

$$Q_2 = -\frac{\partial}{\partial x_2} \left(D_{12} \frac{\partial^2 w}{\partial x_1^2} + D_2 \frac{\partial^2 w}{\partial x_2^2} \right), \tag{6.13b}$$

where the notation

$$D_{12} = \nu_{21} D_1 + 2D_k = \nu_{12} D_2 + 2D_k \tag{6.14}$$

is introduced again.

6.1.5 Balance of forces (displacement – shearing force relation)

The last step is to develop Newton's second law in radial direction, which differs from the plate's one in one term. The in-plane normal force intensity N_1 has due to the curvature

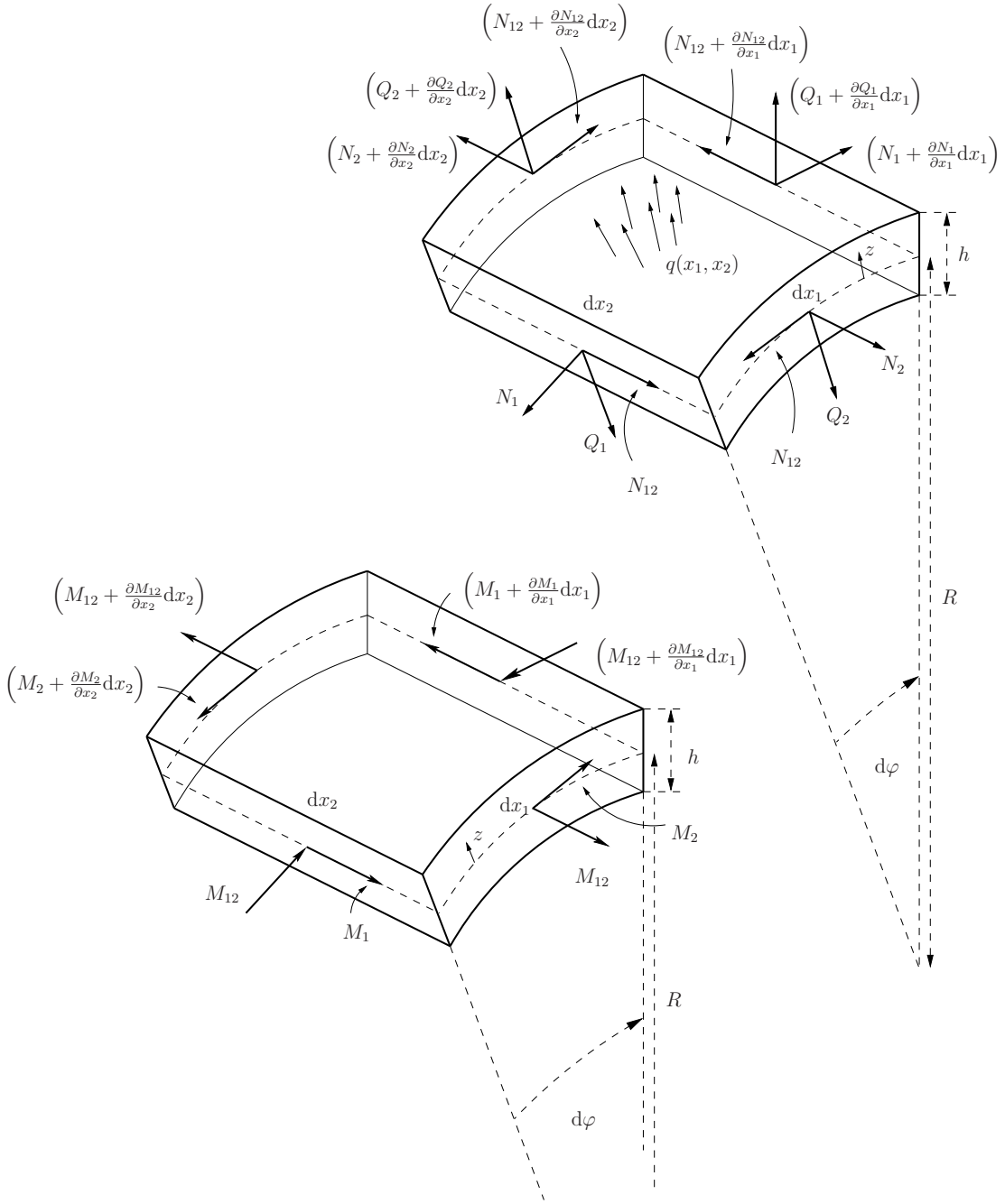

Figure 6.1: *Forces and moments acting on the differential element of a cylindrical shell.*

a much relevant component in radial direction. The equation is thus

$$\begin{aligned}\rho\, h\, \mathrm{d}x_1\, \mathrm{d}x_2\, \frac{\partial^2 w}{\partial t^2} = {} & \frac{\partial Q_1}{\partial x_1}\, \mathrm{d}x_1\, \mathrm{d}x_2 + \frac{\partial Q_2}{\partial x_2}\, \mathrm{d}x_1\, \mathrm{d}x_2 - \\ & - N_1 \mathrm{d}x_2 \left(\frac{\partial w}{\partial x_1} + \frac{\mathrm{d}x_1}{2\, R} \right) + \\ & + \left(N_1 + \frac{\partial N_1}{\partial x_1} \mathrm{d}x_1 \right) \mathrm{d}x_2 \left(\frac{\partial w}{\partial x_1} + \frac{\partial^2 w}{\partial x_1^2} \mathrm{d}x_1 - \frac{\mathrm{d}x_1}{2\, R} \right) - \\ & - N_2 \mathrm{d}x_1 \frac{\partial w}{\partial x_2} + \left(N_2 + \frac{\partial N_2}{\partial x_2} \mathrm{d}x_2 \right) \mathrm{d}x_1 \left(\frac{\partial w}{\partial x_2} + \frac{\partial^2 w}{\partial x_2^2} \mathrm{d}x_2 \right) - \\ & - N_{12} \mathrm{d}x_1 \frac{\partial w}{\partial x_1} + \left(N_{12} + \frac{\partial N_{12}}{\partial x_2} \mathrm{d}x_2 \right) \mathrm{d}x_1 \left(\frac{\partial w}{\partial x_1} + \frac{\partial^2 w}{\partial x_1 \partial x_2} \mathrm{d}x_2 \right) - \\ & - N_{12} \mathrm{d}x_2 \frac{\partial w}{\partial x_2} + \left(N_{12} + \frac{\partial N_{12}}{\partial x_1} \mathrm{d}x_1 \right) \mathrm{d}x_2 \left(\frac{\partial w}{\partial x_2} + \frac{\partial^2 w}{\partial x_1 \partial x_2} \mathrm{d}x_1 \right) + \\ & + q\, \mathrm{d}x_1\, \mathrm{d}x_2, \end{aligned} \tag{6.15}$$

which turns by means of the simplifications introduced in section 5.1.5 into

$$\frac{\partial Q_1}{\partial x_1} + \frac{\partial Q_2}{\partial x_2} + N_1 \frac{\partial^2 w}{\partial x_1^2} + N_2 \frac{\partial^2 w}{\partial x_2^2} + 2\, N_{12} \frac{\partial^2 w}{\partial x_1 \partial x_2} - \frac{N_1}{R} + q = \rho\, h\, \frac{\partial^2 w}{\partial t^2}. \tag{6.16}$$

The in-plane force intensities N_1, N_2 and N_{12} were neglected at this stage in the case of the plate. Now, we can perform it partly only, since the term $\frac{N_1}{R}$ is accountable for the additive restoring force caused by the cylindrical geometry. The other three terms containing in-plane force intensities are much smaller, since they are multiplied by the derivatives of the deflection. Furthermore they arise due to the bending motion of the shell, not due to the radial dilatation. Accordingly, the latter terms will be considered negligible in the followings and our equation simplifies to

$$\frac{\partial Q_1}{\partial x_1} + \frac{\partial Q_2}{\partial x_2} - \frac{N_1}{R} + q = \rho\, h\, \frac{\partial^2 w}{\partial t^2}. \tag{6.17}$$

Substituting the transversal shearing and in-plane force intensities from equations 6.13 and 6.8 we get the governing equation of the radial motion of the orthotropic cylindrical shell

$$D_1 \frac{\partial^4 w}{\partial x_1^4} + 2 D_{12} \frac{\partial^4 w}{\partial x_1^2 \partial x_2^2} + D_2 \frac{\partial^4 w}{\partial x_2^4} + \rho\, h\, \frac{\partial^2 w}{\partial t^2} + \frac{E_1}{1 - \nu_{12}\nu_{21}} \frac{w\, h}{R^2} = q. \tag{6.18}$$

Comparing our result with the plate equation 5.27 it is apparent, that they differ only in the term

$$\frac{E_1}{1 - \nu_{12}\nu_{21}} \frac{w\, h}{R^2}. \tag{6.19}$$

This term contains the deflection only but no derivatives. Thus, it is effortless to convert the functional transformation model of plate with periodic boundary condition into the model of the cylindrical shell. The transformation kernels remain the same, the imaginary part of the poles alters only, as we will see.

This equation can be adapted to variable thickness similar to the plate equation, but

also an other generalization can be done, by which we are able to describe general, in two direction curved shells too. This will be presented in the next section.

It is important to note, that we performed a strong simplification in this section, which causes an exaggeration of the stiffness arising due the curvature. In our model every point of the shell moves radially only, and it is apparent that the mode shapes and modal frequencies will be altered compared to the real one for this reason.

6.2 Shells with Variable Curvature

During the development of the shell equation we considered a differential element of the shell only. Thus we based our equation upon local properties of the shell, and the value of R can be treated as a local value. We did not have to know anything about the values of R in the adjacent points, thus it can change point by point. Thus our model is capable to describe shells with variable radius of curvature, where

$$R = R(x_1, x_2). \tag{6.20}$$

Due to the symmetry the curvature in direction x_2 can be considered in the same way. Thus the model can be adapted to shells curved in both directions, and possessing variable curvature.

Let us introduce the notations $R_1 = R_1(x_1, x_2)$ and $R_2 = R_2(x_1, x_2)$ for the radius of curvatures in directions x_1 and x_2 respectively. This way we get for the strains that

$$\epsilon_1 = \frac{w}{R_1} - z\frac{\partial^2 w}{\partial x_1^2}, \tag{6.21a}$$

$$\epsilon_2 = \frac{w}{R_2} - z\frac{\partial^2 w}{\partial x_2^2}, \tag{6.21b}$$

$$\gamma_{12} = \frac{\partial}{\partial x_2}\left(\frac{wx_1}{R_1}\right) + \frac{\partial}{\partial x_1}\left(\frac{wx_2}{R_2}\right) - 2z\frac{\partial^2 w}{\partial x_1 \partial x_2}, \tag{6.21c}$$

from which the stresses are

$$\sigma_1 = \frac{E_1}{1-\nu_{12}\nu_{21}}\left(\frac{w}{R_1} - z\frac{\partial^2 w}{\partial x_1^2} + \nu_{21}\frac{w}{R_2} - \nu_{21}z\frac{\partial^2 w}{\partial x_2^2}\right), \tag{6.22a}$$

$$\sigma_2 = \frac{E_2}{1-\nu_{12}\nu_{21}}\left(\frac{w}{R_2} - z\frac{\partial^2 w}{\partial x_2^2} + \nu_{12}\frac{w}{R_1} - \nu_{12}z\frac{\partial^2 w}{\partial x_1^2}\right), \tag{6.22b}$$

$$\tau_{12} = G_{12}\left(\frac{\partial}{\partial x_2}\left(\frac{wx_1}{R_1}\right) + \frac{\partial}{\partial x_1}\left(\frac{wx_2}{R_2}\right) - 2z\frac{\partial^2 w}{\partial x_1 \partial x_2}\right). \tag{6.22c}$$

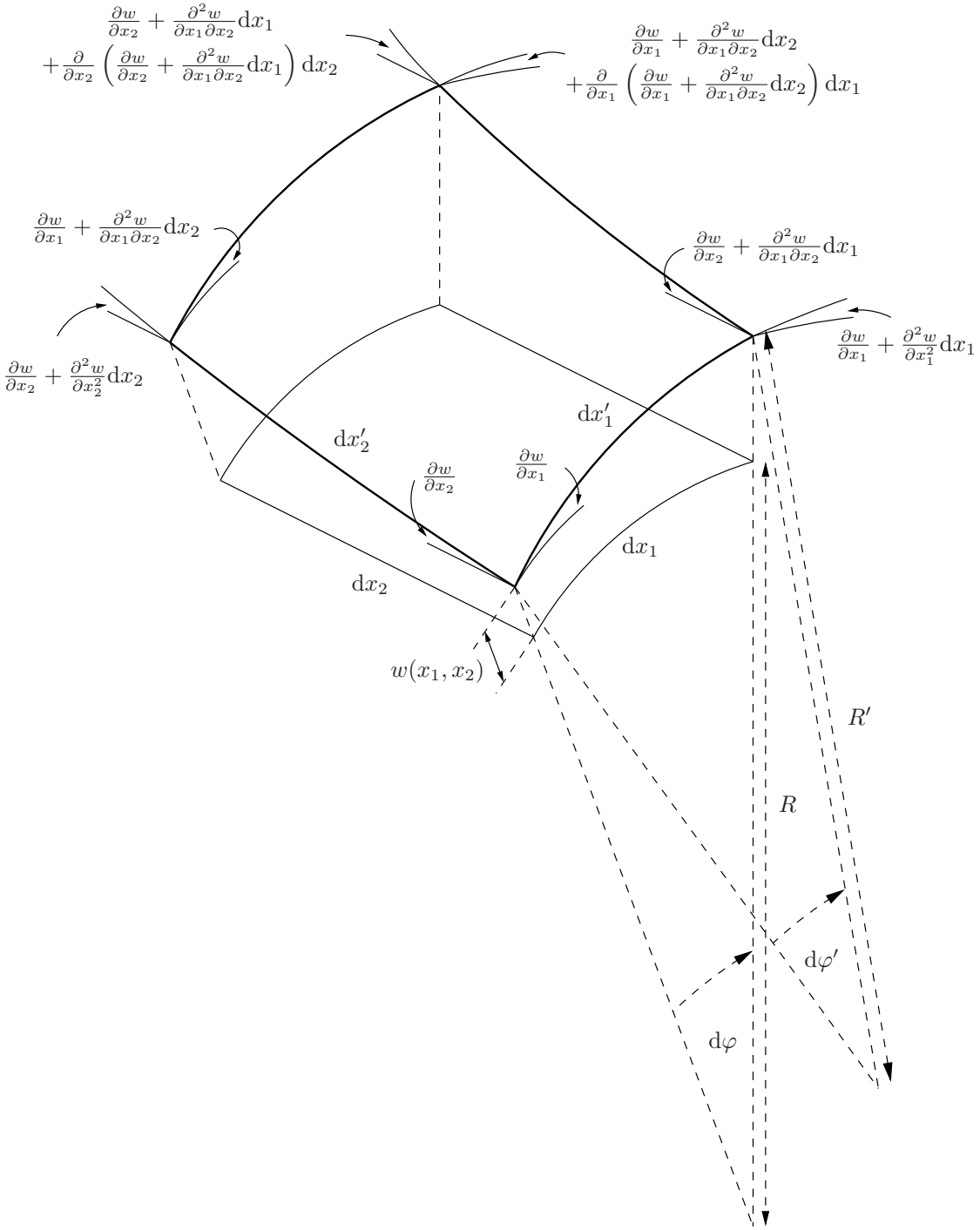

Figure 6.2: *The deformed neutral plane of the cylindrical shell and the slopes on the edges.*

The in-plane force densities according to these stresses are

$$N_1 = \frac{E_1 h}{1 - \nu_{12}\nu_{21}} \left(\frac{w}{R_1} + \nu_{21} \frac{w}{R_2} \right) \tag{6.23a}$$

$$N_2 = \frac{E_2 h}{1 - \nu_{12}\nu_{21}} \left(\frac{w}{R_2} + \nu_{12} \frac{w}{R_1} \right) \tag{6.23b}$$

$$N_{12} = G_{12} h \left(\frac{\partial}{\partial x_2} \left(\frac{w x_1}{R_1} \right) + \frac{\partial}{\partial x_1} \left(\frac{w x_2}{R_2} \right) \right). \tag{6.23c}$$

Due to the mutual symmetry of directions x_1 and x_2 Newton's second law in radial direction gives in this case

$$\frac{\partial Q_1}{\partial x_1} + \frac{\partial Q_2}{\partial x_2} - \frac{N_1}{R_1} - \frac{N_2}{R_2} + q = \rho\, h\, \frac{\partial^2 w}{\partial t^2}. \tag{6.24}$$

We arrive at the equation of general shells by substituting the in-plane force densities from equation (6.23)

$$\begin{aligned} q = {} & D_1 \frac{\partial^4 w}{\partial x_1^4} + 2 D_{12} \frac{\partial^4 w}{\partial x_1^2 \partial x_2^2} + D_2 \frac{\partial^4 w}{\partial x_2^4} + \rho\, h\, \frac{\partial^2 w}{\partial t^2} \\ & + \frac{E_1\, h}{1 - \nu_{12}\nu_{21}} \left(\frac{w}{R_1^2} + \nu_{21} \frac{w}{R_1 R_2} \right) + \frac{E_2\, h}{1 - \nu_{12}\nu_{21}} \left(\frac{w}{R_2^2} + \nu_{12} \frac{w}{R_1 R_2} \right). \end{aligned} \tag{6.25}$$

This equation can be simplified in the case of isotropy too, and also variable thickness can be introduced. Both can be executed in the same way as in the case of the plate. The in-plane force densities in the last two terms are not differentiated, thus cause no difficulty.

Chapter 7

Application of the Model to Shells

This section presents the second step of physics-based modeling, which is the solution of the differential equations derived in the preceding two chapters, with given initial and boundary conditions and excitation, respectively. The functional transformation method is applied, but the transformation kernels are determined by means of the finite different method.

Although the determined shell equations are capable to describe general curved shells, we focus on shells with cylindrical symmetry. A cylindrical shell with constant thickness is considered first, then the model is adapted to arbitrary variable thickness and along the height variable cross-section. In this way we can try to apply our model to bell shaped shells.

Not all the steps of the functional transformation method need to be executed again, it is enough to compute the coefficients of the filters and the transformation kernels, since these determine the filter bank completely. Practically, the solution of the Sturm–Liouville eigenvalue problem is our main problem.

7.1 Cylindrical Shell

Although the cylindrical shell with constant cross-section can be treated as the model of the tubular bell, it is more expedient to base the model on a beam equation, since the dominant modal frequencies of the tubular bell are closely related to the ones of the beam equation (see [3]). The modes arising due to the vibration of the tube as a shell play not an important role in the sound.

We set out from the cylindrical shell in spite of these considerations, because it is a relatively simple example to examine and introduce our model whereby. Furthermore it can converted to the more general bell shaped shell.

Let us thus consider the governing equation of the cylindrical shell (6.18). We are not concerning the losses for the moment, because we are interested in the modal frequencies and mode shapes mostly. Thus our starting-point is the appropriately rearranged equation

$$S_1 \frac{\partial^4 w}{\partial x_1^4} + 2S_{12} \frac{\partial^4 w}{\partial x_1^2 \partial x_2^2} + S_2 \frac{\partial^4 w}{\partial x_2^4} + \frac{\partial^2 w}{\partial t^2} + Fw = e, \tag{7.1}$$

where

$$S_1 = \frac{D_1}{\rho\, h} \quad , \quad S_{12} = \frac{D_{12}}{\rho\, h} \quad , \quad S_2 = \frac{D_2}{\rho\, h} \quad , \quad F = \frac{E_1}{\rho(1-\nu_{12}\nu_{21})R^2} \quad , \quad e = \frac{q}{\rho\, h}. \tag{7.2}$$

Initial & boundary conditions: We have to lay down the boundary and initial conditions too. The initial conditions are now and hereinafter the followings:

$$w(x_1, x_2, t)\big|_{t=0} = 0, \tag{7.3a}$$

$$\left.\frac{\partial w(x_1, x_2, t)}{\partial t}\right|_{t=0} = 0, \tag{7.3b}$$

thus the shell is in rest at the beginning. The boundary conditions can be determined according to the physical constraints on the edges. Since the shell is constructed by locking the opposite edges, the moment, shear and in-plane force densities have to cross this connection continuously, that is

$$M_1|_{x_1=0} = M_1|_{x_1=L_1}\,, \tag{7.4a}$$

$$M_{12}|_{x_1=0} = M_{12}|_{x_1=L_1}\,, \tag{7.4b}$$

$$Q_1|_{x_1=0} = Q_1|_{x_1=L_1}\,, \tag{7.4c}$$

$$N_1|_{x_1=0} = N_1|_{x_1=L_1}\,, \tag{7.4d}$$

$$N_2|_{x_1=0} = N_2|_{x_1=L_1}\,, \tag{7.4e}$$

$$N_{12}|_{x_1=0} = N_{12}|_{x_1=L_1}\,, \tag{7.4f}$$

where $L_1 = 2R\pi$. The other two edges are so-called free edges, here, the moment and shear force densities have to be equal to zero since external forces do not act on them, that is

$$M_2|_{x_2=0,L_2} = 0, \tag{7.5a}$$

$$M_{12}|_{x_2=0,L_2} = 0, \tag{7.5b}$$

$$Q_2|_{x_2=0,L_2} = 0. \tag{7.5c}$$

It can be shown, that the conditions on shear moment density M_{12} and shear force densities Q_i combine and give a single condition[1], which is by means of equations (6.11), (6.12) and

[1] For the sake of this one has to express M_{12} by means of force couples perpendicular to the middle plane. These with Q_i form the quantity V_i. See [5] or [19].

(6.8c) the following:

$$V_i = Q_i - \frac{\partial M_{12}}{\partial x_j} = -\frac{\partial}{\partial x_i}\left[D_i\left(\frac{\partial^2 w}{\partial x_i^2} + \nu_{ji}\frac{\partial^2 w}{\partial x_j^2}\right)\right] - 4\frac{\partial}{\partial x_j}\left(D_k\frac{\partial^2 w}{\partial x_i \partial x_j}\right), \quad i,j = \{1,2\}, \quad i \neq j. \tag{7.6}$$

We are able now to express the boundary conditions by means of the partial derivatives of w, which are according to (7.6), (6.8a), (6.8b) and (6.13)

$$\begin{aligned} -V_1|_{x_1=0} &= \frac{\partial}{\partial x_1}\left[D_1\left(\frac{\partial^2 w}{\partial x_1^2} + \nu_{21}\frac{\partial^2 w}{\partial x_2^2}\right)\right] + 4\frac{\partial}{\partial x_2}\left(D_k\frac{\partial^2 w}{\partial x_1 \partial x_2}\right)\Bigg|_{x_1=0} = \\ &= -V_1|_{x_1=L_1} = \frac{\partial}{\partial x_1}\left[D_1\left(\frac{\partial^2 w}{\partial x_1^2} + \nu_{21}\frac{\partial^2 w}{\partial x_2^2}\right)\right] + 4\frac{\partial}{\partial x_2}\left(D_k\frac{\partial^2 w}{\partial x_1 \partial x_2}\right)\Bigg|_{x_1=L_1}, \end{aligned} \tag{7.7a}$$

$$\begin{aligned} -M_1|_{x_1=0} &= D_1\left(\frac{\partial^2 w}{\partial x_1^2} + \nu_{21}\frac{\partial^2 w}{\partial x_2^2}\right)\Bigg|_{x_1=0} = \\ &= -M_1|_{x_1=L_1} = D_1\left(\frac{\partial^2 w}{\partial x_1^2} + \nu_{21}\frac{\partial^2 w}{\partial x_2^2}\right)\Bigg|_{x_1=L_1}, \end{aligned} \tag{7.7b}$$

$$-V_2|_{x_2=0,L_2} = \frac{\partial}{\partial x_2}\left[D_2\left(\frac{\partial^2 w}{\partial x_2^2} + \nu_{12}\frac{\partial^2 w}{\partial x_1^2}\right)\right] + 4\frac{\partial}{\partial x_1}\left(D_k\frac{\partial^2 w}{\partial x_1 \partial x_2}\right)\Bigg|_{x_2=0,L_2} = 0, \tag{7.7c}$$

$$-M_2|_{x_2=0,L_2} = D_2\left(\frac{\partial^2 w}{\partial x_2^2} + \nu_{12}\frac{\partial^2 w}{\partial x_1^2}\right)\Bigg|_{x_2=0,L_2} = 0. \tag{7.7d}$$

The initial and boundary value problem is thus given. The first step if the functional transformation method is to apply the Laplace Transformation on the equation.

The Laplace-transform This can be carried out in the same way as in the case of the string. Since the spatial and temporal derivatives are independent, the spatial derivatives can be liberated from the integral of the Laplace transform. The resulting boundary value problem, taken the initial conditions into account too, is

$$S_1\frac{\partial^4 W}{\partial x_1^4} + 2S_{12}\frac{\partial^4 W}{\partial x_1^2 \partial x_2^2} + S_2\frac{\partial^4 W}{\partial x_2^4} + s^2 W + FW = E, \tag{7.8}$$

where $W(x_1, x_2, s) = \mathcal{L}\{w(x_1, x_2, t)\}$ and $E(x_1, x_2, s) = \mathcal{L}\{e(x_1, x_2, t)\}$. The boundary conditions on $W(x_1, x_2, s)$ remain the same as the ones on $w(x_1, x_2, t)$ thanks to the linearity of the Laplace transform.

Sturm–Liouville-transform We arrived thus at the main task, the determination of the Sturm–Liouville transform. For the sake of this we have to solve the eigenvalue-problem of the adjoint differential operator (see section 3.2.2). The differential operator is in this case

$$L\{.\} = S_1\frac{\partial^4}{\partial x_1^4} + 2S_{12}\frac{\partial^4}{\partial x_1^2 \partial x_2^2} + S_2\frac{\partial^4}{\partial x_2^4}, \tag{7.9}$$

while the the corresponding boundary conditions are given by (7.7). The eigenvalue problem

$$\tilde{L}\{K\} = \beta(n)K \tag{7.10}$$

concerning $K(x_1, x_2, n)$ is hardly solvable analytically, while in more complicated cases, such as variable thickness or curvature, it is unsolvable. Hence, we use the finite difference method for the solution. We construct the matrix $\mathbf{L}$ corresponding to the differential operator L and the boundary conditions. The adjoint $\tilde{\mathbf{L}}$ of this will be the matrix corresponding to the adjoint differential operator. The eigenfunctions of this are $K(x_1, x_2, n)$, while the corresponding eigenvalues give the values of $\beta(n)$. Note that the $K(x_1, x_2, n)$ functions will be given in the vector form, introduced in section 4.1.4.

For the help of the construction of matrix $\mathbf{L}$ in MatLab we define a structure which stores the i, j coordinates, the $n = (i-1)n_1 + n_2$ serial number of the vector form, and the numbers of those adjacent points, which are concerned by the finite difference stencil for each points. It is worthwhile to construct a matrix which gives the serial number n of each point on the basis of its coordinates i, j. With these help structures, those rows of the matrix $\mathbf{L}$, which belong to points far from the boundaries can be filled up by the help of a relatively short MatLab code. In those points, however, which are close to the boundaries enough to let the stencil point out from the domain, we have to distort the stencil according the boundary conditions. On the both meeting edges we have to set the fields containing the numbers of the adjacent points such a way that they refer to the corresponding points on the opposite edge. In this way all the boundary conditions on these edges are satisfied. Dealing with the two free edges is rather complicated. We used the method of virtual points, which resulted in long MatLab code based on conditional executions.

The matrix $\mathbf{L}$ corresponding to the operator L can thus be constructed. The adjoint of this is simply the transpose due to the finite size and real elements. Since our matrices contain relatively few non-zero elements it would be worthwhile to treat them as sparse matrices and to solve the eigenvalue problem by the MatLab function `eigs`. According to our experiences, however, the function `eigs` uses such an iteration algorithm, which results not in a biorthogonal system for the eigenvectors of $\mathbf{L}$ and $\tilde{\mathbf{L}}$. Hence we use the the function `eig` with big memory and computation demand. If the matrix $\tilde{\mathbf{L}}$ is given, the eigenvectors K and eigenvalues $\beta(n)$ can be computed by the help of the following code for example, where `n_modes` is the number of the modelled modes (n_{max}), while `vect_uns` and `value`

```
n_modes=800;
[vect_uns,value]=eig(L','nobalance');
[eigvalues,indices] = sort(diag(value));
vect = vect_uns(:,indices);
K=zeros(n2,n1,n_modes);
beta=eigvalues(1:n_modes);
for i=(1:1:15)
  K(:,:,i) = (reshape(vect(:,i),n1,n2))';
end
```

are the eigenvectors and eigenvalues determined by `eig`. These have to be sorted on the

basis of the eigenvalues, this is done by the following two commands. Vector `beta` contains the first n_{max} eigenvalues $(\beta(1), \beta(2), \ldots \beta(n_{max}))$, while the three-dimensional `K` contains the eigenvectors in two-dimensional form. This latter is filled up in the iteration.

We will need functions $J(x_1, x_2, n)$ too, to perform the inverse Sturm–Liouville transform, the approximation of these can be determined in the same way. These are actually the mode shapes. The first fifteen of them, that is functions $(J(x_1, x_2, 1),\ J(x_1, x_2, 2),\ -\ldots J(x_1, x_2, 15))$ are depicted on figure 7.1 The first two modes are so-called rigid body modes, which reflects the fact, that one of the possible transverse modes of the plate[2] (on which our shell model is based on) is the shifting without distortion. If one unfolds the modes in mind, it becomes apparent that these are the transversal shiftings of the plate. Since the plate has no resistance against this shifting, the corresponding frequency is zero.

The first of the displayed frequencies corresponds to the simple coiled plate, while the second one to our shell model. It is apparent, that the relative distances of the modal frequencies decreased, this happened due to the inaccuracy of the model. As we mentioned earlier, the model exaggerates the stiffness arising due to the curvature. In the case of the bell shaped shell the situation will be much better.

There are more mode shape pairs on the figure with identical frequencies, that is eigenvalues, these are the so-called degenerate modes. This means in the language of the eigenvalue-problems that to the eigenvalue belongs an eigensubspace, instead of a single eigenvector. This subspace is spanned by the degenerate eigenvectors. In this case every linear combination of these eigenvectors are solution of the eigenvalue-problem with the same eigenvalue. Degeneracy arises in this case due to the cylindrical symmetry of the shell. Namely, every non-symmetrical mode can be directed arbitrary, and at least two vectors are needed to describe them. This accounts for the fact that the order of degeneracy is in our case always two.

The MatLab command `eig` gives on certain reason complex valued eigenvectors in the case of several degenerated mode shape pairs, in these cases the real parts coincide and the imaginary parts differ only. Designating the vectors by J_1' and J_2', they have thus the form of

$$J_1' = a + jb_1, \tag{7.11a}$$

$$J_2' = a + jb_2. \tag{7.11b}$$

$$\tag{7.11c}$$

Since every pair of linearly independent vectors of the subspace suits, we can rewrite these

[2]Since the term FW is not considered yet, our model describes a plate for the present, with the boundary conditions of the cylindrical shell. This model is identical with the one used in [13] and [6] apart from the mixed derivative and some refinements of the boundary conditions.

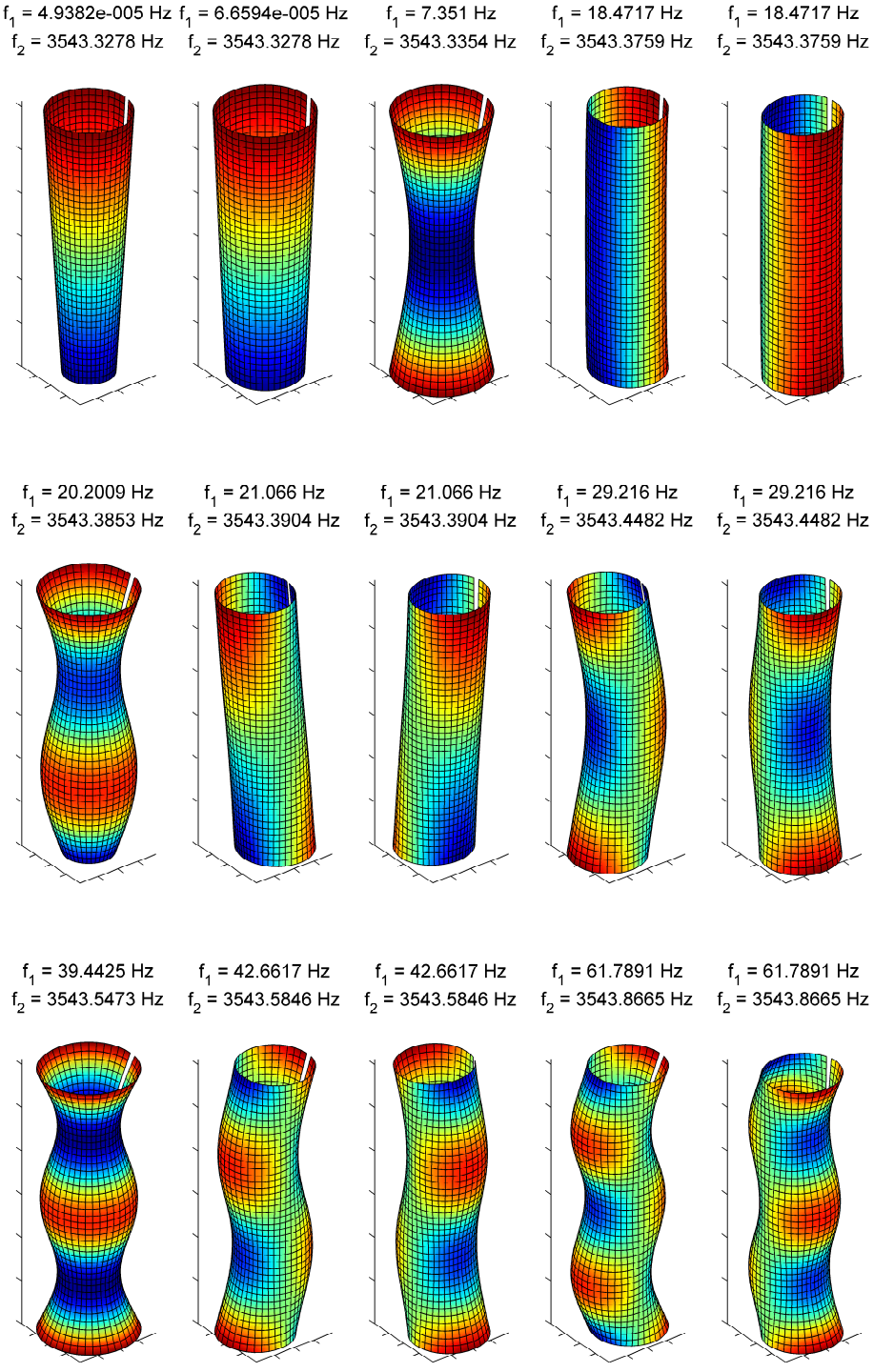

Figure 7.1: *Several modes and the corresponding frequencies of a cylindrical shell.*

mode shapes to real valued ones. Let the new modes be

$$J_1 = -j(J_1' - J_2') = b_1 - b_2, \tag{7.12a}$$

$$J_2 = \left(\frac{b_2}{b_2 - b_1}\right) J_1' - \frac{b_1}{b_2} J_2' = a, \tag{7.12b}$$

$$\tag{7.12c}$$

thus the difference of the imaginary parts, and the real part. This can be carried out by means of the following code in MatLab.

```
for q=1:n_modes
  for r=q+1:n_modes
    if abs(beta(q)-beta(r))<1 && ...
       abs(max(max(real(J(:,:,q))./real(J(:,:,r))))-...
       min(min(real(J(:,:,q))./real(J(:,:,r)))))<1e-3,
      J(:,:,r) = imag(J(:,:,q))-imag(J(:,:,r));
      J(:,:,q) = real(J(:,:,q));
    end
    if abs(beta(q)-beta(r))<1 && ...
       abs(max(max(real(K(:,:,q))./real(K(:,:,r))))-...
       min(min(real(K(:,:,q))./real(K(:,:,r)))))<1e-3,
      K(:,:,r) = imag(K(:,:,q))-imag(K(:,:,r));
      K(:,:,q) = real(K(:,:,q));
    end
  end
end
```

An other problem is that the computed eigenvectors of $\mathbf{L}$ and $\tilde{\mathbf{L}}$ corresponding to the multiple eigenvalues are not biorthogonal, that is

$$\langle K_1'(x_1, x_2, n), J_2(x_1, x_2, n)\rangle \neq 0, \tag{7.13a}$$

$$\langle K_2'(x_1, x_2, n), J_1(x_1, x_2, n)\rangle \neq 0. \tag{7.13b}$$

In this case we can proceed similar to the Gram–Schmidt process of orthogonalisation[3]. Let us thus alter the degenerate mode pairs K' to form a biorthogonal system with the corresponding vectors J. It can be shown that seeking the function pair K_1 and K_2 in the form of

$$K_1(x_1, x_2, n) = K_1'(x_1, x_2) + aK_2'(x_2, x_1), \tag{7.14a}$$

$$K_2(x_1, x_2, n) = K_2'(x_1, x_2) + bK_1(x_2, x_1), \tag{7.14b}$$

than the choice of

$$a = -\frac{\langle K_1', J_2\rangle}{\langle K_2', J_2\rangle}, \tag{7.15a}$$

$$b = -\frac{\langle K_2', J_1\rangle}{\langle K_1, J_1\rangle} \tag{7.15b}$$

results in an appropriate pair of functions. This orthogonalisation is carried out by the following MatLab code.

[3]See for example in [2]

```
found=0;
for q=1:n_modes
  degen_num=1;
  V=K(:,:,q);
  W=J(:,:,q);
  for r=(q+1):n_modes
    if abs(beta(q)-beta(r))<1e-2,
      Vold = V;
      Wold = W;
      degen_num=degen_num+1;
      V=zeros(n2,n1,degen_num);
      W=zeros(n2,n1,degen_num);
      V(:,:,1:degen_num-1)=Vold;
      V(:,:,degen_num)=K(:,:,r);
      W(:,:,1:degen_num-1)=Wold;
      W(:,:,degen_num)=J(:,:,r);
      num_r=[q,r];
      found=1;
    end
  end
  if found==1
    found=0;
    a = -num_inner_product(V(:,:,1),W(:,:,2),d1,d2)/...
      num_inner_product(V(:,:,2),W(:,:,2),d1,d2);
    K(:,:,num_r(1)) = V(:,:,1)+a*V(:,:,2);
    b = -num_inner_product(V(:,:,2),W(:,:,1),d1,d2)/...
      num_inner_product(V(:,:,1),W(:,:,1),d1,d2);
    K(:,:,num_r(2)) = V(:,:,2)+b*V(:,:,1);
  end
end
```

We have determined the sampled approximations of the eigenfunctions $K(x_1, x_2, n)$ and $J(x_1, x_2, n)$ and the corresponding eigenvalues $\beta(n)$ we can thus proceed the next step of the functional transformation method and determine the multidimensional transfer function.

Note that there are several modes depicted on figure 7.1, which are the bending modes of a beam at first sight. These would be so in the case of a completely correct model, which deals with the in-plane motion too, but now, these only are the modes of the plate with one period along the circumference, unfortunately. The real bending modes of the beam have much higher frequencies.

The multidimensional transfer function Let us transcribe equation (7.8) to multidimensional transfer function form

$$\beta(n)\overline{W} + s^2\overline{W} + F\overline{W} = \overline{E}, \tag{7.16}$$

that is

$$\frac{\overline{W}}{\overline{E}} = \frac{1}{s^2 + \beta(n) + F}. \tag{7.17}$$

This equation corresponds to (3.21), but $d_1 s$ is missing now, as we do not deal with the losses. Accordingly, the imaginary part of the poles are

$$\omega(n) = \sqrt{\beta(n) + F}, \tag{7.18}$$

while the real parts are equal to zero ($\sigma(n) = 0$) due to the absence of losses.

We do not have to follow the steps of the functional transformation method any further,

as they are the same as in the case of the string. As a result we obtain the coefficients of the filters, and the weighting factors of the outputs on the grounds of the same formulas. These are the followings

$$c_1(n) = 2\cos\left(\sqrt{\beta(n)+F}\,T\right), \tag{7.19a}$$

$$c_2(n) = -1, \tag{7.19b}$$

$$a(x_1,x_2,n) = \frac{1}{N(n)}\frac{\sin\left(\sqrt{\beta(n)+F}\,T\right)}{\sqrt{\beta(n)+F}}\bar{f}_x(n)J(x_1,x_2,n), \tag{7.19c}$$

where

$$N(n) = \langle J(x_1,x_2,n), K(x_1,x_2,n)\rangle, \tag{7.20a}$$

$$\bar{f}_x(n) = \langle f_x(x_1,x_2), K(x_1,x_2,n)\rangle. \tag{7.20b}$$

Since $K(x_1,x_2,n)$ and $J(x_1,x_2,n)$ are numerically given functions, the integral of the inner product have to be executed numerically. The simplest method of numerical integration is the midpoint rule, which means the multiplication of the matrices element by element and weighting by the differential areas. This is a good approximation in the case of the first modes, which are the most important for us. Our inner product function in MatLab is thus the following, where `f` and `g` are the matrices corresponding the functions we want

```
function pr = num_inner_product(f,g,d1,d2)
pr = sum(sum(f.*g*d1*d2));
```

to multiply, while `d1` and `d2` the step-sizes of the partition.

In the MatLab code of the functional transformation method we have to determine the former two inner products first, then the filter parameters for each filter. The value of $a(x_1,x_2,n)$ has to be calculated in the points, where the motion of the body is sought. If we want to visualise the oscillation, we have to determine a filter for each point, calculate the motion in the points, and depict the obtained values in an appropriate way. As an example a few milliseconds after the strike is depicted on figure 7.2. Note that for the visualisation we used the simple coiled plate model, since the other one has such a big dispersion that the wavefront can not be recognised on it.

If we are concerned in the resulting voice only, it is enough to calculate the motion in a few points and take a weighted sum of them[4] Note that the factor F of our shell model, representing the stiffness arising due the curvature, appears in the formula of $\omega(n)$ only. This means that each modal frequency is shifted upwards, but the mode shapes are unaffected. The resulting oscillation differs, however greatly. If we leave the factor F, that is we consider the coiled plate model, the frequencies corresponding to the rigid body modes becomes zero, and thus these modes increase to the infinity, if they are excited. In the case of the plate this is correct. In the case of the cylindrical shell, however, this

[4]If we would investigate one point only, all the modes that have a node in that point would fall out from the resulting sound.

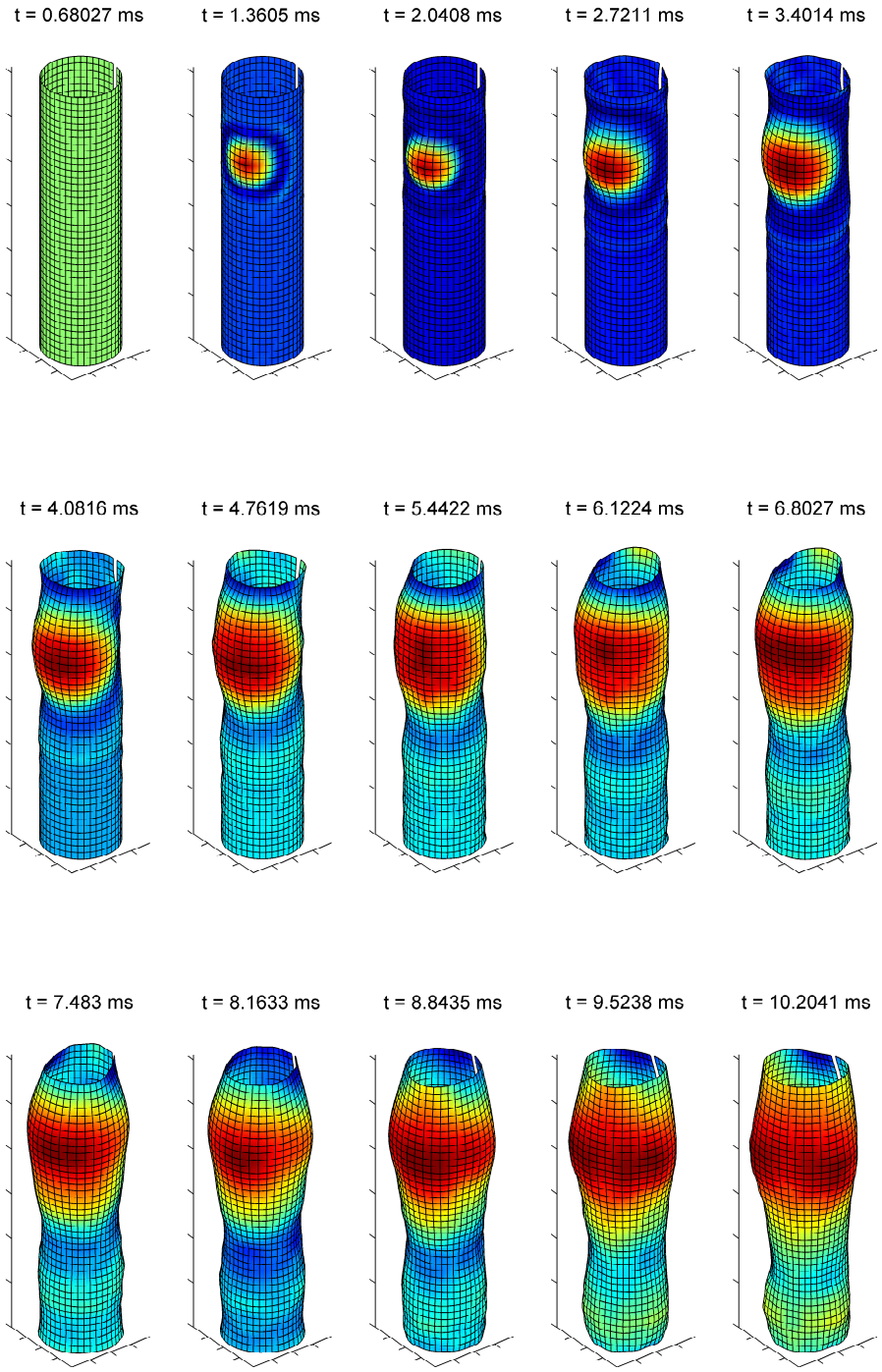

Figure 7.2: *The vibration patter of the coiled plate after the strike, computed by the help of the functional transformation method.*

corresponds to the infinite growth or fall of the radius (this can be seen on figure 7.2 too). This is unnatural, and our shell equation offers a solution to this. Namely, if we take F in the formula of $\omega(n)$ into account, then the frequencies of the rigid body modes becomes nonzero, and the infinite growth or fall is avoided, since the rigid body modes start to oscillate too.

7.1.1 Variable Thickness

If we want to model the vibrations of the cylindrical shell with variable thickness of wall, we have to modify our finite difference matrix, because our starting point is in this case equation (6.17) instead of (6.18), where the shear force densities are

$$Q_1 = \frac{\partial M_1}{\partial x_1} + \frac{\partial M_{12}}{\partial x_2} = -\frac{\partial}{\partial x_1}\left[D_1\left(\frac{\partial^2 w}{\partial x_1^2} + \nu_{21}\frac{\partial^2 w}{\partial x_2^2}\right)\right] - \frac{\partial}{\partial x_2}\left[2D_k\frac{\partial^2 w}{\partial x_1 \partial x_2}\right], \tag{7.21a}$$

$$Q_2 = \frac{\partial M_2}{\partial x_2} + \frac{\partial M_{12}}{\partial x_1} = -\frac{\partial}{\partial x_2}\left[D_2\left(\frac{\partial^2 w}{\partial x_2^2} + \nu_{12}\frac{\partial^2 w}{\partial x_1^2}\right)\right] - \frac{\partial}{\partial x_1}\left[2D_k\frac{\partial^2 w}{\partial x_1 \partial x_2}\right]. \tag{7.21b}$$

Here the thickness h and thus D_1, D_2 and D_k are each space dependent. Executing the partial derivatives we get the coefficients of the various partial derivatives of w. These terms are certain functions of the upper space dependent parameters and their derivatives. Thus it is worthwhile to construct a MatLab code which generates these derivatives. For this sake the values of D_i and h are stored in matrices, and we generate the derivatives by the help of shiftings. Because of the great number of the occurring types of derivative the resulting code is a relatively long on conditional execution based function, the first rows are copied here. The columns and rows of the input `Min` and output matrices `Mout`

```
function Mout=finitediff_SLEP_old(Min,dim,n,m,d1,d2,n1,n2)

            switch dim          %the independent variable(s), with respect to...
                                %the derivative should be taken
                case 1
                    Mout=(Min(n,mod(m+1-1,n1)+1)...
                        -Min(n,mod(m-1-1,n1)+1))/(2*d1);
                case 2
                    Mout=(Min(min(n+1,n2),mod(m-1,n1)+1)...
                        -Min(max(n-1,1),mod(m-1,n1)+1))/(2*d2);
                case 11
                    Mout=(Min(n,mod(m+1-1,n1)+1)...
                        -2*Min(n,mod(m-1,n1)+1)...
                        +Min(n,mod(m-1-1,n1)+1))/d1^2;
                case 22
                    Mout=(Min(min(n+1,n2),mod(m-1,n1)+1)...
                        -2*Min(n,mod(m-1,n1)+1)...
                        +Min(max(n-1,1),mod(m-1,n1)+1))/d2^2;
                case {12,21}
                    Mout=(Min(min(n+1,n2),mod(m+1-1,n1)+1)...
                        -Min(max(n-1,1),mod(m+1-1,n1)+1)...
                        -Min(min(n+1,n2),mod(m-1-1,n1)+1)...
                        +Min(max(n-1,1),mod(m-1-1,n1)+1))/(4*d1*d2);
                    .
                    .
```

correspond to the coordinates x_1 and x_2. With the help of the expression `mod(m-1,n1)+1` in the second indices we can address the adjacent points on the meeting edges. On the free

edges it is undecided how to determine the values of the thickness. It is seems evident to treat the thickness zero beyond the edges, but in the case of constant thickness it is always treated constant beyond the edges too. We also considered the thickness constant at the boundaries, because it simplified the resulting MatLab code greatly. The expressions of type `max(n-1,1)` in the first indices are accountable for this treatment.

Thus the matrix of the difference operator can be created in this case also. We use MatLab to solve the eigenvalue-problem again.

As an application let us break the cylindrical symmetry of the system, and let the thickness be variable around the circumference

$$h(x_1, x_2) = C_1 + C_2 \cos(\frac{2\pi}{L_1} x_1), \tag{7.22}$$

where $C_2 < C_1$ are arbitrary constants. The degenerate mode pairs have to disappear in this case, since they arose even due to the cylindrical symmetry. The arisen mode shapes and corresponding modal frequencies can be investigated in figure 7.3. It is apparent that each modal frequencies are different as we expected.

7.2 Cylindrical Shell with Variable Radius of Curvature (Bell)

If we want to apply our model to a bell-shaped shell, we have to generalize our MatLab code further. The filter bank of the functional transformation method remains the same, the matrix according to the differential operator alters however. Namely we have to take into account the variable cross-section too beside the variable thickness. The bell can be treated as a cylindrical shell which curvature $R = R_1$ alters along the axis of symmetry. This change in the curvature induces a curvature R_2 in the perpendicular direction. Due to the variation of the circumference the step-size Δx_1 alters too. Step-size Δx_2 could be treated constant, but for the sake of generality we consider it variable. The cylindrical symmetry remains however, thus the step-sizes are functions of coordinate x_2 only

$$\Delta x_1 = \Delta x_1(x_2), \tag{7.23a}$$

$$\Delta x_2 = \Delta x_2(x_2). \tag{7.23b}$$

We will exploit this symmetry, but the finite difference quotients get fairly complicated despite of this.

The step-sizes have to be stored in vectors, and the stencils of the difference operators will be variable. Let see two examples. The first order central difference quotients are relatively simple:

$$\left.\frac{\partial w}{\partial x_1}\right|_{(x_1,x_2)=(i\Delta x_1, j\Delta x_2)} \approx \frac{w_{i+1,j} - w_{i-1,j}}{2\Delta x_{1j}}, \tag{7.24a}$$

$$\left.\frac{\partial w}{\partial x_2}\right|_{(x_1,x_2)=(i\Delta x_1, j\Delta x_2)} \approx \frac{w_{i,j+1} - w_{i,j-1}}{\Delta x_{2j} + \Delta x_{2j-1}}, \tag{7.24b}$$

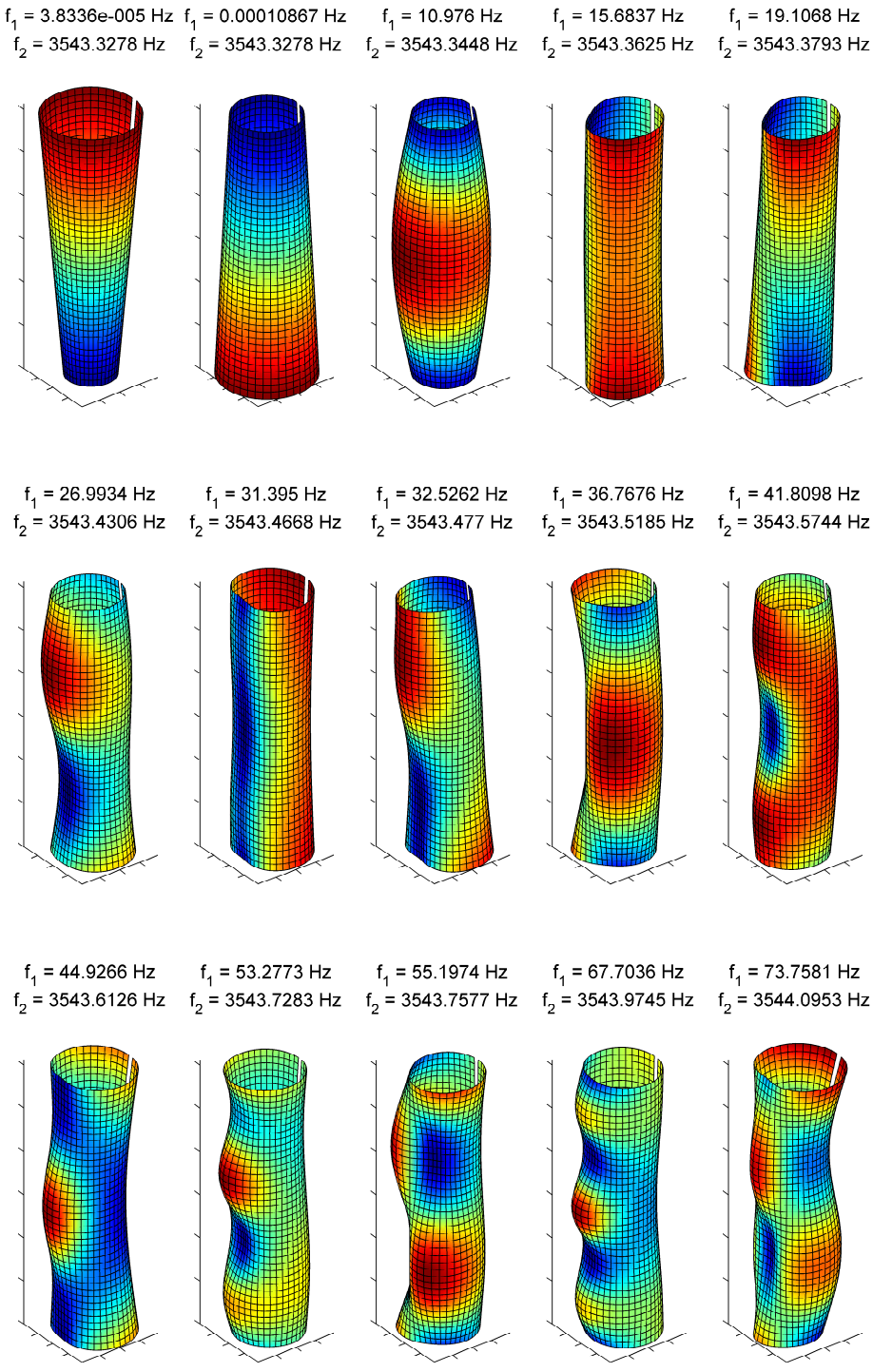

Figure 7.3: *Several mode shapes and modal frequencies of the non symmetric cylindrical shell.*

where $\Delta x_{1j} = \Delta x_1|_{x_2=j\Delta x_2}$ and $\Delta x_{2j} = \Delta x_2|_{x_2=(j+1/2)\Delta x_2}$. The second order difference quotient with respect to x_2 is yet much more complicated as earlier

$$\left.\frac{\partial^2 w}{\partial x_2^2}\right|_{(x_1,x_2)=(i\Delta x_1,j\Delta x_2)} \approx \frac{2}{\Delta x_{2j}\left(\Delta x_{2j}+\Delta x_{2j-1}\right)} w_{i,j+1} - \frac{2}{\Delta x_{2j}\Delta x_{2j-1}} w_{i,j} + \frac{2}{\Delta x_{2j-1}\left(\Delta x_{2j}+\Delta x_{2j-1}\right)} w_{i,j-1}. \tag{7.25}$$

The higher order ones are complicated increasingly. We present the code calculating the third order difference quotient with respect to x_2. Here are `d1` and `d2` vectors already and

```
function Mout=finitediff_SLEP(Min,dim,n,m,d1,d2,n1,n2)

d2M = d2(max(n-2,1));
d2m = d2(max(n-1,1));
d2p = d2(min(n,n2-1));
d2P = d2(min(n+1,n2-1));
d1m = d1(max(n-1,1));
d1p = d1(min(n+1,1));
switch dim          %the independent variable(s), with respect to...
                    %the derivative should be taken
                    .
                    .
    case 222
        Mout=Min(min(n+2,n2),mod(m-1,n1)+1) *2 /d2P /(d2P+d2p) /(d2p+d2m)...
            -2*Min(min(n+1,n2),mod(m-1,n1)+1) *2 /d2P /d2p /(d2m+d2p)...
            +Min(n,mod(m-1,n1)+1) *2 *( 1/(d2p*(d2P+d2p)*(d2m+d2p)) -...
                 1/(d2m*(d2m+d2M)*(d2m+d2p)) )...
            +2*Min(max(n-1,1),mod(m-1,n1)+1) *2 /d2m /d2M /(d2m+d2p)...
            -Min(max(n-2,1),mod(m-1,n1)+1) *2 /d2M /(d2M+d2m) /(d2m+d2p);
                    .
                    .
end
```

store the step-sizes, the variables of type `d2M` are the shifted copies of these. It is apparent, that the middle term is not zero any more.

The formulas of the boundary conditions have to be reformed according the new difference quotients too. The boundary conditions themselves remain the same except of one of the free edges. The shell of the bell is modeled up to the shoulder, where the shell can be treated as it would be clamped, thus the deflection w and its derivative with respect to x_2 is zero

$$w|_{(x_1,x_2)=(x_1,0)} = 0, \tag{7.26a}$$

$$\left.\frac{\partial w}{\partial x_2}\right|_{(x_1,x_2)=(x_1,0)} = 0. \tag{7.26b}$$

$$\tag{7.26c}$$

Our starting-point is in this case the governing equation of the universally curved shell

(6.24) which is, divided by $\rho\, h$ and Laplace transformed, the followings

$$\begin{aligned} E = &\frac{\partial^2}{\partial x_1^2}\left[S_1\left(\frac{\partial^2 W}{\partial x_1^2} + \nu_{21}\frac{\partial^2 W}{\partial x_2^2}\right)\right] + \frac{\partial^2}{\partial x_1 \partial x_2}\left[2S_k\frac{\partial^2 W}{\partial x_1 \partial x_2}\right] \\ &+ \frac{\partial^2}{\partial x_2^2}\left[S_2\left(\frac{\partial^2 W}{\partial x_2^2} + \nu_{12}\frac{\partial^2 W}{\partial x_1^2}\right)\right] + \frac{\partial^2}{\partial x_1 \partial x_2}\left[2S_k\frac{\partial^2 W}{\partial x_1 \partial x_2}\right] \\ &+ \frac{E_1}{\rho(1-\nu_{12}\nu_{21})}\left(\frac{1}{R_1^2} + \nu_{21}\frac{1}{R_1 R_2}\right)W + \frac{E_2}{\rho(1-\nu_{12}\nu_{21})}\left(\frac{1}{R_2^2} + \nu_{12}\frac{1}{R_1 R_2}\right)W + s^2 W. \end{aligned} \tag{7.27}$$

where shear force stresses are given by (7.21) and we introduced the coefficients S again. Here, the additive term arising due to the curvature is not constant, but the function of x_2

$$\begin{aligned} F(x_2) = &\frac{E_1}{\rho(1-\nu_{12}\nu_{21})}\left(\frac{1}{R_1(x_2)^2} + \nu_{21}\frac{1}{R_1(x_2)R_2(x_2)}\right) \\ &+ \frac{E_2}{\rho(1-\nu_{12}\nu_{21})}\left(\frac{1}{R_2(x_2)^2} + \nu_{12}\frac{1}{R_1(x_2).R_2(x_2)}\right) \end{aligned} \tag{7.28}$$

Accordingly, it can not be liberated from the Sturm–Liouville transform. Thus we have to consider it as the part of the spatial differential operator. It do not present any difficulty, since only a diagonal matrix has to be added to the matrix $\mathbf{L}$, which contains the values of F for each point (keeping to our convention of reshaping matrices into vectors, see section 4.1.4).

The matrix $\mathbf{L}$ of the difference operator can be constructed with these considerations again. We measured the necessary data, that is the curvature R_1 and thickness values h from a cross-section figure of a bell off. Curvature R_2 can be computed from R_1, since this latter one is represented on the cross-section by means of a function of one variable. The curvature R_2 is accordingly

$$R_2 = \left|\frac{\left[1 + \left(\frac{\mathrm{d}R_1}{\mathrm{d}l}\right)\right]^{3/2}}{\frac{\mathrm{d}^2 R_1}{\mathrm{d}l^2}}\right|, \tag{7.29}$$

where l is the height measured along the axis of symmetry. Since R_1 is a sampled function we evaluated this formula by the help of the finite difference method too.

The arisen mode shapes and modal frequencies are depicted on figure 7.4. The important modes of the bell can be found on the figure, but other type of modes appear too. If we search for the modes hum, prime and tierce[5], the frequencies of which should be in the ratio of about $(0.5 : 1 : 1,2)$, we find that in our case these are in the ratio of $(2425 : 3940 : 6260) = (0,5 : 0,81 : 1,29)$. Which is thus much better what we espected on the grounds of arisen modal frequencies of the cylindrical shell. The lowest mode is, however not the hum, but an expansion-type mode, which in the reality have a much higher frequency, since it is far harder to expand the sound ring as press it according the hume-shape. There are several other unespected modes in the figure too.

In the case of the ordinary cylindrical shell the modal frequencies where affected by the

[5]See [3] or [15] about the sound properties of the bells for example.

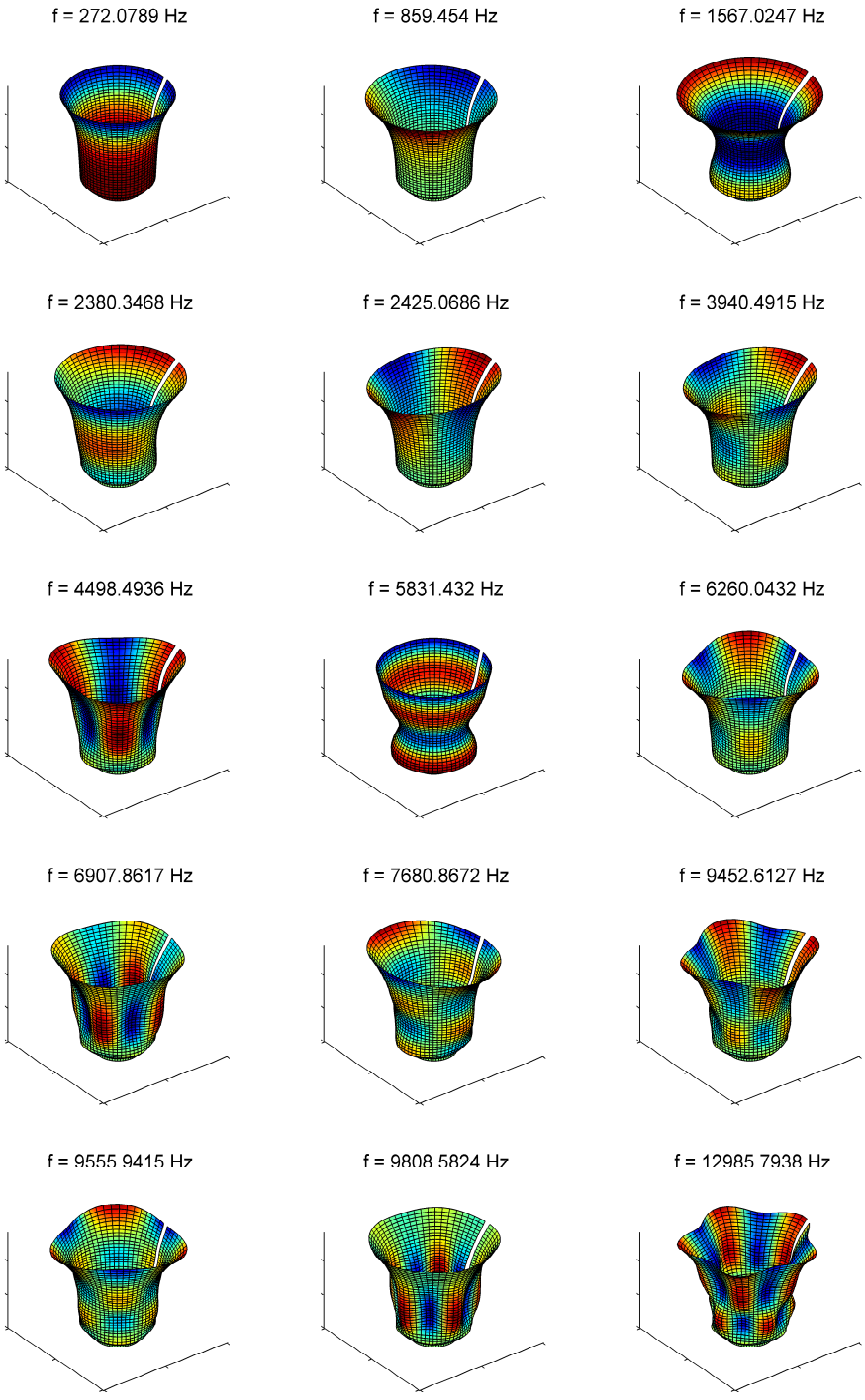

Figure 7.4: *Several mode shapes and the corresponding modal frequencies of the bell-shaped shell.*

additional term F of our shell model, here it affects the difference operator, and act on the modal frequencies and mode shapes through it.

The frequency spectrum of the synthesized sound is depicted on figure 7.5 evaluated in two different points. It is apparent how these points affect the resulting spectrum. The information about how these points have to affect the sound is hidden in the weighting factors $a(x_1, x_2, n)$ of the filters.

7.2.1 Losses

We concentrated only on the modal shapes and mode frequencies so far. However, we have to introduce the losses, if we want to produce acceptable musical sounds. According to the experience, a damping of perceptually good quality can be achieved by introducing the following two additional terms in the governing equation (see [1])

$$D_1 = d_1 \frac{\partial w}{\partial t}, \tag{7.30a}$$

$$D_2 = d_2 \frac{\partial}{\partial t} \left(\frac{\partial^2 w}{\partial x_1^2} + \frac{\partial^2 w}{\partial x_2^2} \right). \tag{7.30b}$$

The firs term causes a frequency independent damping, while the second one damps the modes with higher frequencies increasingly. The frequency independent damping can be incorporated in the same way as in the case of the string. The second term, however can not attached to the spatial differential operator, since it contains the factor s due to the Laplace transform, and this variable can not be handled by means of our numerical process.

We know, however, that this term have to appear in the real part of the poles $\sigma(n)$. In the case of the string it arose as a multiple of the square of n in the formula. This means that the damping grows with increasing n, that is with increasing frequency. We want to achieve a same behaviour in this case too, thus a possible solution is the imitate the $\sigma(n)$ of the string. Let us thus concern it as

$$\sigma(n) = \frac{1}{2} \left(d_3' n^2 - d_1 \right), \tag{7.31}$$

where d_3' is different from d_3 since the upper formula is just an approximation. If we would determine how d_3 arises in σ it would be probably a much more elaborate formula, since the mode frequencies are located unevenly. The formula of $\sigma(n)$ can be modified, however, arbitrarily, the exponent could be a fraction either for example.

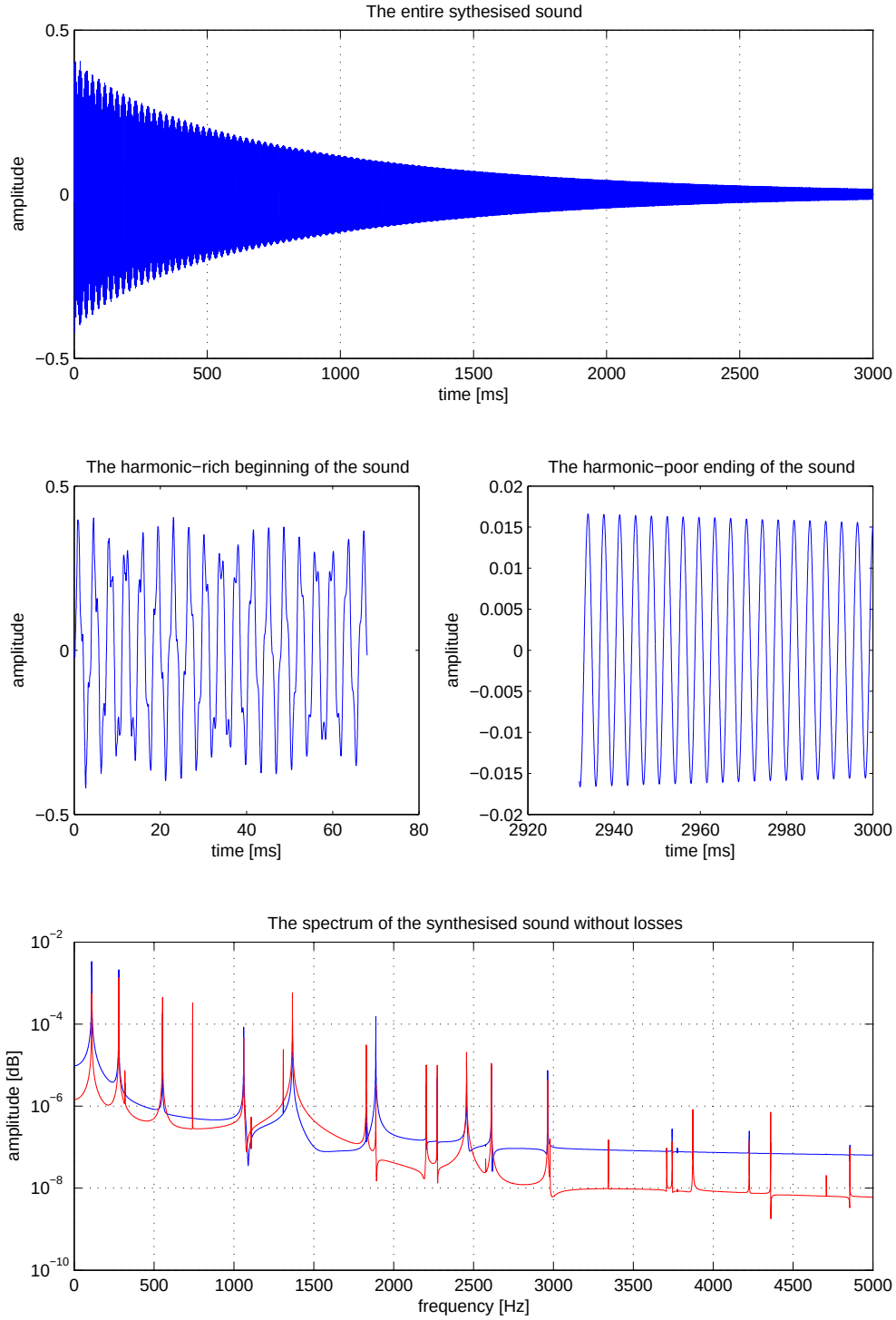

Figure 7.5: *The waveform and spectrum of the synthesized sound of bell-shaped shell.*

Chapter 8

Conclusion and Possibilities of Development

8.1 Results

We have thus managed to create a simple model for the modeling of two-dimensional vibrating bodies and to apply it to the cylindrical and the bell-shaped shell. We had to execute two main tasks for this sake, first we had to deduce an appropriate differential equation, then to solve the Sturm–Liouville eigenvalue-problem by the help of the finite difference method. Our method has proved to be operable, but we have seen its limits too.

We wanted to avoid the nonlinear system of differential equations, but to be able to represent the stiffness arising due to the curvature, for the sake of this we have constructed a simplified differential equation, in which the curvature is represented by means of a term of no derivatives. In the case of the ordinary cylindrical shell, where the factor of this term was a constant number, it influenced the modal frequencies only and shifted them unnaturally high. In the case of the bell, where the factor was space dependent, it acted through the spatial differential operator. Using our master bell cross-section we managed to obtain the frequency ratio of the main modes approximately, the modal shapes were acceptable too.

We have managed to convert the finite difference method into a form which is given by a matrix and is capable to compute the mode shapes and modal frequencies. The resulting MatLab code can be applied to arbitrary shells with variable thickness but having cylindrical symmetry. We have performed two transformations on the resulting mode shapes to let them form a biorthogonal system in every case.

The MatLab code of the filter bank of the functional transformation method is based on numerical integration according to the numerical given mode shapes, and it computes the resulting wave form, or sound.

This is thus a possible way to avoid the application of coupled nonlinear system of differential equations in the case of curved shells. We have to keep in mind, however, that some of the modes appear with highly false frequencies in the spectrum.

Our model can not be treated as a substitute model for the present, but it behaves

musical instrument-like anyway. It can be treated as a physical-abstract method rather, since we have used physical concepts in the derivation of the method, but have not managed to get an accurate model.

8.2 Possible Developments

8.2.1 Nonlinear Coupled Differential Equation

The adaptation of the coupled system of differential equations introduced in section 5.2 would be a much better approximation of the problem. This needs the ability of dealing with nonlinearities. By the help of ordinary finite difference method this is not difficult. We have developed such a model to the cylindrical shell, but we had not enough time to investigate it. One can read about the handling of nonlinearities by the help of the functional transformation method in [11]. It seems, that this method can be adapted to our problem too, but it needs further investigation.

8.2.2 Modeling the Excitation and Sound Radiation

The modeling of excitation has been proved very important in the case of the piano (see [1]) and drums (see [4]) and during our former investigations of the tubular bell and glockenspiel. This is a crucial point in the case of percussion instruments, since the auditory system is very sensitive to short-course strike notes. It is worthwhile to create the excitation model also based on the physical background. The ordinary finite difference method can be connected to physics-based excitation models, for this sake we use the deflection values in the striking points. Since these quantities are available in the case of the functional transformation method too, the modeling of the excitation could be executed probably similarly. A hybrid method could be built, in which the excitation is modeled by means of finite different method, while the motion of the resonator by means of the functional transformation method.

It would be worthwhile too, to model the radiated sound, or the directionality and frequency response of the instrument as a sound source leastwise. The determination of the directionality is rather a matter of principle, since it would be difficult to reproduce electro acoustically. The frequency response could be modeled by means of a filter, which coefficients would be determined on the grounds of acoustic considerations.

8.2.3 Curvilinear Coordinates

The description of general curved shells by means of curvilinear coordinates would be a natural and very smart way. From the point of view of such a coordinate system, suited to the shell, it would have the same structure as the plate has in the cartesian coordinate system. The derivatives are in this system rather complicated but well determined however[1]. It can be worthwhile to use this description.

[1] About curvilinear coordinates see [10] for example.

Appendix

F.1 Concepts of Dynamics and Elasticity Theory

This Appendix gives an outline about the basic physical concepts, used to derive the governing equations of the mechanical structures in chapters 5 and 6.

In Appendices F.1.1 and F.1.2 the relevant basic laws of linear and circular motion will be reviewed. According to Euler's rotation theorem every motion of a physical body can be decomposed into a linear motion of any point of the body, and a circular motion around an axis through that point, respectively. Thus it is sufficient to analyse these two types of motion. The linear motion is described by means of the concept of linear momentum, or simply momentum, the circular motion can be described by help of the angular momentum.

The simplest model of the solid bodies, like rods, plates or cylindrical shells is the rigid body, in which deformations are negligible. That is, independently from the external forces acting on it, the relative position of all point pairs within the rigid body are constant. It is clear, however that this model is inappropriate to describe the elastic properties of the solid bodies being examined. Thus, we have to assume that under external forces these bodies suffer some deformation and also internal stresses rise within them. These concepts are examined by the elasticity theory. In Appendices F.1.3 and F.1.4 the basic concepts of elasticity theory, the stress and strain, and their relevant properties will be introduced. Appendix F.1.5 will present the relationship between stress and strain, the method for its description, and four significant types, the anisotropy, the orthotropy, the transversely isotropy and the isotropy, respectively. Appendix 1.3 presents some additional considerations about the derivation of the governing equations and its general steps.

The unit vectors of the coordinate systems will be denoted by $\mathbf{e}_1$, $\mathbf{e}_2$ and $\mathbf{e}_3$, and the coordinates by x_1, x_2 and x_3, respectively. The advantage of this representation is the easiness of summation along the indices.

F.1.1 Momentum

The linear motion of physical bodies of finite size can be described by means of the momentum, or quantity of motion[2]. The momentum of a particle is a vector quantity, the product of it's mass and the velocity

$$\mathbf{p} = m\frac{\mathrm{d}\mathbf{r}}{\mathrm{d}t} = m\dot{\mathbf{r}} = m\mathbf{v}, \tag{F.1.1}$$

[2]Newton's original denomination.

where m is the mass, $\mathbf{r}$ the position and $\dot{\mathbf{r}} = \mathbf{v}$ the velocity. Dot denotes derivative with respect to time.

In the case of a body consisting of more particles, we can introduce the center of mass by means of the equation

$$\mathbf{R} = \frac{\sum_{i=1}^{n} m_i \mathbf{r}_i}{\sum_{i=1}^{n} m_i}, \tag{F.1.2}$$

where $\mathbf{r}_i$ is the position, m_i the mass of the i-th particle. With this, it can be proven that

$$\mathbf{P} = \sum_{i=1}^{n} \mathbf{p}_i = \sum_{i=1}^{n} m_i \dot{\mathbf{R}} = m\mathbf{V}, \tag{F.1.3}$$

where $m = \sum_{i=1}^{n} m_i$ is the total mass of the body, and $\mathbf{V} = \dot{\mathbf{R}}$ the velocity of the center of mass, respectively. That is, the sum of the moments of the particles equals the product of the total mass and the velocity of the center of mass. Thus, from the point of view of momentum, the body behaves as if the total mass was concentrated in the center of mass. For a body with continuously distributed mass the center of mass can be computed of course by integration over the entire volume V of the body

$$\mathbf{R} = \frac{\int \rho(\mathbf{r})\mathbf{r}\mathrm{d}V}{\int \rho(\mathbf{r})\mathrm{d}V}, \tag{F.1.4}$$

where $\rho(\mathbf{r})$ is the mass density of the body.

The statements about the momentum are summarized by Newton's laws

1. **Law of inertia:** There exist such reference frames – which are called inertial reference frames –, relative to which the moment of every body is invariant as long as there is no interaction with a field or other body.

2. **Newton's second law:** Observed from an inertial reference frame, the net force acting on a particle is equal to the time derivative of its momentum, that is

   $$\mathbf{F} = \frac{\mathrm{d}\mathbf{p}}{\mathrm{d}t} = \dot{\mathbf{p}}. \tag{F.1.5}$$

   In a closed system, where the m mass is invariant, we get the well-known relation

   $$\mathbf{F} = m\frac{\mathrm{d}\mathbf{v}}{\mathrm{d}t} = m\mathbf{a} \tag{F.1.6}$$

   results.

3. **Law of reciprocal actions:** By the interaction of two bodies, on both of them acts a force of the same magnitude, but opposite direction.

4. **Superposition principle:** The influences of two or more forces acting on a body simultaneously, are summed independently, without altering each other.

One of the starting points of derivation of the governing equations in chapters 5 and 6 will be always Newton's second law about a differential element of the mechanical structure

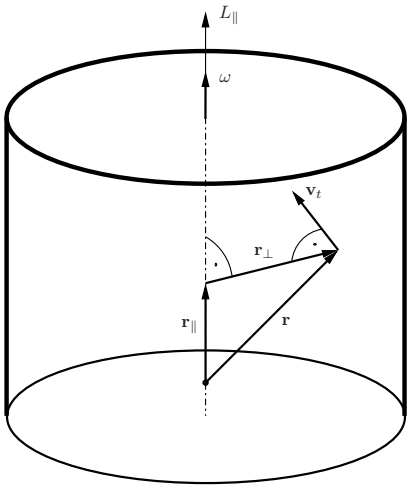

Figure F.1.1: *Interpretation of angular momentum in the case of rotation about an axis of symmetry.*

in question.

F.1.2 Angular momentum

The description of circular motion is possible by means of the angular momentum, however every type of motion has angular momentum. In a closed system angular momentum is also constant, like the momentum. The angular momentum $\mathbf{L}$ of a particle is

$$\mathbf{L} = \mathbf{r} \times \mathbf{p}, \tag{F.1.7}$$

where $\mathbf{r}$ and $\mathbf{p}$ are the position and momentum vectors. For the examination of variation of angular momentum over time, let us take the first derivative, which is

$$\dot{\mathbf{L}} = \dot{\mathbf{r}} \times \mathbf{p} + \mathbf{r} \times \dot{\mathbf{p}}. \tag{F.1.8}$$

The fist term is zero, since $\dot{\mathbf{r}} = \mathbf{v}$ is the velocity, which is parallel to the $\mathbf{p}$ momentum. In the second term, according to Newton's second law $\dot{\mathbf{p}} = \mathbf{F}$, thus the equation becomes

$$\dot{\mathbf{L}} = \mathbf{r} \times \mathbf{F} = \mathbf{M}, \tag{F.1.9}$$

where the quantity denoted by $\mathbf{M}$ is the torque, or moment acting on the particle, created by the $\mathbf{F}$ force. We will refer to this equation as the balance of moments. We need torque to alter the angular momentum, as we need force to alter the momentum. In the case of a solid body rotating about an axis of symmetry, it is practical to place the origin on the axis. According to the distributivity of the cross product in the definition of the angular momentum, and some geometrical considerations it can be seen that it is enough to take the angular momentum's projection on the axis of rotation. Let us resolve the position vector according to figure F.1.1 into an $\mathbf{r}_\parallel$ component parallel to the axis of rotation, and

an $\mathbf{r}_\perp$ component to it, respectively. With this the projection of the angular momentum on the axis of rotation is

$$\mathbf{L}_\parallel = \mathbf{r}_\perp \times \mathbf{p}. \tag{F.1.10}$$

Since the orientation of $\mathbf{L}_\parallel$ is known, it is enough to calculate the amplitude, thus

$$L = r_\perp \, p, \tag{F.1.11}$$

where $r_\perp = \|\mathbf{r}_\perp\|$ and $p = \|\mathbf{p}\|$ are the amplitudes of the vectors. The sign of the cross product is important, however. It is positive in the case of a counterclockwise rotation, and negative for a clockwise rotation, respectively. Note, that by a rotation about an axis, the $\mathbf{p}$ momentum is always tangential, thus there is no need for decomposition.

Let us resolve equation F.1.11

$$L = r_\perp \, p = r_\perp \, mv = mr_\perp^2 \, \omega, \tag{F.1.12}$$

where v is the tangential, ω the angular velocity. In the case of a system of particles the net angular momentum is the sum of the particle's angular momentums, for a continuous distribution with mass density $\rho(\mathbf{r})$ the sum becomes an integral, however. Thus the net angular momentum is

$$L = \omega \int \rho(\mathbf{r}) \, r_\perp^2 \, \mathrm{d}V, \tag{F.1.13}$$

where the domain of integration is the entire volume of the body in question. This integration is called moment of inertia, and denoted by I

$$I = \int \rho(\mathbf{r}) \, r_\perp^2 \, \mathrm{d}V. \tag{F.1.14}$$

The magnitude of the angular momentum is

$$L = I \, \omega. \tag{F.1.15}$$

Note, that the angular momentum vector can be written generally in the same form

$$\mathbf{L} = \mathbf{I}\boldsymbol{\omega}, \tag{F.1.16}$$

where $\boldsymbol{\omega}$ is the angular velocity vector and $\mathbf{I}$ the moment of inertia tensor, respectively.

In chapters 5 and 6 we will develop also a balance of moments equation for the differential element of the mechanical structure in question.

F.1.3 Stress

Stress is the force exerted per unit area of a surface within a body on which external forces act. The acting external forces are transmitted from point to point within the body, in a way, that Newton's second law and the balance of moments equation are satisfied in every point of the body. In behalf of the interpretation of the concept stress, let's look at figure

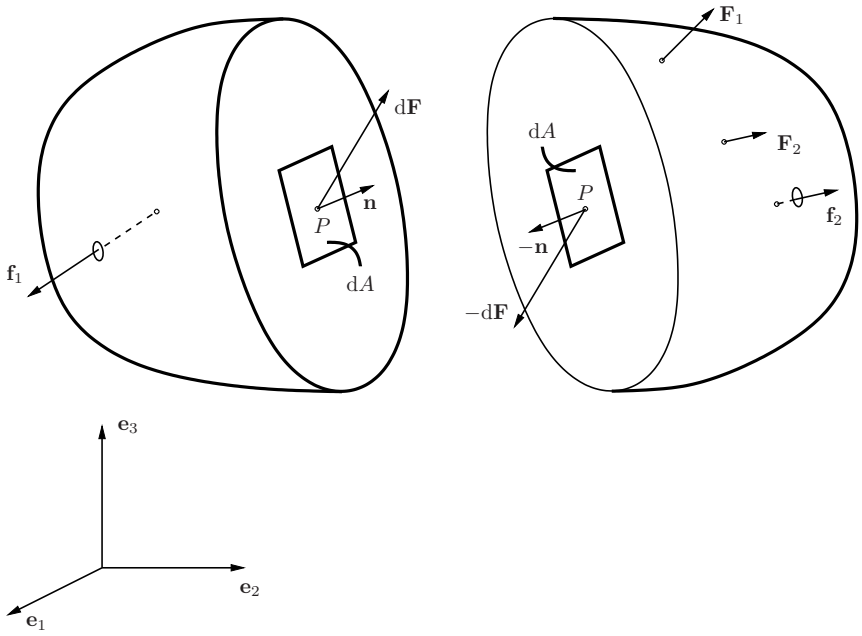

Figure F.1.2: *Interpretation of stress.*
Body ($\boldsymbol{f}_i$) and surface forces ($\boldsymbol{F}_i$) acting on the body in the reference frame determined by the unit vectors $\boldsymbol{e}_1$, $\boldsymbol{e}_2$, $\boldsymbol{e}_3$. $\mathrm{d}\boldsymbol{F}$ is the internal force acting on the surface element with a normal vector $\boldsymbol{n}$ passing through the point P, generated by the external forces.

F.1.2. Let us consider an imaginary plane dividing the body into two segments. P is a point on the plane, $\mathrm{d}A$ a differential small area with normal vector $\mathbf{n}$, passing through the point P. The stress in this point corresponding to direction $\mathbf{n}$ is

$$\mathbf{T}^{\mathbf{n}} = \frac{\mathrm{d}\mathbf{F}}{\mathrm{d}A} = \lim_{\Delta A \to 0} \frac{\Delta \mathbf{F}}{\Delta A}. \tag{F.1.17}$$

$\Delta\mathbf{F}$ is the force exerted on the small area ΔA, which generated by the interaction of the two segments of the body. According to the law of reciprocal actions the same force with the opposite direction is acting on the small area $\mathrm{d}A$ on the other segment, thus

$$\mathbf{T}^{-\mathbf{n}} = -\mathbf{T}^{\mathbf{n}}. \tag{F.1.18}$$

It is worthwhile to resolve the vector $\mathbf{T}^{\mathbf{n}}$ into two components, a parallel to $\mathbf{n}$ one, and a perpendicular one. These are called normal and shearing stresses and are represented by σ and τ, respectively. Normal stress arises for example in a prismatic bar subjected to axial force. In this case internal force arises only in axial direction, thus the average normal stress on the cross section is the fraction of the axial force and the cross sectional area. Shearing stress arises in a bar clamped at one end, and exerted by a force next to the clamp in a direction perpendicular to the axis.

The shearing and normal stresses have different characters, the shearing stress acts to slip the planes of the body, in turn by normal stress the planes push or pull each other. In

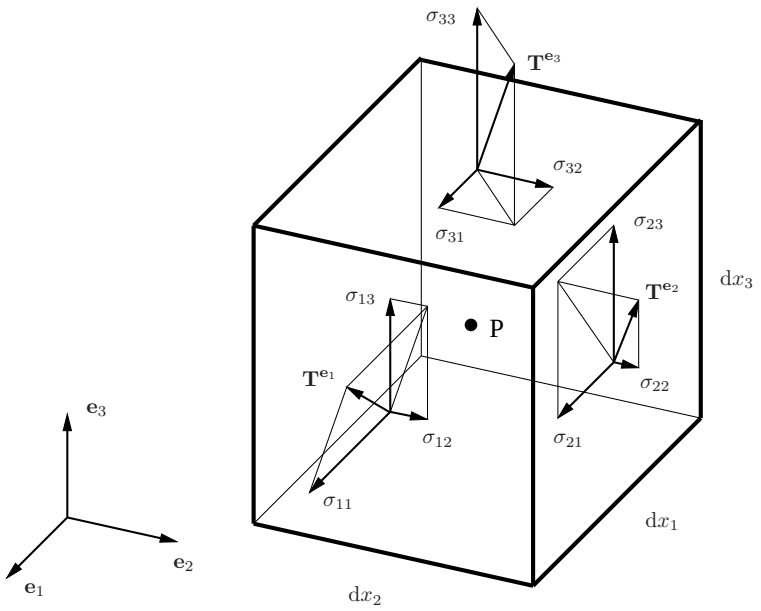

Figure F.1.3: *Interpretation of the stress components.*
The force $\boldsymbol{T}^{\mathbf{e}_i}$ acting on the planes of normal vector $\boldsymbol{e}_i$ can be decomposed into a normal and two shear components. The normal component $\sigma_{ii}\,\boldsymbol{e}_i$ is the normal stress, the planar component $\sum_{i\neq j}\sigma_{ij}\,\boldsymbol{e}_j$ is the shear stress.

the case of the prismatic bar exerted to axial force there is not any shearing force[3]. We can consider a small area perpendicular to the cross section, but the axial force alternating along it will not cause a net d$\mathbf{F}$ force. Thus the shearing force in the plane perpendicular to the axis does not equal the normal stress on the cross section. The stress vectors corresponding to differently oriented planes have different components in the same direction, i.e. stress is not a vector variable, we need more than three scalars to describe it.

The stress depends on two vector variables, the normal vector of the plane on which the stress is acting on, and the location vector. The state of stress at a point is defined by all the stress vectors $\mathbf{T}^{\mathbf{n}}$ associated with all planes that pass through that point, these can always be determined from the stress vectors of three mutually perpendicular planes, however. Thus, it is enough to determine the stress on the coordinate planes of the frame of reference. Let us consider according to figure F.1.3 a differential cube around the point P. The $\mathbf{T}^{\mathbf{e}_i}$ stress vectors can be decomposed into three components according to the normal vectors $\mathbf{e}_1$, $\mathbf{e}_2$ and $\mathbf{e}_3$, this gives

$$\begin{aligned}
\mathbf{T}^{\mathbf{e}_1} &= T_1^{\mathbf{e}_1}\mathbf{e}_1 + T_2^{\mathbf{e}_1}\mathbf{e}_2 + T_3^{\mathbf{e}_1}\mathbf{e}_3,\\
\mathbf{T}^{\mathbf{e}_2} &= T_1^{\mathbf{e}_2}\mathbf{e}_1 + T_2^{\mathbf{e}_2}\mathbf{e}_2 + T_3^{\mathbf{e}_2}\mathbf{e}_3,\\
\mathbf{T}^{\mathbf{e}_3} &= T_1^{\mathbf{e}_3}\mathbf{e}_1 + T_2^{\mathbf{e}_3}\mathbf{e}_2 + T_3^{\mathbf{e}_3}\mathbf{e}_3.
\end{aligned} \tag{F.1.19}$$

It is worthwhile to simplify the notation as follows

[3]In isotropic case (see F.1.5).

$$T_j^{\mathbf{e}_i} = \sigma_{ij}. \tag{F.1.20}$$

With this, equation F.1.19 written in shorter form becomes

$$\begin{pmatrix} \mathbf{T}^{\mathbf{e}_1} \\ \mathbf{T}^{\mathbf{e}_2} \\ \mathbf{T}^{\mathbf{e}_3} \end{pmatrix} = \begin{pmatrix} \sigma_{11} & \sigma_{12} & \sigma_{13} \\ \sigma_{21} & \sigma_{22} & \sigma_{23} \\ \sigma_{31} & \sigma_{32} & \sigma_{33} \end{pmatrix} \begin{pmatrix} \mathbf{e}_1 \\ \mathbf{e}_2 \\ \mathbf{e}_3 \end{pmatrix}. \tag{F.1.21}$$

It is clear, that the stress can be determined by means of nine numbers in every point. This nine parameters are called Cauchy stress tensor.

For the investigation of the stress tensor, let us develop Newton's second law for the differential cube element of volume $V = \mathrm{d}x_1\,\mathrm{d}x_2\,\mathrm{d}x_3$ in the point P. In linear approximation, assuming external force per unit of volume[4] $\mathbf{f}_i$ too,

$$\begin{aligned} &\frac{\partial \sigma_{1i}}{\partial x_1}\mathrm{d}x_1\mathrm{d}x_2\mathrm{d}x_3 + \frac{\partial \sigma_{2i}}{\partial x_2}\mathrm{d}x_2\mathrm{d}x_1\mathrm{d}x_3 + \frac{\partial \sigma_{3i}}{\partial x_3}\mathrm{d}x_3\mathrm{d}x_1\mathrm{d}x_2 + \\ &+ f_i\,\mathrm{d}x_1\mathrm{d}x_2\mathrm{d}x_3 = \rho\,\mathrm{d}x_1\mathrm{d}x_2\mathrm{d}x_3\frac{\partial^2 u_i}{\partial t^2}, \qquad (i = 1,2,3) \end{aligned} \tag{F.1.22}$$

where ρ is the mass density and $u_i = u_i(\mathbf{r})$ the deflection in direction x_i of the particle originally been in point $\mathbf{r}$. Dividing with the volume $\mathrm{d}x_1\mathrm{d}x_2\mathrm{d}x_3$ gives

$$\sum_{j=1}^{3} \frac{\partial \sigma_{ji}}{\partial x_j} + f_i = \rho\,\frac{\partial^2 u_i}{\partial t^2} \qquad (i = 1,2,3)\,. \tag{F.1.23}$$

If there is not any force per unit of volume present and the point p is in equilibrium, i.e. $f_i = 0$ and $u_i = 0$ the equation simplifies to

$$\sum_{j=1}^{3} \frac{\partial \sigma_{ji}}{\partial x_j} = 0 \qquad (i = 1,2,3)\,. \tag{F.1.24}$$

From the balance of moment equation of the differential cube element follows the symmetry of the stress tensor, i.e.

$$\sigma_{ij} = \sigma_{ji}. \tag{F.1.25}$$

With this, the number of scalars required to describe the state of stress in a point reduces to six.

In the case of the duplicated index of the normal stress it is common to use only one index

$$\sigma_{ii} = \sigma_i. \tag{F.1.26}$$

For the sake of better distinguishing between normal and shearing stress, the shearing stress is often denoted by

$$\sigma_{ij} = \tau_{ij}, \tag{F.1.27}$$

[4] e.g. force of gravity

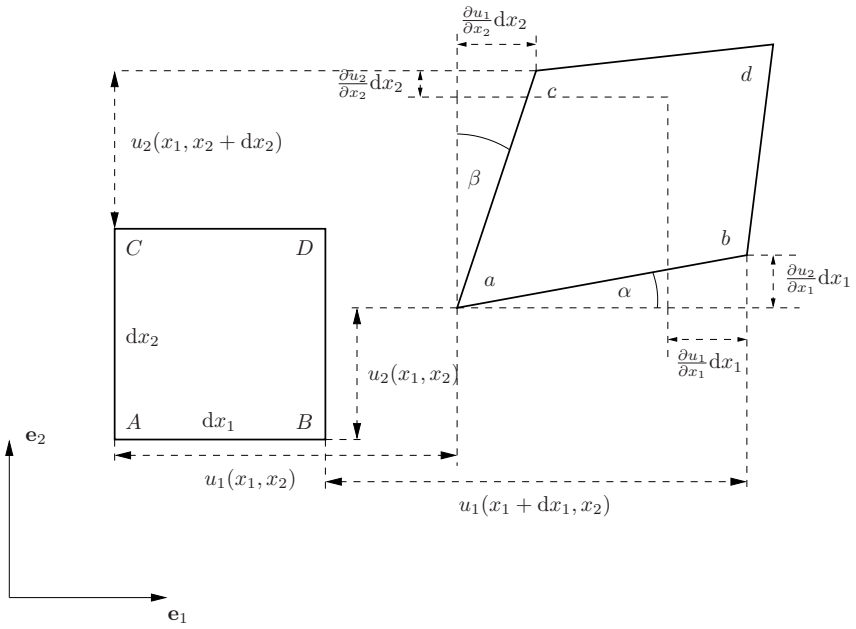

Figure F.1.4: *Interpretation of stress in two dimensions. Points A, B, C and D moves to a, b, c and d, respectively. The displacements are expressed by means of the components of displacement vector u_i and its derivatives, respectively.*

where $i \neq j$. With these new notations the Cauchy stress tensor becomes

$$\underline{\underline{\sigma}} = \begin{pmatrix} \sigma_1 & \tau_{12} & \tau_{13} \\ \tau_{21} & \sigma_2 & \tau_{23} \\ \tau_{31} & \tau_{32} & \sigma_3 \end{pmatrix}. \tag{F.1.28}$$

F.1.4 Strain

An elastic body subjected to external forces and therefore to stress too, undergoes a displacement. The material point $\mathbf{r}$ shifts with an amount of $\mathbf{u}(\mathbf{r})$, thus gets into the location $\mathbf{r} + \mathbf{u}(\mathbf{r})$. If the displacement vector $\mathbf{u}(\mathbf{r})$ is not constant over the entire body, i.e. $\nabla u_i \neq 0$ we speak about deformation. ∇ is the nabla operator, that is ∇u_i denotes the gradient of u_i. The degree of deformation ∇u_i depends upon the material, in the case of metals it is much smaller than unit, i.e. $\|\nabla u_i\| \ll 1m$. Strain is the measure of deformation, representing the relative displacements between particles in the material body. Since the deformation is caused by the stress, there are normal and shearing deformations according to the two types of stress. For the interpretation of the strain let us consider a square on the plane according to figure F.1.4. Generalization to three dimension can be carried out without any difficulty. The corners a, b, c and d of the deformed square correspond to the corners A, B, C and D in the undeformed case.

The normal deformation is measured by the normal strain. In the x_1 direction it is the

relative extension of the differential section $\overline{\mathrm{AB}}$, that is

$$\epsilon_1 = \frac{\overline{\mathrm{ab}} - \overline{\mathrm{AB}}}{\overline{\mathrm{AB}}}. \tag{F.1.29}$$

The length of the deformed section $\overline{\mathrm{ab}}$ can be written with the components of the displacement vector $\mathbf{u}$

$$\begin{aligned}\overline{\mathrm{ab}} &= \sqrt{\left(\mathrm{d}x_1 + \frac{\partial u_1}{\partial x_1}\mathrm{d}x_1\right)^2 + \left(\frac{\partial u_2}{\partial x_1}\mathrm{d}x_1\right)^2} = \\ &= \sqrt{1 + 2\frac{\partial u_1}{\partial x_1} + \left(\frac{\partial u_1}{\partial x_1}\right)^2 + \left(\frac{\partial u_2}{\partial x_1}\right)^2}\,\mathrm{d}x_1.\end{aligned} \tag{F.1.30}$$

For small deformations

$$\begin{aligned}\left(\frac{\partial u_1}{\partial x_1}\right)^2 &\ll \frac{\partial u_1}{\partial x_1}, \\ \left(\frac{\partial u_2}{\partial x_1}\right)^2 &\ll \frac{\partial u_2}{\partial x_1},\end{aligned} \tag{F.1.31}$$

and with this, employing, that for $x \ll 1$ the linear approximation

$$\sqrt{1+x} \approx 1 + \frac{1}{2}x \tag{F.1.32}$$

holds, we get

$$\overline{\mathrm{ab}} \approx \sqrt{1 + 2\frac{\partial u_1}{\partial x_1}}\,\mathrm{d}x_1 \approx \mathrm{d}x_1 + \frac{\partial u_1}{\partial x_1}\mathrm{d}x_1. \tag{F.1.33}$$

Thus, the normal strain in direction x_1 is

$$\epsilon_1 = \frac{\overline{\mathrm{ab}} - \overline{\mathrm{AB}}}{\overline{\mathrm{AB}}} = \frac{\mathrm{d}x_1 + \frac{\partial u_1}{\partial x_1}\mathrm{d}x_1 - \mathrm{d}x_1}{\mathrm{d}x_1} = \frac{\partial u_1}{\partial x_1}. \tag{F.1.34}$$

We can express the normal strain in direction x_2 and x_3 in the same way, which gives

$$\begin{aligned}\epsilon_2 &= \frac{\partial u_2}{\partial x_2}, \\ \epsilon_3 &= \frac{\partial u_3}{\partial x_3}.\end{aligned} \tag{F.1.35}$$

The measure of the shearing deformation is the shearing strain. It is by definition in a given point the change of angle between two lines initially perpendicular to each other and passing through that point. On the figure in the case of the x_1 – x_2 plane the shearing strain is the sum $\alpha + \beta$, which is assuming small angles

$$\gamma_{12} = \gamma_{21} = \alpha + \beta \approx \tan\alpha + \tan\beta = \frac{\frac{\partial u_2}{\partial x_1}\mathrm{d}x_1}{\mathrm{d}x_1 + \frac{\partial u_1}{\partial x_1}\mathrm{d}x_1} + \frac{\frac{\partial u_1}{\partial x_2}\mathrm{d}x_2}{\mathrm{d}x_2 + \frac{\partial u_2}{\partial x_2}\mathrm{d}x_2}. \tag{F.1.36}$$

This can be further simplified for small deformations

$$\gamma_{12} = \gamma_{21} = \alpha + \beta = \frac{\partial u_2}{\partial x_1} + \frac{\partial u_1}{\partial x_2}. \tag{F.1.37}$$

We get completely similar results for the other two coordinate planes

$$\begin{aligned} \gamma_{13} = \gamma_{31} &= \frac{\partial u_3}{\partial x_1} + \frac{\partial u_1}{\partial x_3}, \\ \gamma_{23} = \gamma_{32} &= \frac{\partial u_3}{\partial x_2} + \frac{\partial u_2}{\partial x_3}. \end{aligned} \tag{F.1.38}$$

We can set up a strain tensor from the quantities ϵ_i and γ_{ij}

$$\underline{\underline{\epsilon}} = \begin{pmatrix} \epsilon_1 & \gamma_{12}/2 & \gamma_{13}/2 \\ \gamma_{21}/2 & \epsilon_2 & \gamma_{23}/2 \\ \gamma_{31}/2 & \gamma_{32}/2 & \epsilon_3 \end{pmatrix}. \tag{F.1.39}$$

It is clear according to equations F.1.37 and F.1.38 that the strain tensor is also symmetrical, thus the strain is described by means of six independent scalars.

F.1.5 Hooke's law

Hooke's Law determines the relation between stress and strain in linear-elastic materials. The linear-elastic attribute alludes to, that in these materials under a certain limit of load, the stress and strain are in a linear relation, i.e. Hooke's law can be expressed by a system of linear equations. In the case of metal this assumption holds.

We need at least 36 independent elastic material properties to relate the six stress components to the six strain components. Towards to be able to write the relation in matrix form, we have to introduce the notation, which represents the six-six independent stress and strain data by two six dimensional vectors as following

$$\underline{\sigma} = \begin{pmatrix} \sigma_1 \\ \sigma_2 \\ \sigma_3 \\ \tau_{23} \\ \tau_{31} \\ \tau_{12} \end{pmatrix} = \begin{pmatrix} \sigma_1 \\ \sigma_2 \\ \sigma_3 \\ \sigma_4 \\ \sigma_5 \\ \sigma_6 \end{pmatrix} \qquad \underline{\epsilon} = \begin{pmatrix} \epsilon_1 \\ \epsilon_2 \\ \epsilon_3 \\ \gamma_{23} \\ \gamma_{31} \\ \gamma_{12} \end{pmatrix} = \begin{pmatrix} \epsilon_1 \\ \epsilon_2 \\ \epsilon_3 \\ \epsilon_4 \\ \epsilon_5 \\ \epsilon_6 \end{pmatrix}. \tag{F.1.40}$$

With this notation the relation can be written as

$$\begin{pmatrix} \sigma_1 \\ \sigma_2 \\ \sigma_3 \\ \sigma_4 \\ \sigma_5 \\ \sigma_6 \end{pmatrix} = \begin{pmatrix} C_{11} & C_{12} & C_{13} & C_{14} & C_{15} & C_{16} \\ C_{21} & C_{22} & C_{23} & C_{24} & C_{25} & C_{26} \\ C_{31} & C_{32} & C_{33} & C_{34} & C_{35} & C_{36} \\ C_{41} & C_{42} & C_{43} & C_{44} & C_{45} & C_{46} \\ C_{51} & C_{52} & C_{53} & C_{54} & C_{55} & C_{56} \\ C_{61} & C_{62} & C_{63} & C_{64} & C_{65} & C_{66} \end{pmatrix} \begin{pmatrix} \epsilon_1 \\ \epsilon_2 \\ \epsilon_3 \\ \epsilon_4 \\ \epsilon_5 \\ \epsilon_6 \end{pmatrix}, \tag{F.1.41}$$

or in shorter form

$$\sigma_i = \sum_{j=1}^{6} C_{ij}\,\epsilon_j \qquad i = 1, 2, .., 6, \tag{F.1.42}$$

where $\underline{\underline{C}}$ is called stiffness matrix, or stiffness tensor. It represents the amount of stress is needed to achieve the specified strain. The bigger the stiffness tensor is, the more stiff the material and harder to create strain is.

Often is necessary to determine the strain caused by the stress, which is described by the compliance tensor $\underline{\underline{S}}$, that is

$$\epsilon_i = \sum_{j=1}^{6} S_{ij}\sigma_j. \tag{F.1.43}$$

It is clear, that $\underline{\underline{S}}$ is the inverse of $\underline{\underline{C}}$

$$\underline{\underline{S}} = \underline{\underline{C}}^{-1}. \tag{F.1.44}$$

It can be shown, that both the stiffness and compliance tensor are symmetrical

$$\begin{aligned} C_{ij} &= C_{ji}, \\ S_{ij} &= S_{ji}, \end{aligned} \tag{F.1.45}$$

thus the number of the independent elastic material properties reduces to 21. In many cases, however, this number can be lowered further according to symmetric properties of the material. The most general materials, where no simplifications are possible are called anisotropic materials.

It will be demanded in three steps even stronger symmetric properties in the following sections, which will yield even less independent elastic material properties. The corresponding denominations are orthotropy, transverse isotropy and isotropy. Orthotropic materials are the wood and rolled metals, transversely isotropic are the so-called unidirectional fiber composite materials, and isotropic are the most metals on macroscopic scale.

F.1.6 Orthotropy

At first, let's assume, that the material has three mutually orthogonal two-fold axis of rotational symmetry. That is, rotating it by π radian along either of these axis of symmetry, its elastic properties remain the same. In this case it is worthwhile to develop Hooke's law in a frame of reference with axes parallel to the axes of symmetry.

In such a frame of reference the result of these restrictions is, that some of the stresses become independent from some of the strains. The normal stresses do not cause shearing strain, and the shearing stresses do not cause normal strain any more. The shearing strains and shearing stresses in different planes of the coordinate system become also independent from each other. These involve the vanishing of many entries of the stiffness and compliance

tensor, respectively. The compliance tensor, for example has a structure of

$$\begin{pmatrix} \epsilon_1 \\ \epsilon_2 \\ \epsilon_3 \\ \epsilon_4 \\ \epsilon_5 \\ \epsilon_6 \end{pmatrix} = \begin{pmatrix} S_{11} & S_{12} & S_{13} & 0 & 0 & 0 \\ S_{21} & S_{22} & S_{23} & 0 & 0 & 0 \\ S_{31} & S_{32} & S_{33} & 0 & 0 & 0 \\ 0 & 0 & 0 & S_{44} & 0 & 0 \\ 0 & 0 & 0 & 0 & S_{55} & 0 \\ 0 & 0 & 0 & 0 & 0 & S_{66} \end{pmatrix} \begin{pmatrix} \sigma_1 \\ \sigma_2 \\ \sigma_3 \\ \sigma_4 \\ \sigma_5 \\ \sigma_6 \end{pmatrix}. \tag{F.1.46}$$

Note, that this holds only if the axes of the frame of reference coincide with the axes of symmetry. In a different frame of reference the stiffness and compliance tensor must be transformed according the tensor transformation rules, and their structure is not such simple any more.

The connection between the normal and shearing elastic behavior ceased, thus we can derive the twelve elastic properties independently, according to basic elastic rules. Apparently, the connection between the normal stresses and strains of different directions still hold, this agrees to the Poisson effect, the contraction in the perpendicular directions in a stretched material. The twelve elastic properties are, thus the three Young's moduli according the coordinate axes, the six Poisson's ratios according the six coordinate pairs and the three shear moduli according the coordinate planes.

The relation between the normal strain and normal stress is given by Young's modulus, or modulus of elasticity

$$\epsilon_i = \frac{1}{E}\sigma_i \qquad i = 1, 2, 3. \tag{F.1.47}$$

According to the Poisson effect strains arise in the perpendicular directions too, the Poisson's ratio is the ratio of the strain in the perpendicular direction and the strain in the direction of the load

$$\nu_{ij} = \frac{\epsilon_j}{\epsilon_i}. \tag{F.1.48}$$

On the grounds of equations F.1.47 and F.1.48 can be showed, that if $\nu \ll \nu^2$ and $\nu^2 \ll 1$ holds, the relation between the normal strains and normal stresses are given, more accurate by the equations

$$\epsilon_i = \frac{1}{E_i}\sigma_i - \sum_{j \neq i} \left(\frac{\nu_{ij}}{E_i}\sigma_j \right) \qquad i = 1, 2, 3. \tag{F.1.49}$$

The relation between the stress τ_{ij} and the caused strain γ_{ij} in the plane $x_i - x_j$

$$\gamma_{ij} = \frac{1}{G_{ij}}\,\tau_{ij}, \tag{F.1.50}$$

where G_{ij} is the shear modulus according to the plane $x_i - x_j$. The compliance matrix is,

thus

$$\begin{pmatrix} \epsilon_1 \\ \epsilon_2 \\ \epsilon_3 \\ \gamma_{23} \\ \gamma_{31} \\ \gamma_{12} \end{pmatrix} = \begin{pmatrix} \frac{1}{E_1} & -\frac{\nu_{12}}{E_1} & -\frac{\nu_{13}}{E_1} & 0 & 0 & 0 \\ -\frac{\nu_{21}}{E_2} & \frac{1}{E_2} & -\frac{\nu_{23}}{E_2} & 0 & 0 & 0 \\ -\frac{\nu_{31}}{E_3} & -\frac{\nu_{32}}{E_3} & \frac{1}{E_3} & 0 & 0 & 0 \\ 0 & 0 & 0 & \frac{1}{G_{23}} & 0 & 0 \\ 0 & 0 & 0 & 0 & \frac{1}{G_{31}} & 0 \\ 0 & 0 & 0 & 0 & 0 & \frac{1}{G_{12}} \end{pmatrix} \begin{pmatrix} \sigma_1 \\ \sigma_2 \\ \sigma_3 \\ \tau_{23} \\ \tau_{31} \\ \tau_{12} \end{pmatrix}. \tag{F.1.51}$$

Since the compliance matrix has to be symmetric, the Young's moduli and Poisson's ratios have to satisfy the following system of equations

$$\frac{\nu_{12}}{E_1} = \frac{\nu_{21}}{E_2}, \tag{F.1.52a}$$

$$\frac{\nu_{13}}{E_1} = \frac{\nu_{31}}{E_3}, \tag{F.1.52b}$$

$$\frac{\nu_{23}}{E_2} = \frac{\nu_{32}}{E_3}. \tag{F.1.52c}$$

These restrictions reduce the number of independent elastic properties to nine.

F.1.7 Transverse isotropy

As a second step let's assume, that the material has two mutually perpendicular two-fold axes of rotational symmetry and an axis of cylindrical symmetry perpendicular to the former two axes. In the planes perpendicular to the axis of cylindrical symmetry are, thus every direction equal on the grounds of elastic properties. In this plane the material is isotropic.

Let the plane of isotropy the $x_1 - x_2$ plane, in this case the indices 1 and 2 are indistinguishable, thus the equations

$$\begin{aligned} E_2 &= E_1, \\ \nu_{32} &= \nu_{31}, \\ \nu_{23} &= \nu_{13}, \\ \nu_{21} &= \nu_{12}, \\ G_{23} &= G_{31}, \end{aligned} \tag{F.1.53}$$

must hold, and Hooke's law turns into

$$\begin{pmatrix} \epsilon_1 \\ \epsilon_2 \\ \epsilon_3 \\ \gamma_{23} \\ \gamma_{31} \\ \gamma_{12} \end{pmatrix} = \begin{pmatrix} \frac{1}{E_1} & -\frac{\nu_{12}}{E_1} & -\frac{\nu_{13}}{E_1} & 0 & 0 & 0 \\ -\frac{\nu_{12}}{E_1} & \frac{1}{E_1} & -\frac{\nu_{13}}{E_1} & 0 & 0 & 0 \\ -\frac{\nu_{31}}{E_3} & -\frac{\nu_{31}}{E_3} & \frac{1}{E_3} & 0 & 0 & 0 \\ 0 & 0 & 0 & \frac{1}{G_{31}} & 0 & 0 \\ 0 & 0 & 0 & 0 & \frac{1}{G_{31}} & 0 \\ 0 & 0 & 0 & 0 & 0 & \frac{1}{G_{12}} \end{pmatrix} \begin{pmatrix} \sigma_1 \\ \sigma_2 \\ \sigma_3 \\ \tau_{23} \\ \tau_{31} \\ \tau_{12} \end{pmatrix}. \tag{F.1.54}$$

Now, we can write only one further equation according the symmetry of the compliance

tensor

$$\frac{\nu_{13}}{E_1} = \frac{\nu_{31}}{E_3}, \tag{F.1.55}$$

which reduces the seven independent elastic properties by one. In addition, there is a connection between the shear modulus G_{12}, the modulus of elasticity E_1 and the Poisson's ratio ν_{12} in the plane $x_1 - x_2$ as follows

$$G_{12} = \frac{E_1}{2\,(1+\nu_{12})}, \tag{F.1.56}$$

thus five independent elastic properties are enough to describe in isotropic material.

F.1.8 Isotropy

Finally, let's assume that the material has identical elastic property in all direction of the three dimensional space, that is, it posses a spherical symmetry. In this case all directions are identical, it is impossible to distinguish the indices, thus

$$\begin{aligned} E_1 = E_2 = E_3 = E, \\ \nu_{12} = \nu_{13} = \nu_{21} = \nu_{23} = \nu_{31} = \nu_{32} = \nu, \\ G_{23} = G_{31} = G_{12} = G. \end{aligned} \tag{F.1.57}$$

Accordingly, the Hooke's law is

$$\begin{pmatrix} \epsilon_1 \\ \epsilon_2 \\ \epsilon_3 \\ \gamma_{23} \\ \gamma_{31} \\ \gamma_{12} \end{pmatrix} = \begin{pmatrix} \frac{1}{E} & -\frac{\nu}{E} & -\frac{\nu}{E} & 0 & 0 & 0 \\ -\frac{\nu}{E} & \frac{1}{E} & -\frac{\nu}{E} & 0 & 0 & 0 \\ -\frac{\nu}{E} & -\frac{\nu}{E} & \frac{1}{E} & 0 & 0 & 0 \\ 0 & 0 & 0 & \frac{1}{G} & 0 & 0 \\ 0 & 0 & 0 & 0 & \frac{1}{G} & 0 \\ 0 & 0 & 0 & 0 & 0 & \frac{1}{G} \end{pmatrix} \begin{pmatrix} \sigma_1 \\ \sigma_2 \\ \sigma_3 \\ \tau_{23} \\ \tau_{31} \\ \tau_{12} \end{pmatrix}. \tag{F.1.58}$$

The elastic properties are, thus E, ν and G, respectively. However, the equation F.1.56 holds in this case too

$$G = \frac{E}{2\,(1+\nu)}. \tag{F.1.59}$$

The isotropic material is described, thus by means of two independent constants.

F.2 MatLab Code of Filter Bank Model of the Bell

Here the MatLab code of the functional transformation method is presented. The transformation kernels are considered given. The code which determines these kernels is rather long, thus we can not present it here.

```
function voice=FTM_bell(K,J,beta,d1,d2,R1,R2,time,wtd);

% voice=FTM_bell(K,J,beta,d1,d2,R1,R2,time,wtd) computes the vibration of
% a bell-shaped shell by means of the functional transformation method.
%
% K and J are the transformation kernels of the Sturm--Liouville transform
% and inverse Sturm--Liouville transform respectively.
%
% beta is the vector cantaining the eigenvalues
%
% d1 and d2 are the disceritzation step-sizes in each direction
%
% R1 and R2 are the radii of curvature in each direction
%
% time determines how long period is computed
%
% wtd determines if the voice should be computed or the vibration pattern
% visualised,
% it should be either "voi" (=voice) or "vis" (visualisation)


%---Some required variables
fs = 44100;
t = time;
T = 1/fs;
k_max = floor(t/T);
n_modes=size(J,3);
n = (1:n_modes)';
D1 = 1;
D3 = -10e-1;
D3 = 0;
D1 = 0;
n1 = size(J,2);
n2 = size(J,1);
L1 = sum(d2(:,1));

%---Normaliztion factors
N = zeros(1,n_modes);
for q=1:n_modes,
    N(q) = num_inner_product_bell((squeeze(J(:,:,q))),...
    (squeeze(K(:,:,q))),d1,d2,n1);
end

%---Spatial part of the excitation
fx = zeros(n2,n1);
% fx(n2-12:n2-9,n1-12:n1-9) = 1e-3*hanning(4)*hanning(4)';
fx(n2-14,round(2*n1/3)-10)=1e-3;

%---Sturm--Liouville tarnsform of the spatial part of the excitation
f_ = zeros(1,n_modes);
for q=1:n_modes
    f_(q) = num_inner_product_bell(fx,(squeeze(K(:,:,q))),d1,d2,n1);
end

%---Temporal part of the excitation
ft = zeros(1,k_max);
t_hit=2e-4;
k_hit=round(t_hit/T);
ft(1:k_hit) = hann(k_hit);
```

```
%---Filter bank coefficients in vectors
sigma = 0.5*(D3*n.^2 - D1);
omega = sqrt(abs(beta)-sigma.^2);
c1 = 2 * exp(sigma*T) .* cos(omega*T);
c2 = -exp(2*sigma*T);

%---Weighting factor of the filters in vector
a = zeros(n2,n1,n_modes);
for q=1:n_modes
    a(:,:,q) = 1/N(q)/omega(q)*sin(omega(q)*T)*f_(q).*(J(:,:,q));
end


if wtd=='voi' %--- Calculates the sound
    %--- The points where the deflection is calculated
    x1_out=round(n1/3-2);
    x2_out=round(n2-8);
    %--- Matrices of the deflection in three time-step
    z0 = zeros(9,9,n_modes);
    z1 = zeros(9,9,n_modes);
    z2 = zeros(9,9,n_modes);
    out = zeros(9,9);
    voice=zeros(1,k_max);

    for q=1:k_max
         %--- Calculating the filter outputs
        for r=1:9
            for s=1:9
             z0(r,s,:)=c1.*squeeze(z1(r,s,:)) + c2.*squeeze(z2(r,s,:)) + ft(q);
             out(r,s)=sum(squeeze(z0(r,s,:)).*squeeze(a(r+x2_out-4,s+x1_out-4,:)));
            end
        end
        z2 = z1;
        z1 = z0;
        voice(q)=sum(sum(out));
    end

elseif wtd=='vis' %--- Calculates the vibration pattern
    %--- Matrices of the deflection in three time-step
    z0 = zeros(n2,n1,n_modes);
    z1 = zeros(n2,n1,n_modes);
    z2 = zeros(n2,n1,n_modes);
    out = zeros(n2,n1);
    %--- Help ariables for the visualisation
    PHI=ones(n2,1)*(0:2*pi/n1:2*pi-2*pi/n1);
    H=zeros(n2,n1);
    for q=2:n2
        H(q,:)=sum(d2(1:q-1,1))*ones(1,n1);
    end

    figure(2);
    set(gcf,'Color',[1,1,1]);
    colormap(jet);
    for q=1:k_max
         %--- Calculating the filter outputs
        for r=1:n2
            for s=1:n1
                z0(r,s,:)=c1.*squeeze(z1(r,s,:)) + c2.*squeeze(z2(r,s,:)) + ft(q);
                out(r,s)=sum(squeeze(z0(r,s,:)).*squeeze(a(r,s,:)));
            end
        end
        z2 = z1;
        z1 = z0;
         %--- Visualisation
        X=(R1+6e7*out).*cos(PHI);
        Y=(R1+6e7*out).*sin(PHI);
%         subplot(3,5,q);
        surf(X,Y,H,out);
```

```
        set(get(gcf,'CurrentAxes'),'PlotBoxAspectRatio',...
        [2.4*max(R1(:,1)),2.4*max(R1(:,1)),1.02*L1]);
        set(get(gcf,'CurrentAxes'),'Xlim',[-1.2*max(R1(:,1)),1.2*max(R1(:,1))]);
        set(get(gcf,'CurrentAxes'),'Ylim',[-1.2*max(R1(:,1)),1.2*max(R1(:,1))]);
        set(get(gcf,'CurrentAxes'),'Zlim',[0,1.02*L1]);
        set(get(gcf,'CurrentAxes'),'Xgrid','off');
        set(get(gcf,'CurrentAxes'),'Ygrid','off');
        set(get(gcf,'CurrentAxes'),'Zgrid','off');
        set(get(gcf,'CurrentAxes'),'Xticklabel',{''});
        set(get(gcf,'CurrentAxes'),'Yticklabel',{''});
        set(get(gcf,'CurrentAxes'),'Zticklabel',{''});
        set(get(gca,'children'),'facecolor','interp');
        title(['t = ',num2str(q*T*1000),' ms']);
        view([45,45]);
        pause(0);
    end
else error('Please give either "visu" (=visualisaton) or...
 "voi" (=voice) as method!')
end
```

List of Figures

List of Tables

Bibliography

[1] Balázs Bank. *Physics-based Sound Synthesis of String Instruments Including Geometric Nonlinearities*. PhD thesis, Budapest University of Technology and Economics,Department of Measurement and Information Systems, 2006.

[2] N. Bronstejn, I., A. Szemengyajev, K., D. Musiol, and H. Mühlig. *Matematikai kézikönyv*. Typotex kiadó, Budapest, 2006.

[3] H. Fletcher, Neville and D. Rossing, Thomas. *The Physics of Musical Instruments*. Springer-Verlag New York Inc., 2000.

[4] Zsolt Garamvölgyi. Dobhang fizikai alapú szintézise, 2006. TDK dolgozat.

[5] Karl F. Graff. *Wave Motion in Elastic Solids*. Dover Publications, Inc., New York, reprint edition, 1991.

[6] Tilman Koch. Digitale klangsynthese: Simulation von gekrümmten zweidimensionalen klangkörpern, Januar 2008.

[7] Florian Kolbeck. Digitale klangsynthese mit physikalischen und systemtheoretischen parametern, October 2008.

[8] Cornelius Lanczos. *Linear Differential Operators*. D. Van Nostrand Company, Ltd., London, 1961.

[9] A.W. Leissa. *Vibration of plates*. National Aeronautics and Space Administration, Washington, D.C., 1969.

[10] Kornél Lánczos. *A geometriai térfogalom fejlődése*. Gondolat Kiadó, Budapest, 1976.

[11] Rudolf Rabenstein. Simulation of nonlinear multidimensional systems using a functional transformation approach. *Proc. of the 7th European Simulation Symposium ESS'95*, 1995.

[12] Rudolf Rabenstein. Transfer function models for non self-adjoint multidimensional systems. *Proc. 2. IMACS Int. Conf. on Circuits, Systems and Computers (IMACS-CSC'98)*, 1998.

[13] Rudolf Rabenstein, Tilman Koch, and Christian Popp. Tubular bells – a physical and algorithmic model. Universität Erlangen-Nürnberg, Lehrstuhl für Multimediakommunikation und Signalverarbeitung.

[14] Rudolf Rabenstein and Lutz Trautmann. Digital sound synthesis of string instruments with the functional transformation method. *Signal Processing*, 83:1673 – 1688, 2003.

[15] Lajos Rancz. Harang hangjának digitális szintézise, 2004.

[16] Gisbert Stoyan. *MATLAB*. Typotex kiadó, 2005.

[17] Gisbert Stoyan. *Numerikus matematika mérnököknek és programozóknak*. Typotex kiadó, 2007.

[18] Tero Tolonen, Vesa Välimäki, and Matti Karjalainen. *Evaluation of Modern Sound Synthesis Methods*. Helsinki University of Technology, Department of Electrical and Communications Engineering, Laboratory of Acoustics and Audio Signal Processing.

[19] C. Ugural, A. *Stresses in Plates and Shells*. McGraw-Hill Book Company, 1981.